This is to certify that the
thesis entitled

EVALUATION OF PREFABRICATED COMPOSITE STEEL
BOX GIRDER SYSTEMS FOR RAPID BRIDGE
CONSTRUCTION

presented by

Benjamin S. Pavlich

has been accepted towards fulfillment
of the requirements for the

M.S. degree in Civil Engineering

Major Professor's Signature

7/16/2010

Date

E

EVALUATION OF PREFABRICATED COMPOSITE STEEL BOX GIRDER SYSTEMS FOR RAPID BRIDGE CONSTRUCTION

By

Benjamin S. Pavlich

A THESIS

Submitted to
Michigan State University
in partial fulfillment of the requirements
for the degree of

MASTER OF SCIENCE

Civil Engineering

2010

EV

P

enginee

then as

prefab

only

consti

length

feas

emp

resp

the

an

st

h

t

ABSTRACT

EVALUATION OF PREFABRICATED COMPOSITE STEEL BOX GIRDER SYSTEMS FOR RAPID BRIDGE CONSTRUCTION

By

Benjamin S. Pavlich

Prefabrication is a popular practice that has gained widespread use in the bridge engineering community. Often certain components of a bridge are prefabricated and then assembled at the job site. However, this report focuses on the possibility of prefabricating a box girder/slab unit and shipping the entire assembly to a job site, where only placement and transverse post-tensioning would be required to complete the construction. This could drastically reduce construction time, eliminating the need for lengthy and costly road closures.

The objective of the project was to evaluate through numerical simulations the feasibility of creating an entirely prefabricated composite box girder bridge system and employing such a system for highway bridges. This included evaluating the global response of the system, local response of the composite girder/deck units and joints, and the vibration characteristics of the resulting bridge systems. To ensure accuracy, the analytical models were checked against theoretical predictions and experimental data.

Results from the simulation studies of this work indicated that the prefabricated steel/concrete composite girder/deck units are a safe and viable system for short-span highway bridges. It was shown that acceptable joint closure could be maintained below the AASHTO post-tensioning limits.

To my grandparents – Stephen, Velna, C. Wesley, and Miriam – who would have been very proud to see this day.

ACKNOWLEDGEMENTS

This work would never have been possible without the constant guidance and help of my advisor Dr. Rigoberto Burgueño. His knowledge and experience, coupled with the insatiable drive to teach and instill knowledge in his students is unmatched. He has helped me not only with my research, but also with my work ethic, my approach to problem solving, and my overall capabilities as an engineer. For this, and many other things over the 4+ years that I have known him, I will always be grateful.

The research described in this report was carried out under funding from the Michigan Department of Transportation, Contract 2002-0532 – Authorization 12, MSU APP 90038, with Mr. Steve Kahl as the project manager. The financial support of MDOT and the coordination of Mr. Kahl throughout the execution of the experimental program are gratefully acknowledged. Mr. Roger Till (MDOT) provided many helpful suggestions on the direction of the present study and his help is thankfully recognized. Also, Mr. Guy Nelson (Nelson Engineering Services) provided invaluable knowledge and support to this research, which stemmed from his insightful bridge concept, supporting the analytical effort reported in this report with much needed information on the real construction and performance of prefabricated steel-box girder bridges.

Many of my peers at MSU deserve recognition for supporting me and helping me think through problems in my research and schoolwork, as well as lending a hand at the lab including Mahmood Haq, David Bendert, Janelle Musch, Megan Vivian, Zhe Li and Xuejian Liu, among others.

Finally, I would like to thank my family and friends for encouraging me through the times when my outlook was a bit bleak. Thanks to all.

TABLE OF CONTENTS

LIST OF TABLES

LIST OF FIGURES

Images in this thesis are presented in color

1. INTRODUCTION

1.1 Summary

In order to offer faster and, in some cases, less expensive bridge construction, precast superstructures have recently become a topic of much interest to federal and state highway agencies (FHWA, 2004; Shahawy, 2003). Almost any component of a bridge can be precast or prefabricated, including girders, abutments, and decks (FHWA, 2004; Shahawy, 2003). The focus of this research is that of completely prefabricated composite steel box girder sections for rapid construction. While the exact geometry is to be developed with the work from this research project, the basic concept being investigated is presented in Figure 1 below.

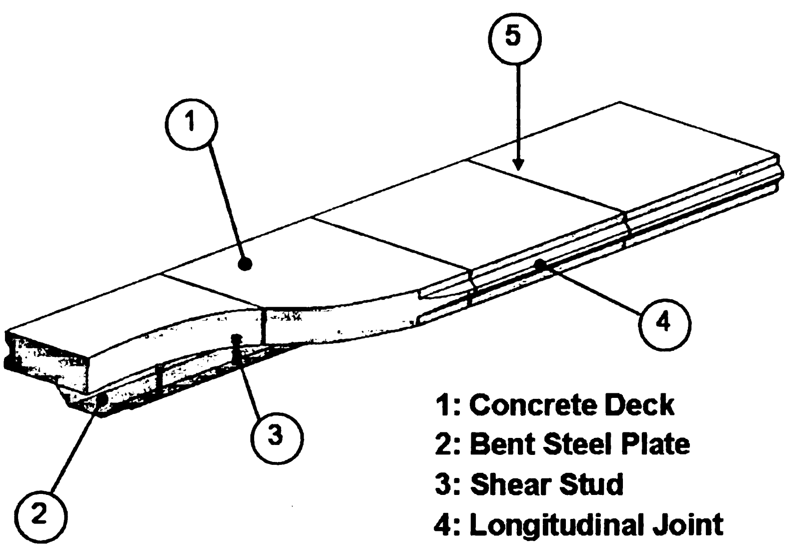

Figure 1. Composite Steel Box Girder Concept

As shown in Figure 1, the prefabricated steel box superstructure system consists of a cast in place or precast deck connected to a press-formed or cold-bent steel plate by means of shear studs. These sections could then be placed side by side and connected transversely, utilizing a shear key or other similar mechanism. While the behavior, design, and analysis of composite steel box girders is well established, several outstanding issues are unresolved for implementation of prefabricated concepts. The information needed in order to make the proposed prefabricated system viable is:

- What, if any systems are already in place
- Design of shear connection
- Design of longitudinal deck connection
- Design and analysis modeling techniques

These topics and their applicability to a prefabricated composite steel box girder system constitute the focus of the work performed in this project.

While the system that originally initiated the interest of the Michigan Department of Transportation (MDOT) in this topic utilized a cold bent plate, the intention of this project is not to limit this system to tubs that can only be press formed. The tub size used in the longer span (100 ft) bridges being studied would require an extremely substantial plate forming and bending operation. The author is not familiar with an operation of such magnitude, and hence tubs for longer spans may require welded plates. Although this would introduce additional cost into the system, it will not affect performance, and will not be discussed further.

1.2 R

syste

objec

elem

som

join

them

chec

the

emp

1.3

Int

1.2 Research Objectives

The overall goal of the project was to gain a working knowledge of the bridge system at hand. This was considered to have been achieved when the following objectives were met:

- Determine global system response of prefabricated composite steel box girder systems due to loads
- Determine localized behavior of joints
- Determine the effect of reduced post-tensioning on both global behavior and joint behavior
- Present design recommendations

The first three objectives were met by developing a hierarchical suite of finite element analyses that could address different aspects of the bridge behavior. While some models were conducive to global analysis, others were more suited for detailed joint analysis. Others yet had reduced complexity that led to smaller run times, making them more adept to parametric studies. These finite element models were meticulously checked against theoretical and experimental results in order to ensure their accuracy.

The final objective was accomplished by analyzing the data compiled throughout the first three objectives. These results allowed the author to make recommendations for employing prefabricated composite steel box girder systems.

1.3 Scope and Organization

The first step toward completing the project was to compile and study existing literature on related topics. This literature review can be found in Chapter 2 of this thesis

here

this p

in Ch

some

be s

cost

repl

can

pre

the

This

stud

des

thesis. Although many similar systems were found, the exact system being investigated here was not. Therefore, it is the belief of the author that this is the first major study of this particular system. The design and analysis considerations for the project are listed in Chapter 3. These included loading conditions and limit states, analysis methods, and some preliminary optimization work.

Once the literature review was performed the possible variations of the system to be studied were pared down using a rating system which accounted for factors such as: cost efficiency, constructability, fatigue performance/durability, and ease of replacement/removal. The highest ranking designs were then chosen for analysis. This can be found in Chapter 4.

Chapter 4 also highlights information gathered from experimental testing of a prefabricated steel box girder system. This experimental evaluation adds credibility to the analytical evaluations performed for this project.

The technical bulk of the work done on this project can be found in Chapter 5. This section details the selection of analysis tools, parametric studies, and detailed studies of joints and connections. The information found here can be used to aid in the design of prefabricated composite box girder systems.

Lastly, design recommendations are presented in Chapter 6.

2.1.1

2.1 (

syste

bein

cons

As a

emp

elem

alon

2.2 I

in

Sha

cor

pro

gir

in

cas

ref

2. LITERATURE REVIEW

2.1 General

A literature and survey review of current prefabricated complete superstructure systems has been conducted to identify prefabricated solutions similar to the system being studied or that address some of the issues noted in Section 1. The review considered available information at the conceptual, research, or implementation stage. As a reference, a brief account of concrete solutions is discussed and then more emphasis is placed on steel composite solutions. In the discussion of connection elements, the girder material type is not relevant and thus they are discussed as stand-alone details.

2.2 Prefabricated Superstructure Systems

As previously mentioned, national and state highway agencies have a high interest in using completely prefabricated bridge systems (AASHTO, 2002; FHWA, 2004; Shahawy, 2003). Technological progress is such that almost all the different elements composing a bridge system have had prefabricated solutions implemented in various projects. Thus, complete superstructure elements should be no different.

The most common type of prefabricated superstructure elements are clearly the girders, which could be prefabricated in either steel or prestressed concrete solutions and in either I or box shapes. These prefabricated beams are usually made composite with a cast-in-place concrete deck. Thus, complete superstructure solutions are typically referred to as those that use prefabricated elements that integrally feature *both* the girder and t

could

prec

adja

succ

supe

(Sh

trans

most

also

with

Prof

for c

or

sup

the

(B

or

199

199

and the deck system. Under this definition, untopped adjacent prestressed box girders could be considered a complete prefabricated system; and clearly so would be precast/prestressed concrete segmental bridges (typically cellular box girders). Both adjacent prestressed box girders and segmental cellular box girders are commonly and successfully used.

Prestressed double-tee beams have also been used as complete prefabricated superstructure solutions in several states (e.g., Colorado, New Mexico, and Wyoming) (Shahawy, 2003). Continuity between adjacent double-tee units is achieved by transverse post-tensioning. While this solution is aimed at highway bridges, it has been mostly used for rural and secondary roads. Complete superstructure deck systems have also been proposed, usually called full-depth prefabricated decks. Systems with and without the requirement of a cast-in-place topping have been developed (FHWA, 2004). Prefabricated prestressed and post-tensioned full-depth deck panels have also been used for complete superstructure replacement in Europe (Shahay, 2003).

A more recent concept is the use of precast/prestressed girder elements with full or partial deck flanges for a prefabricated superstructure element. A complete superstructure would then be assembled by a cast-in-place deck topping or connection of the prefabricated girder/deck elements through transverse connection of the deck flanges (Badie, 1999; FHWA, 2004; Freeby, 2005). These systems have been developed using I- or bulb-tee girders (FHWA, 2004), standard and modified closed box girders (Badie, 1999; Freeby, 2005), and U- or tub-shaped girders with deck flange overhangs (Badie, 1999; Freeby, 2005).

been

asse

Figu

A su

Rich

Figu

cons

Abu

then

trans

The

each

sam

Figu

Prefabricated steel superstructure systems are less common but several have also been developed. Complete superstructure elements have been created by the pre-assembly of I-girders with a composite concrete deck with partial overhangs as shown in Figure 2. If needed, the superstructure unit is prefabricated with transverse diaphragms. A superstructure of this type was used for the James River bridge replacement project in Richmond, Virginia (FHWA, 2004; Ralls, 2003). The contractor used prefabricated steel I-girder/deck units for most of the 101 bridge spans. The girder-deck units were pre-constructed in a casting yard near the site. The old bridge was removed overnight. Abutments were prepared for placement of the new bridge and the composite units were then set in place. The slab joints were sealed and the slab was post-tensioned transversely. For this project, the Virginia DOT did not consider any bids over 220 days. The winning bid was for 179 days and the contractor finished the job in 140 days. For each day under 179 the contractor received $30,000 bonus, and was to be charged the same amount for each day over schedule.

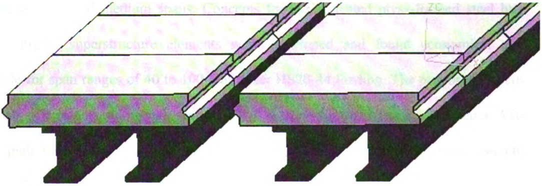

Figure 2. Schematic of Prefabricated Steel Composite Superstructure with I-Girders

2.3. Prefabricated Steel Box Composite Superstructure Systems

Much to the surprise of the author, a literature review on prefabricated steel box composite bridge superstructure elements showed that such a concept has been proposed several times during the past 35 years. The concept, as discussed in Section 1, uses a tub-shaped steel section as the girder element connected compositely to a concrete deck. The steel tub section and the composite deck then define a box section. The prefabricated steel composite box girders are then to be used as complete superstructure units, placed side by side to make up the require bridge width.

2.3.1 Pressed-Formed Steel Box Girder Bridge System – West Virginia University

In reviewing the literature, the first finding of a prefabricated steel composite box girder system was the conceptual designs of Gangarao and Taly (Taly, 1979). In the early 1970s Gangarao and Taly developed and studied several modular bridge systems aimed at short and medium spans. Concepts for prefabricated press-formed steel box girder bridge superstructure elements were developed and found economical and suitable for span ranges of 40 to 100 feet under HS20-44 loading. The proposed system consists of a trapezoidal trough section which is press-formed from a 3/8-in. thick A36 steel plate (see Figure 3). The deck consists of 5-in. thick precast prestressed concrete panels. The concrete deck is to be precast with the stud-plate embedded in it and then the entire deck assembly is shop-welded to the steel trough section. The precast concrete planks are nominally prestressed to minimize shrinkage cracks.

sam

or c

env

thr

con

sp

sh

s

w

a

c

The composite solution was an alternate to an all-steel designed proposed by the same authors (Taly, 1979). The webs and the bottom flange are not stiffened internally or externally. Different girder sections were suggested for different span lengths. They envisioned the girders to be produced in two top-flange widths, 6 ft and 8 ft, each having three variations in depth: 2.5 ft, 3.0 ft, and 3.5 ft. Their studies showed that a suitable combination of these sections results in various deck width designs at 2 ft intervals for spans up to 65 ft.

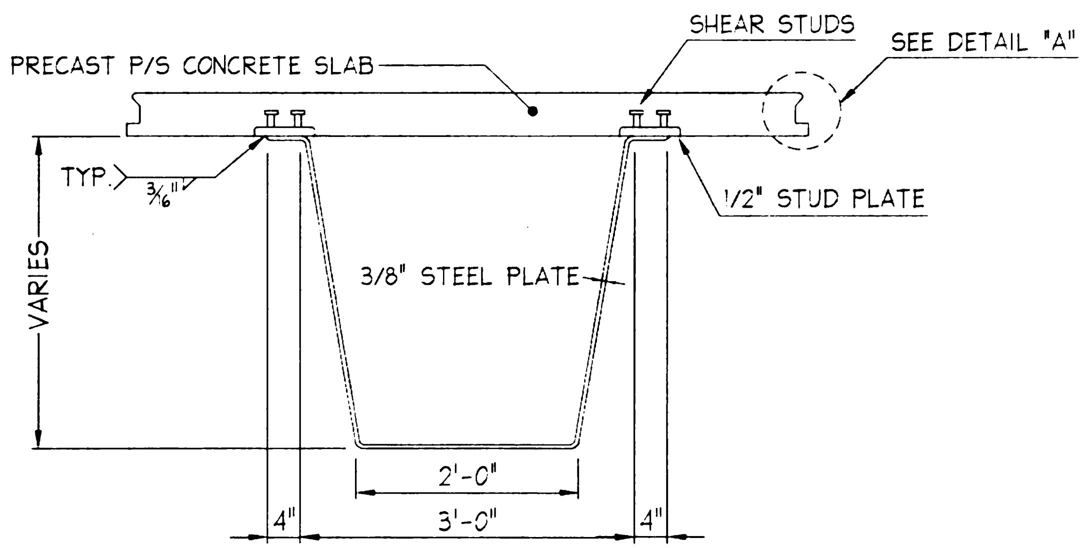

Figure 3. Press-Formed Composite Box Girder from (Taly, 1979)

Lateral load distribution between the adjacent girder units is achieved through shear keys with weld-ties at the junction of the two adjacent beam deck flanges as shown in Figure 4. The ends of the girders are closed by a 3/8-in. thick plate diaphragm welded all around the flanges and webs of the girders. Bearing stiffeners were provided at the beam ends (see Figure 5). Drainage holes were proposed in the bottom flange to drain out moisture from the closed steel box section.

Fi

spe

the

Ins

pr

ha

ins

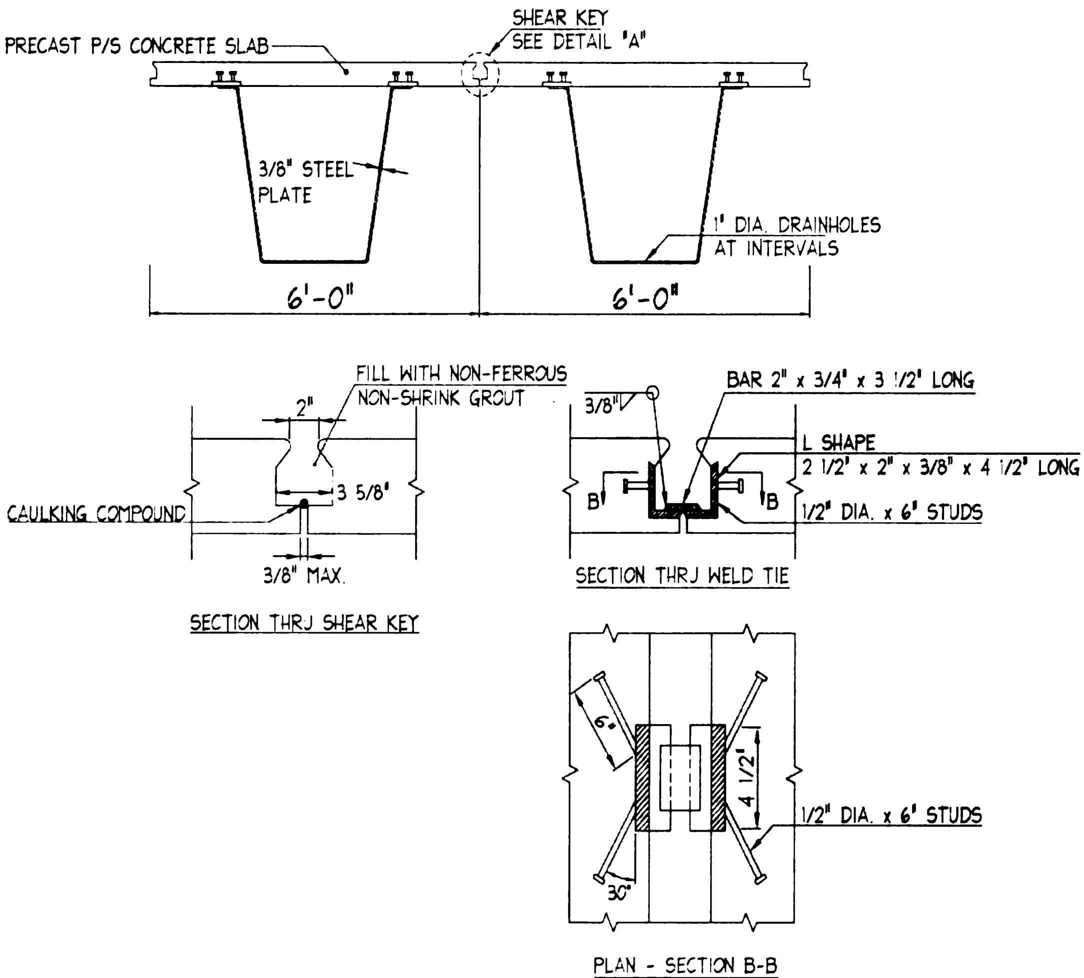

Figure 4. Shear Key Details for Pressed-Formed Steel Box Girders (Taly, 1979)

Since the American Association of Highway Transportation Officials (AASHTO) specifications did not provide any criteria for design with press-formed steel members, the proposed girder was checked according to the 1977 American Iron and Steel Institute specifications. Regarding the maintenance and durability of the system, the proponents note that investigations on several steel bridges with hollow members that had been in service for over 60 years had shown no signs of moisture or corrosion on the inside surfaces. Accordingly, Gangarao and Taly did not suggest corrosion-protective

treat
pain
Cor
2.3
pre
for
the
and
1.35
26

treatment for the interior of the proposed girders. For the exterior, they recommend painting the steel surface to protect it from corrosion, unless weathering steel, such as Corten or Mayari-R, is used for fabrication.

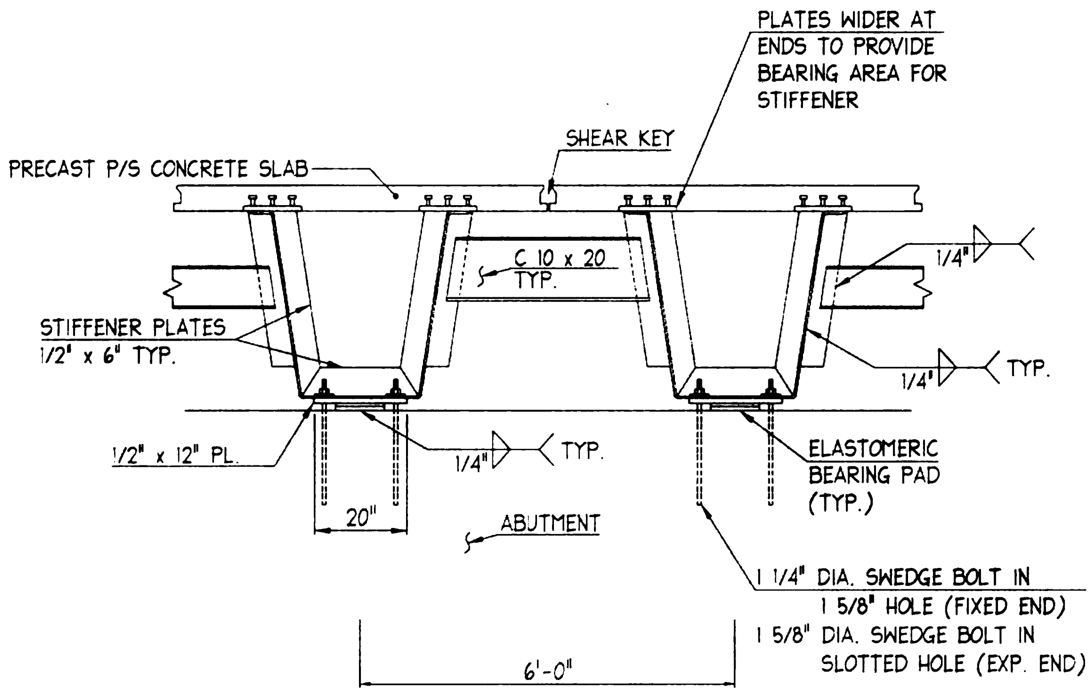

Figure 5. Connection and Stiffener Details at Abutment Support (Taly, 1979)

2.3.2 Texas DOT Prefabricated Steel Tub-Girder System – University of Texas, Austin

A more recent effort to develop steel box girder systems for modular prefabricated bridge superstructures was performed at the University of Texas, Austin for the Texas Department of Transportation (Freeby, 2005). The effort was propelled by the pressure on the Texas DOT to upgrade and expand its on- and off-system roadways and, in particular, the need for the rapid construction of the nearly 150 bridges that cross I-35 in central Texas. Construction of these structures was scheduled to begin in spring 2005.

From the effort noted above, two new prefabricated bridge superstructure systems were developed: a steel tub-girder and a prestressed concrete pre-topped U-beam (Freeby, 2005). Both systems were developed for maximum span lengths of 115 ft and total superstructure depth of 38 in. Only the steel solution is discussed here.

The steel tub-girder system uses a conventional pre-fabricated trapezoidal steel girder topped with a cast-in-place concrete slab before transportation to the bridge site. To achieve a shallow superstructure depth, the beams are shored during placement of the concrete deck to make them composite for all loads. After slab placement, the beam is hauled to the bridge site and erected on the piers/abutments. A cast-in-place closure pour joins the deck girder sections after they are in place. Figure 6 shows a girder section for a 115 ft span. The steel tub-girder has a 29.5-in. deep steel section with an 8.5-in. slab for a total section depth of 38 in. The design used ASTM A709 Grade 50W steel. A typical transverse cross-section of a bridge is shown in Figure 7.

As shown in Figure 6 the steel tub is formed of welded steel plates, as opposed to the bent steel plate proposed in this project. This gives the advantage of variable widths for the webs and flanges, but comes at the expense of requiring costly welds. However, it should be noted that the Texas DOT opted for welded steel plates in order to avoid introducing new bending technology, not on the basis of performance (Freeby, 2006).

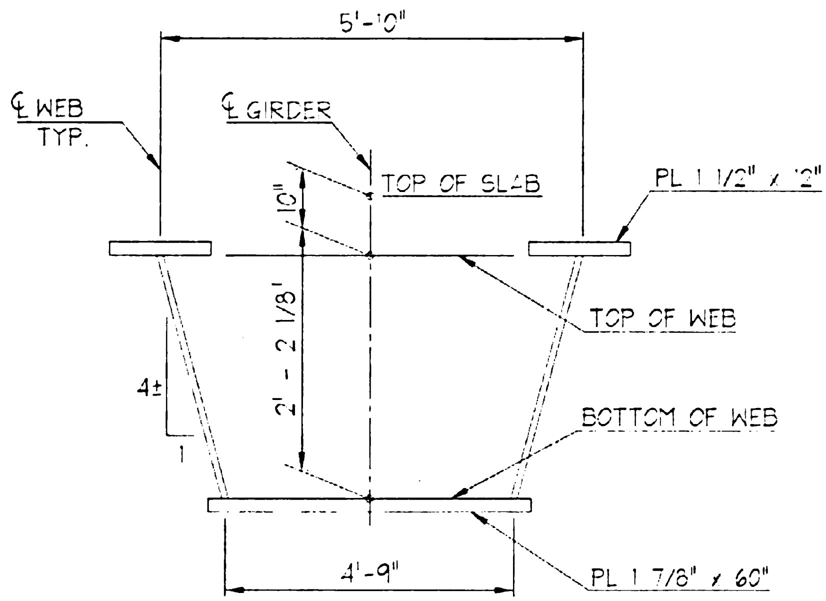

Figure 6. Texas DOT Steel Tub-Girder Section (Freeby, 2005)

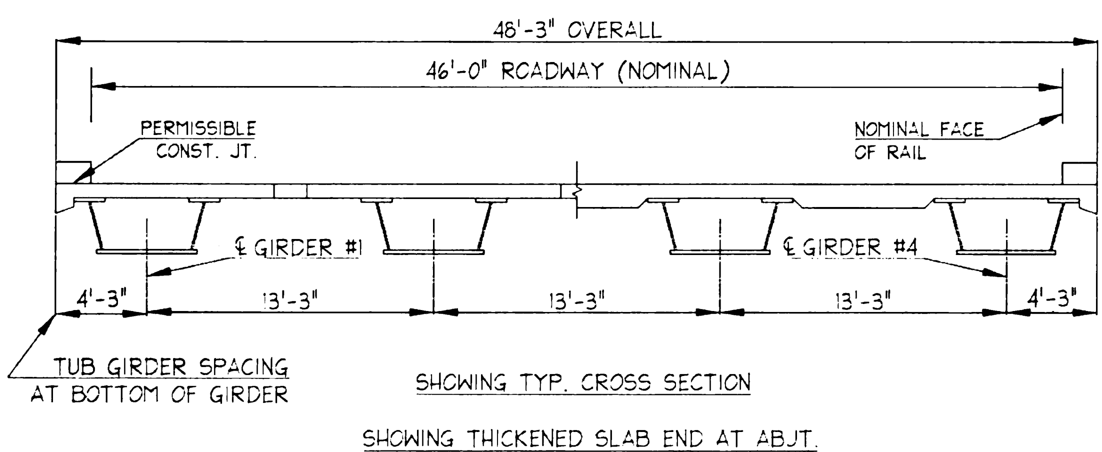

Figure 7. Typical Bridge Cross-Section using TDOT Steel Tub-Girders (Freeby, 2005)

The girder design was developed using the AASHTO LRFD Bridge Design Specifications with HL93 loading (AASHTO, 1998). The design of the girder element was controlled by the Texas DOT imposed live load deflection limit of L/800 and not by allowable strength requirements. Due to the unusually shallow section, the girder was proportioned so that the deck would not crush before the steel tub reached yield.

The transverse deck connections for the prefabricated systems are reported to be undergoing testing at the University of Texas, Austin (Freeby, 2005). The concept for the joint detail used in the steel tub-girder superstructure is shown in Figure 8. Preliminary research results noted that the closure joint behaves as designed and develops the predicted moment and shear capacities with failure due to yielding of the reinforcement, exhibiting ductile behavior (Freeby, 2005). While durability of the joints is a general issue, Texas DOT is not concerned with corrosion due to their weather but plan to monitor the structures closely.

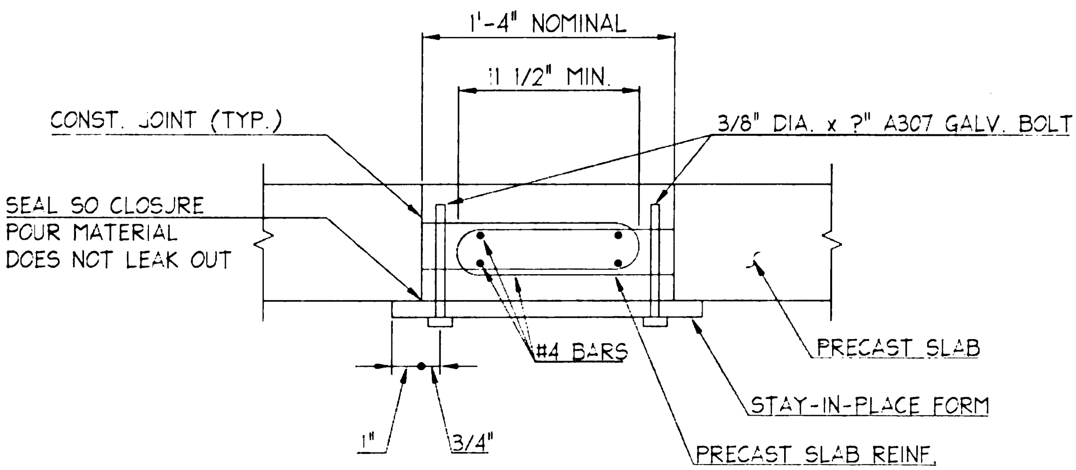

Figure 8. Transverse Deck Connection Detail for Steel Tub-Girder (Freeby, 2005)

Weathering steel was specified for durable performance without maintenance costs. Drip tabs and other details were provided to reduce the potential for substructure staining from the weathering steel. A flexible lifting scheme was incorporated in the des

pre

Au

fel

cor

pla

of

for

2.3

ela

Lu

co

de

sm

Inv

sh

dif

(A

design to give the contractors more options on the lifting and placement of the prefabricated units.

The two competing prefabricated bridge designs were released for letting in August 2004 and the winning bid was of the pretopped prestressed U-beam design. It is felt that the recent rise in steel prices prevented the steel tub-girder design from being competitive. It should also be noted that the steel tub-girder is composed of welded plates, which add a considerable amount of labor. The Texas DOT anticipates that both of the developed prefabricated bridge superstructures will be used over the next 10 years for the rapid construction of the I-35 corridor in central Texas.

2.3.3 Inverted Steel Box Bridge System – University of Nebraska, Lincoln

A new steel configuration for prefabricated steel composite superstructure bridge elements is currently being developed and studied at the University of Nebraska, Lincoln under a contract from the Nebraska Department of Roads (TRB-RIP, 2006). The concept uses an inverted steel tub/box girder connected compositely with a concrete deck. The rationale for inverting the steel tub-girder section follows from the case that small box sections do not permit maintenance workers inside the box for inspection. Inverting the steel box eliminates this problem. A bridge cross section of this system is shown in Figure 9. A United States patent from the same research team shows a different press-formed geometry of the inverted girders, as shown in Figure 10 (Azizinamini, 2006).

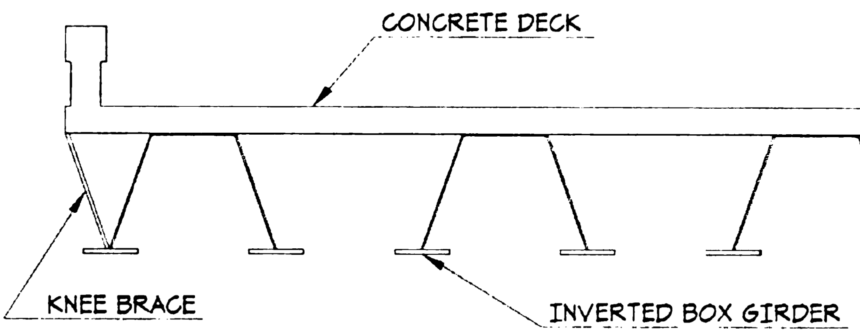

Figure 9. Inverted Box Girder Bridge Diagram (Yakel, 2007)

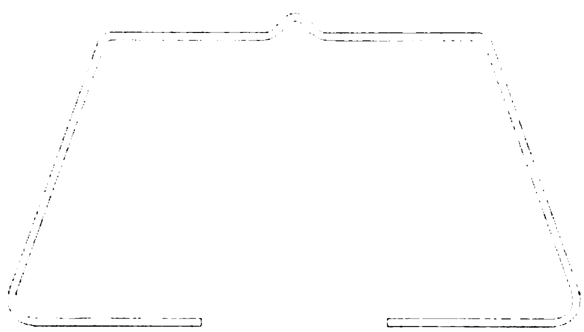

Figure 10. Alternate Inverted Box Girder Geometry (Azizinamini, 2006)

The inverted steel box girder features are:

- A girder consisting of an inverted steel box section. The web and top flange are of the same thickness and the bottom flanges are welded to the end of the web.
- The inverted box girder could be shop-welded or made by bending a flat plate into a U shape.
- Knee braces extending from the bottom flange ends can allow longer deck overhangs, if needed, and can provide horizontal restraint to the bottom flanges since they will have the tendency to "kick-out" (in plan) under flexural demands.
- Initial horizontal curvature (in plan) in the flanges could reduce the tendency of the bottom from "kicking-out" under flexural demands. This approach can also be used to generate an initial compressive force in the

bottom flanges to counteract dead load stresses and increase the live load capacity of the girder.

- The wide top flange of the inverted box provides a convenient platform for construction workers but it may need to be stiffened.

A research project sponsored by the Nebraska Department of Roads (NDOR) published in 2007 provides extensive background on this system (Yakel, 2007). The research suggested that such an inverted box girder system would likely be a viable option for bridges of less than 100-ft span.

2.3.4 Composite Girders with Steel U Section – Tokai University

Professor Shun-ichi Nakamura of Tokai University in Japan studied the bending behavior of composite steel box girders of a "U-shape" in 2002. His research involved testing three different sections of such a girder. One of the sections was prestressed and will not be discussed here. The other two sections can be seen below in Figure 11.

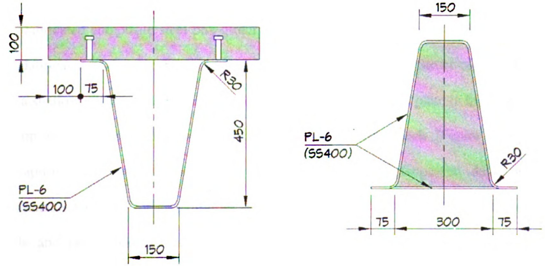

Figure 11. U-Shaped Girder Cross Sections (Nakamura, 2002)

repr

sect

bene

sect

stra

able

and

cons

(197

2.3

pro

pro

of

The

con

elim

sid

di

The second girder configuration shown in Figure 11 is depicted upside-down to represent a section over a support where the section would be in negative bending. The section is filled with concrete to take the compressive forces induced by this negative bending and to stabilize the steel against buckling.

The researchers in this project developed an analysis model that divided the section into vertical "layers" and then analyzed the system assuming a bilinear stress-strain curve for the steel and a parabolic stress-strain curve for the concrete. They were able to match experimental findings closely.

Overall the researchers concluded that the U-girder system was a viable system and could be designed using a plastic design procedure. A three-span continuous bridge consisting of 60m (195 ft) spans was designed, with U-girders reaching heights of 2.5m (97.5 in.) and a plate thickness of 25mm (1 in.) (Nakamura, 2002).

2.3.5 Con-Struct Bridge System – Nelson Engineering Services

Nelson Engineering Services (NES) has developed an innovative concept for a prefabricated composite steel box girder system with an integral road deck for shallow prefabricated bridge superstructures (AASHTO, 1998). The Con-Struct concept is that of a shallow girder element consisting of a cold-formed bent steel plate in the shape of a "bath-tub" connected compositely to a reinforced concrete deck (Figure 12a). The composite box shape is braced for placement by the prefabricated deck, which eliminates the need for cross-frames. Prefabricated girder units can be placed side by side and post-tensioned transversely at the deck level or at intermediate concrete diaphragms to build up the desired superstructure width (Figure 12b).

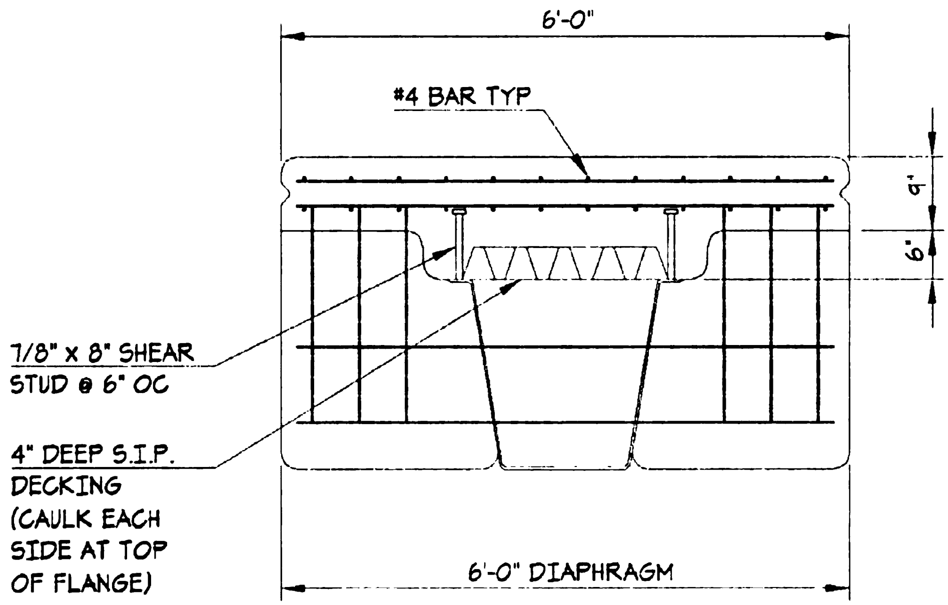

a) Beam-Cross Section at Intermediate Diaphragm

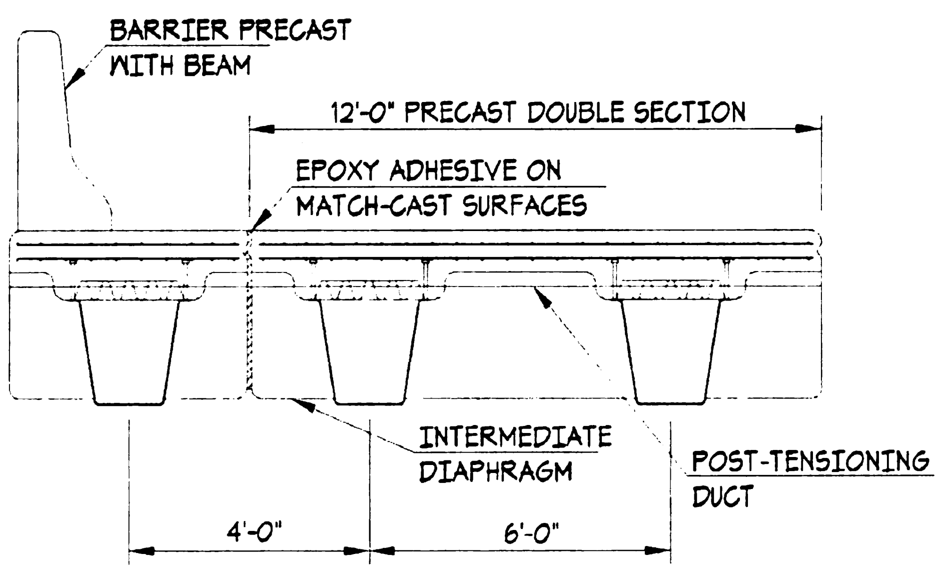

b) Partial Deck Cross-Section

Figure 12. Preliminary Concept for Composite Steel Box Girder (Nelson, 2004)

Unique to the Con-Struct system from Nelson Engineering is their concept to prestress the steel plate to increase the composite girder capacity for live loads. This is achieved by propping the steel tub section at mid-span and stabilizing it, but not supporting it from its ends. A cast-in-place deck is then poured and a Styrofoam block or metal decking is used to form the deck on top of the tub-girder void. The self weight of the deck introduces negative bending on the steel plate when propped on its center. This negative moment introduces an initial compressive state in the bottom of the tub-girder soffit. Once cured, the concrete slab and the steel girder act compositely and the compressive stress in the steel tub is "locked-in." This stress can be further controlled by using tensioning devices at the end of the steel tub-girder. The concept is to use the initial pre-compressive stress to provide camber to the section and to counteract dead load stresses. This also increases the service live load capacity of the section.

The Con-Struct system is built using galvanized steel for durability measures. To the knowledge of the author, Nelson Engineering has not yet developed or validated transverse deck connection details to connect multiple girder sections for wider bridge solutions. The system, however, has been effectively used in several private pedestrian bridges in Michigan. A picture of a 40 ft long pedestrian bridge using the Con-Struct system is shown in Figure 13.

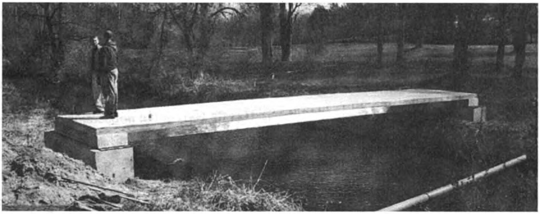

Figure 13. Pedestrian Bridge over Tyler Creek (MI) with Con-Struct System (Nelson, 2006)

2.4. Deck Systems

In designing a composite bridge girder system, even if it is prefabricated, a decision must be made between decks cast-in-place, decks made of precast elements with cast-in-place overlays, decks made of precast elements with wet joints, and totally precast decks.

Decks cast-in-place have strong advantages. They are simple to erect and easy to connect. However, these deck systems may suffer high tensile strains produced by shrinkage, which is resisted by the steel beam. Slabs made from precast elements also have advantages: low cost, fast construction, and high product quality. Connection of a precast deck to a steel girder is achieved by distributing the connection in groups that are anchored in pockets left in the precast deck and which, after placement, are filled with non-shrink grout. Problems with this solution may include connector density, corrosion between the girder and the deck, and shrinkage of the concrete in the pockets. The best solution is to prefabricate the deck and to prestress it longitudinally before connecting it to the steel girder (Virlogeux, 1999). The only concern would be creep in the concrete, which could be reduced through prefabrication. Thus, the slab could be made of precast elements made continuous through longitudinal joints before prestressing the deck; leaving the connection to the steel girder last.

2.5. Longitudinal Girder-Deck Shear Connections

Shear connections in composite beams are obviously essential. The nature of composite action induces large shear forces at the interface between the steel and concrete. Traditionally, these shear forces are carried by means of a shear stud welded to the steel, which is then embedded into the concrete deck. When a cast-in-place deck is used, embedding of the shear studs is simple. Shear studs are shop-welded and the deck is poured around them. However, if the deck is prefabricated, pockets are left in the precast slabs that correspond to the location of the shear studs on the steel. These pockets are then filled with a non-shrink grout, which hardens to achieve the composite action. The design of the shear studs, as well as the properties of the grout used, can have large effects on the response of the entire section.

Considerable information exists both in code guidelines and research findings to guide the design of girder-deck shear connections. This research will study further the guidelines in the AASHTO LRFD specifications. Considerable information was also found from activities in Korea on the development of composite box girder sections with precast decks (Chang, 2001). General guidelines on steel and concrete composite construction were also found (Ohelers, 1995).

2.6. Transverse Deck Joints

Also of consideration are the transverse connections between prefabricated deck segments. Transverse deck joints will be less critical for the concept under investigation here since the sections are to be used as simple spans. Therefore, negative moments, and the associated tensile stresses will not occur at the transverse joints. Despite this, transverse deck connections between prefabricated panels should not be ignored as they are responsible for transferring the longitudinal shear in the deck element. An inadequate transverse shear connection can lead to slip between adjacent precast panels and limit the flexural and shear capacity of the overall system.

Typically, the joints connecting prefabricated panels are made by means of shear keys of two basic types: female-to-female or tongue-and-groove type joints. After installation, the joints are filled with high-strength non-shrink grout or with an epoxy mortar. Longitudinal post-tensioning is sometimes necessary to provide sufficient compression to keep the joints from opening.

Use of precast concrete panels for full depth decks has been in use since the 1970s (Taly, 1979) and new efforts closely related to steel box construction have been recently published (Chang, 2001). Thus, extensive literature exists on the topic (Issa, 1995).

2.7. Longitudinal Deck Connections

The capacity of a deck system to distribute loads transversely between girders defines the load distribution characteristics of the bridge system. Thus, the ability to connect the prefabricated sections transversely, at the deck flanges, will be of great importance for the system under consideration. The longitudinal deck connections for prefabricated decks seem to be designed on a project specific basis for connecting prefabricated double tees (Shahawy, 2003) as well as the prefabricated steel box tub-girder concepts presented in Section 2.3.1 and Section 2.3.2. An overview of the concepts identified follows.

In general, to maintain continuity between adjacent prefabricated deck elements (or the flanges of prefabricated girder/deck elements), the flange edges, or sides, are shaped to create a continuous shear key that can be filled with a non-shrink grout or epoxy mortar. Different types of longtitudinal deck connections are feasible:

1. Grouted female-to-female shear keys. In this connection detail shear is transferred by friction and by the creation of an internal diagonal compression strut inside the shear key cavity.
2. Grouted tongue-and-groove shear keys. In this connection detail shear is transferred largely by friction and by the diagonal compression transferring load between the groove part of the key onto the tongue part in the other component.
3. Reinforced (confined or unconfined) shear keys blocks. This connection requires the provision of long pockets inside the prefabricated deck system. The pockets are asymmetrical such that the reinforcement is placed first on one side and then slid across the joint once the adjacent member is in place – see Figure 14.
4. Reinforced (confined or unconfined) female-to-female shear keys. In this connection, a full depth shear key is reinforced with splicing bars extending from the adjacent panels. The reinforcement could be a simple splice or confined as shown in Figure 15.
5. Post-tensioned grouted female-to-female shear keys. This connection concept is as described in (1) above with additional post-tensioning forces to avoid cracking or opening of the joint and increase its shear capacity.
6. Post-tensioned grouted tongue-and-groove shear keys. This connection concept is as described in (2) above with additional post-tensioning forces to avoid cracking or opening of the joint and increase its shear capacity.
7. Welded plate grouted shear key blocks. In this concept, a steel plate or reinforcement bar is embedded at the end of the flange and fabricated with the precast deck. A plate

is then welded in the field to provide a shear connection. The block-out cavity is then grouted. This connection detail is shown in Figure 16. This concept was utilized for the connection design of Gangarao & Taly's pressed-formed steel box girder bridge system (see Figure 4).

8. Reinforced grouted moment key blocks. A full-depth block-out is reinforced with hair-pin reinforcement protruding from both sides of the prefabricated deck component and crossing in the region of the connection block. The region is grouted and the joint becomes a moment resisting connection. This concept was proposed for the Texas DOT steel tub-girder concept, see Figure 8.

9. Post-tensioned grouted female-to-female moment keys. This connection concept is an extension of that in (5) with the difference that the tendon would be placed such as to give the section moment capacity. Passive compression reinforcement would probably be necessary to control cracking induced by post-tensioning.

10. Post-tensioned grouted tongue-and-groove moment keys. This connection concept is the same as that in (9) but applied to a tongue-and-groove geometry.

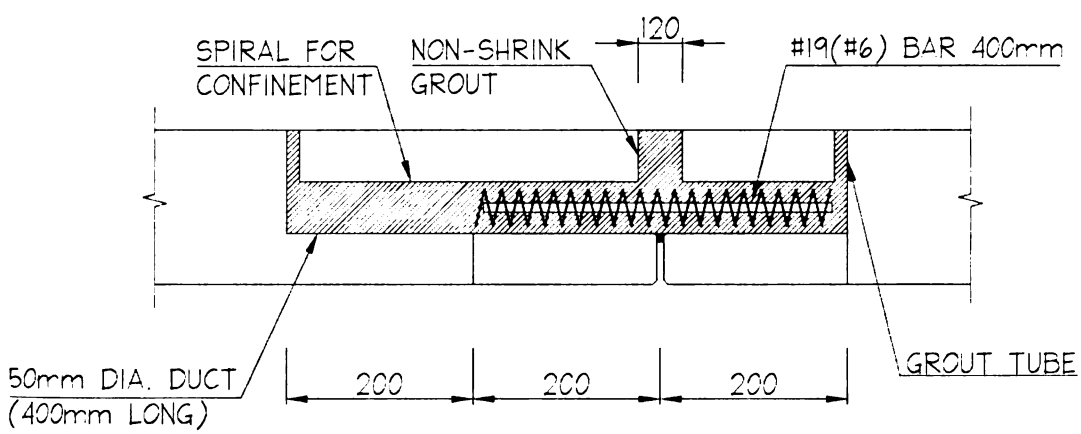

Figure 14. Deck Connection Detail using Reinforcement in Precast Pockets (Badie, 1999)

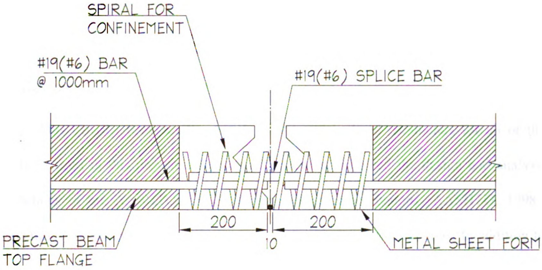

Figure 15. Deck Connection Detail using Confined Reinforcement in Full-Depth Key (Badie, 1999)

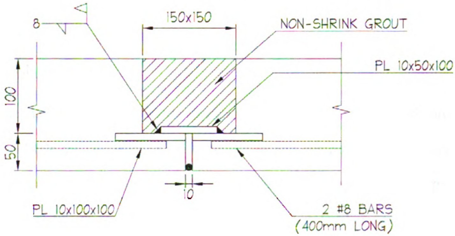

Figure 16. Deck Connection Detail using Welded Steel Plate (Badie, 1999)

The advantages and disadvantages of the above listed connections will be considered with respect to cost, structural performance, constructability, design ease, etc., in order to identify three options for further study under this project (see Chapter 4).

3. DESIGN AND ANALYSIS CONSIDERATIONS

3.1 General

This Chapter provides the details of the standardized parameters for all of the analyses used in this project. In general, the project followed the design and analysis guidelines in the AASHTO LRFD Bridge Design Specifications (AASHTO, 1998). Deviations from these specifications are noted in the respective sections. In addition to general analysis and design specifications, this section also presents the implementation of these guidelines in a design optimization process aimed at providing a parametric evaluation.

3.2 Materials

The material properties for the design and analysis tasks in this study are listed in Table 1. While the construction of the steel/concrete composite prefabricated bridges requires diverse materials, only a few parameters of these are needed for the preliminary design tasks and for the service-load numerical modeling. Further, some specific details are not required such as the type of post-tensioning strands for the transverse connection of the units since only the pressure by them is considered in the analysis.

Table 1. Material Properties

Material	Properties		
Concrete	fc = 4,000 psi	Ec = 3605 ksi	γ = 8.68 x 10E-5 kips/cu. in.
Structural Steel	Fy = 50,000 psi	Es = 29,000 ksi	γ = 2.83 x 10E-4 kips/cu. in.

3.3 Loading

Loading for this study followed the AASHTO LRFD Bridge Design Specifications (AASHTO, 1998). Only the considerations applying to dead load (DC), live load (LL), and impact factor (IM) were used. When considering dead load, the self-weight of the superstructure and a barrier were considered. These loads were calculated by finding the volume of each component per unit length, and then multiplying that by unit weight found in Table 1.

When considering live load, two separate entities are identified by AASHTO. First, the vehicular live load is represented by a design lane load, which is defined to be ten-feet wide and centered in each lane, running the length of the bridge. The magnitude of this load is 0.064 ksf, evenly distributed across the width of the lane. This equates to a load of 0.64 kips for each foot of each lane considered. The second part of the live load is the design truck. The design truck has three axles, spaced at 14 feet. The front axle carries a load of 8 kips (4 kips per tire), and the rear axles carry a load of 32 kips (16 kips per tire). When applicable, the tire loads are applied to an area that is 20 inches wide and 10 inches long. Otherwise, they are applied as point loads. A schematic of the design truck is shown in Figure 17. The impact factor is applied to the design truck only.

D

F

s

n

3.

st

cc

yi

(u

lo

w

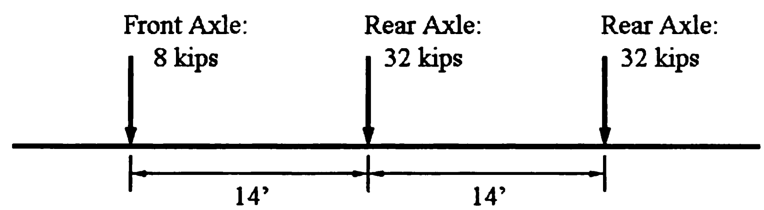

Figure 17. Design Truck Schematic

For this project, the HS-20 design truck was used. Although the MDOT Bridge Design Specifications use a heavier design truck (HS-25), the HS-20 was used in this project in order to draw appropriate parallels to AASHTO specifications. Calculations showed that the using the HS-25 truck would increase moments by 10-12%, and increase deflections by 17-18%.

3.4 Design Limit States

The limit states considered for the design and analysis of the prefabricated steel/concrete bridge structures were: Strength I (to assess strength under basic load combination to represent normal operating conditions of a bridge), Service II (to control yielding of steel structures under vehicular loading) and the optional Deflection Control (under live load only) limit state (AASHTO, 1998). The load combinations (loads and load factors) used for these limit states were:

- Strength I: 1.25D + 1.75(L x IM)
- Service II: 1.00D + 1.30(L x IM)
- Deflection Control: 1.00(L x IM)

where D = dead load, L = vehicular live load, and IM = impact factor = 1.33.

3.5 AASHTO Simplified Analysis and Design Methods

Although the prefabricated systems being studied here are not directly addressed by the AASHTO code, the specifications for composite steel box girders were considered applicable to the type of structure under study and thus were followed.

To demonstrate the AASHTO method, a sample bridge was analyzed. The bridge was assumed to be a 50-ft simple span composed of five girder/deck prefabricated units as shown in Figure 18. The load, along with corresponding bending moment and shear demands are listed in Table 2 and Table 3, respectively.

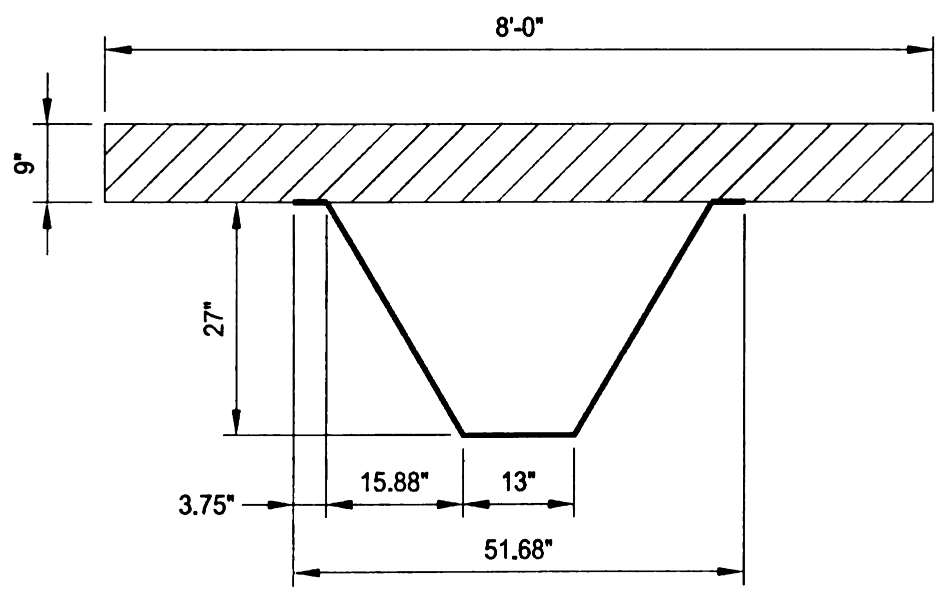

Figure 18. Bridge Geometry Used in AASHTO Analysis

Distribution of moment and shear demands on the individual girder units was estimated with the AASHTO load-distribution factors. The distribution factor for a box section with a steel girder is given by (AASHTO, 1998):

$$DF = 0.05 + \left(0.85\frac{N_L}{N_B}\right) + \frac{0.425}{N_L} \tag{3-1}$$

Table 2. Loading and Moment Demands for Beam Analysis

AASHTO Load	Component	Magnitude	Moment at Midspan (kip*ft)
DC	Concrete Self-Weight	0.90 kip/ft	281.3
	Steel Self-Weight	0.156 kip/ft	23.3
	Barrier	0.18 kip/ft	55.1
		Total:	359.7
LL	Vehicular Lane Load	0.64 kip/ft	200
	Design Truck (Axle 1)	8 kip	34
	Design Truck (Axle 2)	32 kip	360
	Design Truck (Axle 3)	32 kip	216
		Total:	810
IM	All Cases Other Than Fatigue: 1.33		

Table 3. Loading and Shear Demands for Beam Analysis

AASHTO Load	Component	Magnitude	Shear @ 1 (kips)	Shear @ 2 (kips)
DC	Concrete Self-Weight	0.90 kip/ft	22.5	22.5
	Steel Self-Weight	0.156 kip/ft	3.9	3.9
	Barrier	0.18 kip/ft	4.5	4.5
		Total:	30.9	30.9
LL	Vehicular Lane Load	0.64 kip/ft	16	16
	Design Truck (Axle 1)	8 kip	6.6	1.4
	Design Truck (Axle 2)	32 kip	17.6	14.4
	Design Truck (Axle 3)	32 kip	8.6	23.4
		Total:	48.8	55.2
IM	All Cases Other Than Fatigue: 1.33			

For the bridge under consideration, Equation (3-1) becomes:

$$DF = 0.05 + \left(0.85 \cdot \frac{2}{5}\right) + \frac{0.425}{2} = 0.6 \tag{3-2}$$

The maximum bending moment (M_u) under the Strength-I load case is determined with Equations (3-3).

$$[(DC)(1.25) + (VLL)(1.25) + (DT)(IM)(1.75)] \times DF \tag{3-3a}$$

$$[(359.6)(1.25) + (200)(1.25) + (610)(1.33)(1.75)] \times 0.6 = 1337\ kip - ft \tag{3-3b}$$

Design follows from satisfying

$$M_u = \phi_f M_n \tag{3-4}$$

where M_u is the moment demand, M_n is the flexural capacity and the strength reduction factor φ_f is given to be 1.0 in AASHTO Article 6.5.4.2.

To determine the section capacity, the AASHTO bridge design specifications outline a simplified approach for obtaining the nominal plastic moment of composite sections in Appendix 6-A (AAHTO, 1998). A depiction of the variables to be used in the AASHTO equations is shown in Figure 19.

Inspection of force equilibrium for the bridge model units showed that in all cases the section neutral axis was located in the slab above the level of the bottom deck reinforcement. This situation is defined as Case III, IV, or V in Appendix 6-A of the AASHTO Specifications (all three cases are identical when no deck reinforcement is present). For such cases, with reference to Figure 19, section force equilibrium, the plastic neutral axis depth, and the section plastic moment is given, respectively by:

$$P_t + P_w + P_c + P_{rb} = \left(\frac{c_{rb}}{t_s}\right) P_s + P_{rt} \tag{3-5}$$

$$\bar{y} = t_s \left[\frac{P_{rb} + P_c + P_w + P_t - P_{rt}}{P_s}\right] \tag{3-6}$$

$$M_p = \left(\frac{\bar{y}^2 P_s}{2t_s}\right) + \left[P_{rt} d_{rt} + P_{rb} d_{rb} + P_c d_c + P_w d_w + P_t d_t\right]. \tag{3-7}$$

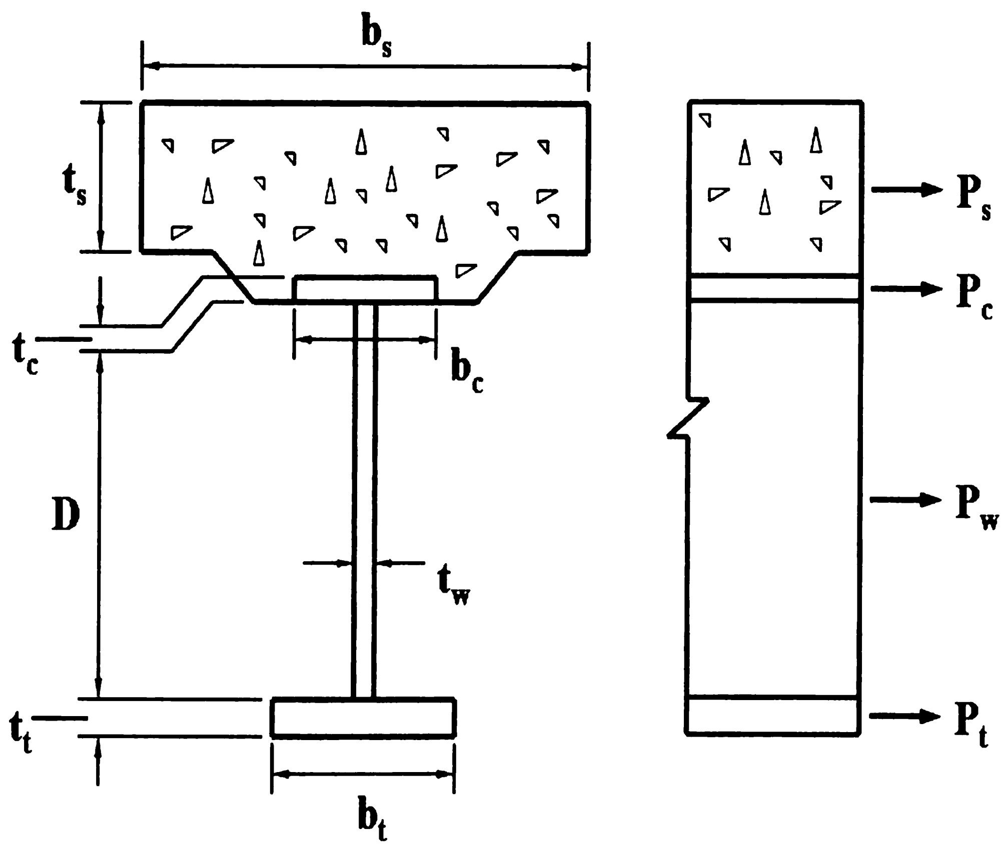

Figure 19. Variables for AASHTO Nominal Plastic Moment of Composite Girders (AASHTO, 1998)

For the test units under consideration, the force components at the deck reinforcement can be neglected and thus P_{rb} and P_{rt} are set equal to zero. Considering a deck concrete compressive strength of 3.6 ksi, solution of the above equations yields a plastic neutral axis depth ($\bar{y}$) of 3.66 inches and a nominal plastic capacity (M_p) of 1987 kip-ft. Since the deck is nine inches deep, the plastic neutral axis is in the deck.

AASHTO Article 6.10.4.1.2-1 (AASHTO, 1998) states that the section is compact if

$$\frac{2D_{cp}}{t_w} \leq 3.76\sqrt{\frac{E}{F_y}}\,. \tag{3-8}$$

Since the plastic neutral axis is in the deck, the depth of web in compression at the plastic moment is zero. Hence, the left side of the inequality in Equation (3-8) is also zero, and the section is compact. For compact sections, the AASHTO specifications direct the user to Article 6.10.4.2.2. Here, a variable D' is defined as

$$D' = \beta\frac{d + t_s + t_h}{7.5} \tag{3-9a}$$

$$D' = 0.9\frac{27 + 9 + 0}{7.5} = 4.32 \tag{3-9b}$$

where β is given as 0.9 for F_y = 36 ksi, d is the depth of the steel, t_h is the haunch thickness, and t_s is the slab thickness. For the section in Figure 18 D' is 4.32 inches.

Since D' is less than the plastic neutral axis depth then M_n=M_p=1969 kip-ft (found with Equation (3-7) above) and $M_u \leq M_r$ making the section adequate in flexure.

The loading values used for the shear calculations are showed in Table 3. As Table 3 shows, the highest shear value occurs at Support 2. The maximum factored shear demand (V_u) under the Strength-I limit state is determined as shown in Equation (3-10):

$$[(DC)(1.25)+(VLL)(1.25)+(DT)(IM)(1.75)]\times DF \tag{3-10a}$$

$$[(30.9)(1.25)+(16)(1.25)+(39.2)(1.33)(1.75)]\times 0.6 = 94.7\ kips \tag{3-10b}$$

Equation (3-10b) gives the V_u, which is described in AASHTO Section 6.10.9.1 as shear in the web at the section under consideration due to factored loads (AASHTO, 1998). Now the shear resistance of the section must be found.

The maximum shear resistance, V_n, of the section is given by (AASHTO, 1998):

$$V_r = \phi_v V_n \tag{3-11}$$

where φ_v is given in AASHTO Article 6.5.4.2 as 1.0, and V_n is found using Equation (3-12) below:

$$V_n = \frac{4.55 t_w^3 E}{D} \tag{3-12a}$$

$$V_n = \frac{4.55(0.375)^3(29,000)}{27} = 258 \text{ kips} \tag{3-12b}$$

where t_w is the thickness of the web, and D is the depth of the steel girder. With a maximum shear demand (V_u) of 94.7 kips, the section is adequate in shear.

3.6 Refined Analysis Methods

There are many other methods to analyze a bridge structure with improved refinement. In this project, two other methods were employed. The first is the grillage method. A grillage model is a means of representing a structure with a series of line-type elements that have been given properties appropriate for representing the stiffness, torsion and unit weight properties of the structure being modeled. Grillage models reduce the number of required elements and degrees of freedom, thereby reducing the number of equations that need to be solved to evaluate system response. Grillage models can be two- or three-dimensional, although only two-dimensional models were used in this project.

The second analysis method that was used is the finite element (FE) method. The FE method is an approximate method of structural analysis that breaks the structure into discrete pieces, or elements, connected by means of nodes. The nodes are forced to satisfy compatibility requirements and the way in which they interact with nodes of other elements or boundary conditions is determined by the force-deformation properties of the elements. This method is very powerful, and it can be used to analyze very

complex structures to a high degree of accuracy. Care must be taken, however, to ensure the method is used correctly. In this project, three-dimensional FE models were created and analyzed with linear elements.

3.7 Joint Performance Criteria

As a reference point to evaluate the acceptability of the joint openings, the author consulted the AASHTO LRFD Bridge Design Specifications (AASHTO, 1998). While unable to locate a specific tolerance for crack opening in segmental construction, the limit for acceptable crack width in a reinforced concrete bridge was found. This threshold has been included in the plots of the joint opening of the models in Section 5.4.5 as a reference to the reader. However, it should be kept in mind that this is simply a comparison that the author found to give a reasonable benchmark, not an actual requirement by any code or governing body.

The equation used to establish the acceptability threshold was given in Article 5.7.3.4 of the AASHTO LRFD Bridge Design Specifications. The crack tolerance varies depending on performance criteria, therefore the code lists multiple conditions. Condition (1) applies when cracks can be tolerated due to reduced concerns of appearance and/or corrosion. Condition (2) applies to transverse design of segmental concrete box girders for any loads prior to full concrete strength and when there is increased concern for appearance and/or corrosion. Because of the harsh environment to which Michigan bridges are exposed, Condition (2) was chosen for the acceptability threshold. The AASHTO Specifications for Condition (2) is

$$w_c = (0.75) \times (0.017 \text{ in.}) = 0.0128 \text{ in.} \tag{3-13}$$

where w_c is the maximum width of a crack. Therefore, the acceptability threshold for this project was set at 0.0128 inches.

3.8 Parametric and Optimization Analyses

To create a starting point for bridge geometries to be studied in this project, a simple optimization program was created using Microsoft Excel. The program incorporated the AASHTO criteria detailed in Section 3.5. This section describes the way the spreadsheet optimization program was created and the obtained results.

3.8.1 Optimization Problem

Optimization analyses were formulated and conducted at the section level in order to identify possible improvements to the basic design concept of a composite steel box girder component and also to conduct parametric studies. The optimization analysis was conducted using the nonlinear quadratic solver of Microsoft Excel. The section being investigated is shown in Figure 20 and a view of the system using a beam-line analysis assumption is shown in Figure 21. The problem at hand is to find the best combination of dimensions for the girder represented in Figure 20 such that cost is minimized.

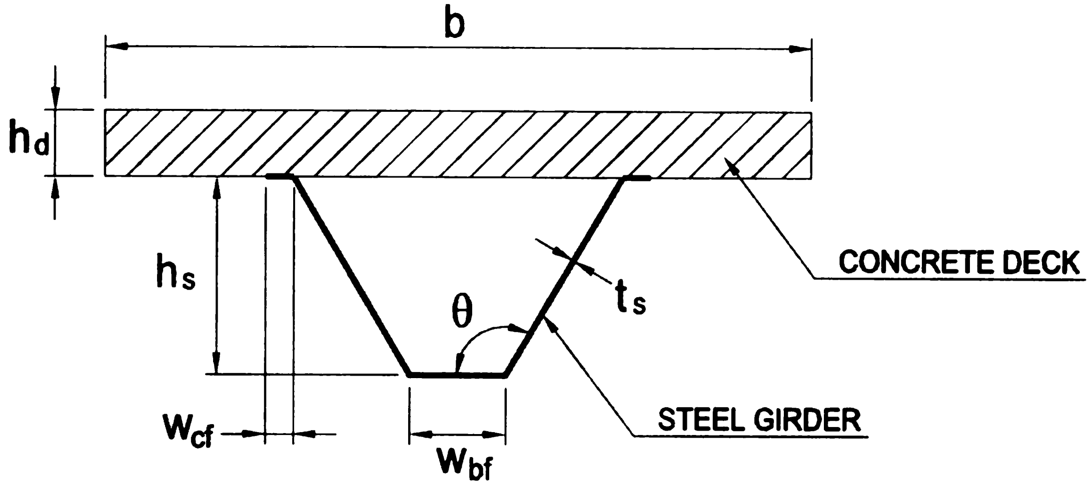

Figure 20. Composite Steel Box Girder Cross-Sectional Geometry

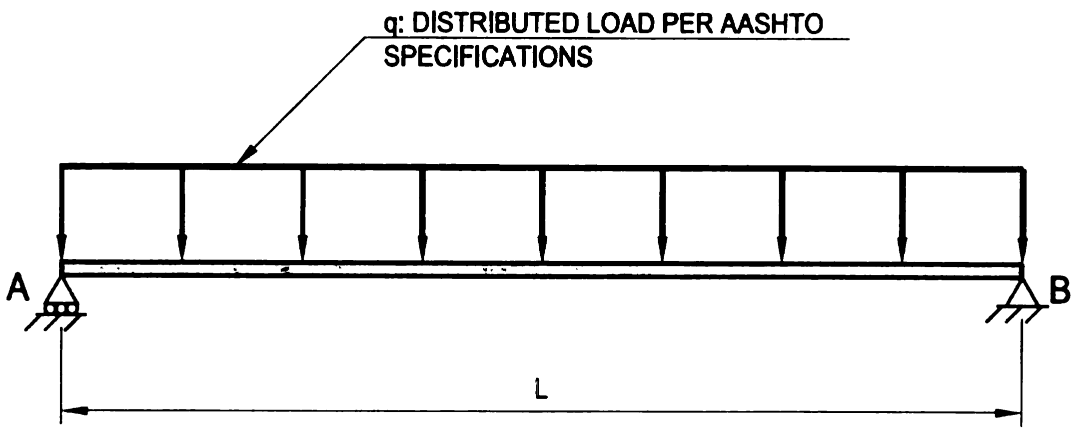

Figure 21. Bridge System Profile under Beam-Line Analysis Assumption

3.8.2 Problem Formulation

Optimization algorithms are numerical methods that allow selection of structural or material parameters for maximum efficiency through an objective function that measures the "goodness" or "efficiency" of a structural design. The objective function is defined by design variables, which are parameters that change during the design process.

Design variables can be continuous or discrete depending on whether they can take values from a continuum or are limited to a set of values. The optimization process is then to improve the goodness of the design by automated changes in the design variables. Optimization processes are generally performed with some limits that restrict the choice of a design. Such limits are called constraints and usually include performance criteria. Optimization algorithms are thus a general and versatile technique for optimal structural design.

An optimization problem is typically defined in standard mathematical terms as:

Objective: Minimize $f(x)$

Subject to: $g_i(x) \le 0$ i = 1 to m

$h_j(x) = 0$ j = 1 to p

$X^L \le x \le X^U$

where x is the design variables vector, X^L and X^U, are the lower and upper bound vectors of the design variables, $f(x)$ is the objective function, and g_i(x) and h_i(x) are the equality and inequality constraints, respectively.

As far as the component geometry being sought, the design variables are obviously chosen as the dimensions of the different components that govern the cross section of the girder component. The selection of the objective function depends on the application. For example, the objective for the current problem could be to maximize

st
im
op

th
mi
op
fo
se
by

stiffness, maximize strength or minimize cost. Finally, the constraints are used to implement design limits such as maximum stresses and displacements to achieve an optimum result.

1) Objective Function. The basis for determining the optimal section was that the section was the least expensive. Consequently, the objective function was to minimize the cross-sectional area of the steel tub-girder. The area of steel used in this optimization was not the area per girder, but rather the area of all the girders required to form a three lane bridge (the bridge width can easily be modified, as noted in subsequent sections). In this way, the individual section is not being optimized, but instead the bridge as a whole is being considered.

2) Independent Variables. The independent variables are the variables that are changed by the solver in order to reach the optimal result. The bridge optimization problem used six independent variables to optimize the section. These variables and their corresponding labels in Figure 20 were:

- Deck Width, b
- Steel Plate Thickness, t_s
- Compression Flange Width, w_{cf}
- Tension Flange Width, w_{bf}
- Web Angle of Inclination, θ
- Steel Section Depth, h_s

3) Parameters. Parameters constitute those values in the design that do not change during the optimization process. The parameters included in the current analyses and their values were:

- Deck Height, h_d = 9 in.
- Concrete Compressive Strength, f'_c = 6 ksi
- Concrete Modulus of Elasticity, E_c = 4,415 ksi
- Steel Yield Strength, f_y = 36 ksi
- Steel Modulus of Elasticity, E_s =29,000 ksi

4) Constraints. When changing the independent variables, limits must be set in order to ensure the optimal solution is a feasible design. The constraints to the independent variable were as shown below:

- 48 in. $\leq b \leq$ 96 in.
- 0.179 in. $\leq t_s \leq$ 0.375 in. (7 ga. – 3/8" plate)
- 4 in. $\leq w_{cf} \leq$ 6 in.
- 10 in. $\leq w_{bf} \leq$ 24 in.
- $60^{\circ} \leq q \leq 76^{\circ}$
- 12 in. $\leq h_s \leq$ 54 in.

Other constraints related to design values were also incorporated, namely:

- Moment Capacity > Nominal Moment
- Steel Section Width < Slab Width
- Enforce Compactness (AASHTO Eq. 6.10.4.1.2-1)

3.8.3 Implementation

The final step in the optimization is to create a set of dependent variables that will change based on the changes made to the independent variables. As presented in Section 3.5, the nominal moment was calculated per the AASHTO LRFD Bridge Design Specifications (AASHTO, 1998). The moment demand per bridge girder component was based on Service II limit state requirements. The loads considered in the analysis were dead load, vehicular live load, and a dynamic load allowance. Distribution factors were calculated based on the AASHTO-LRFD recommendations.

Lastly, the desired span, L, and number of lanes, N_L, was specified. These were constant for a single run of the optimizer, but are user defined in order to find optimal sections for varying bridge lengths and widths.

3.8.4 Results

Because of the high number of variables, there are many local minima in the problem space and the gradient-based search algorithm in Excel easily gets "stuck" in local minima. Therefore, the solution found is highly dependent on the starting values of the independent variables. A table of results returned by the optimizer with the reduced number of variables is shown in Table 4. As mentioned above, Excel has trouble with finding local minima. Therefore, in order to achieve a solution, some of the values were given a specific starting point in order to arrive at reasonable values.

3.4.5 Discussion

The following trends were observed in the data:

- The optimization algorithm seems to always choose the largest available deck width.
- Steeper web angles improve moment capacity.
- The section geometry generally causes the plastic neutral axis to be located in the slab, eliminating compression forces in the steel.
- Acceptable geometries were found for spans ranging between 20'-100', while spans greater than 100' were not investigated.
- Spans ranging from 20' to 40' had identical results, implying that the lower bounds on some of the independent variables were set too high.

Table 4. Sample Results from Cross-Section Optimization Analyses

Parameter	Symbol	Units	Span			
			40'	**50'**	**60'**	**70'**
Deck width (spacing)	*b*	in.	96	96	96	96
Plate thickness	*ts*	in.	0.234	0.268	0.289	0.309
Compression Flange Width	*wcf*	in.	4.0	4.0	4.0	4.0
Bottom Flange Width	*wbf*	in.	10.0	12.0	13.4	14.7
Angle (web-to-horizontal)	*q*	degrees	76.0	76.0	76.0	76.0
Steel depth	*hs*	in.	19.8	27.4	31.6	35.6
Total Steel Area:	*As*	**sq in.**	**68.8**	**102.5**	**125.1**	**148.2**
Parameter	**Symbol**	**Units**	**Span**			
			80'	**90'**	**100'**	
Deck width (spacing)	*b*	in.	96	96	96	
Plate thickness	*ts*	in.	0.327	0.344	0.361	
Compression Flange Width	*wcf*	in.	4.0	4.0	4.0	
Bottom Flange Width	*wbf*	in.	15.9	17.1	18.5	
Angle (web-to-horizontal)	*q*	degrees	76.0	76.0	76.0	
Steel depth	*hs*	in.	39.3	42.8	46.1	
Total Steel Area:	*As*	**sq in.**	**171.8**	**195.4**	**219.4**	

It should also be noted that steel is not available in arbitrary thicknesses or widths. Thus, the results found here would have to be increased to the next available standard size, which could impact the cost of the system. As increasing the steel thickness always results in an increase in moment capacity, the section will not become inadequate when the steel thickness is increased.

4. CONCEPT EVALUATION

4.1 Flexural Performance of Con-Struct Bridge System

Due to MSU's involvement with this MDOT project, the University was approached by Nelson Engineering Services to evaluate the flexural capacity of two scale units of their Con-Struct system, which is the concept that motivated the present investigation. This testing project, while separate from the MDOT research, has given the author an excellent opportunity to experimentally evaluate the prefabricated steel box systems under consideration. With the permission of Nelson Engineering Services (hereafter referred to as NES), an overview of the testing conducted and the evaluation of the results and concept follow.

Two three-point bending tests were conducted on small-scale prototypes of the Con-Struct bridge girder system with cast-in-place and precast decks. The test units were designed by NES and also built under their direction. The test beams were small-scale replicas of the full-scale sections of the Con-Struct system used by NES in field applications. A typical cross section of the low-profile steel-concrete composite box girder section is shown in Figure 22. The steel plate used for the test unit was a lightweight 7-gage steel sheeting unit. The test units were manufactured so that they had an effective span of 12 ft with the beam ends encased on a concrete block for support purposes and laminated elastomeric pads were used between the test unit and support blocks. The overall geometry of the cast-in-place and precast deck test units are shown in Figure 23 and Figure 24, respectively. These drawings and the specifications outlined in them were provided by NES for manufacturing purposes. Overall views of the test setup are shown in Figure 25.

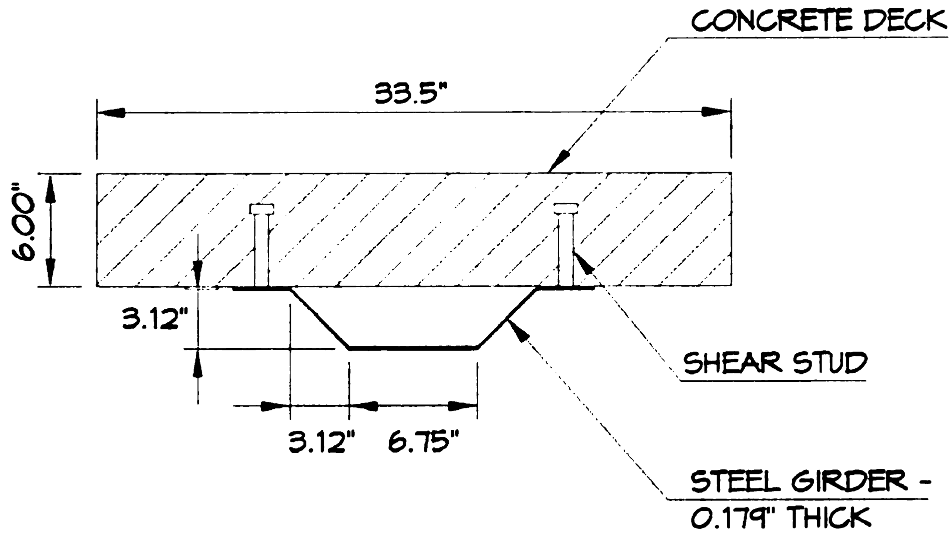

Figure 22. Typical Cross-Section of Con-Struct Test Units (Nelson, 2006)

The flexural tests showed that the overall behavior of the low profile composite box girder system is reliable and that it can effectively exceed the nominal flexural capacity determined according to current AASHTO specifications. As shown in Figure 26, the ultimate moment capacity of the section was found to be 106 kip-ft, while the AASHTO capacity was 80 kip-ft. The yield point shown in Figure 26 was found using strain gauges on the steel girder (see inset). Overall, the performance of both the cast-in-place and precast composite girders was essentially equal, hence the precast results are not presented here. In both cases, their ultimate capacity was limited by detailing of the deck system to effectively carry the longitudinal shear demands.

For the cast-in-place unit the force transfer at the shear connectors introduced longitudinal shear demands in the concrete deck that exceeded the shear strength of the concrete element. In the case of the precast unit, the lack of longitudinal shear keys to transfer shear forces across the joints of the precast panels composite the deck led to the deterioration of the beam load carrying mechanism. In both cases, the failure modes are clearly undesired, but they are not believed to compromise the overall efficiency of the concept as these problems can be easily addressed. Improved performance of the cast-in-place deck can be achieved by better assessment of the forces imposed by the shear connectors and by providing appropriate deck reinforcement to arrest the development of longitudinal shear cracks. Improvements in the precast system can be easily achieved by providing well detailed transverse shear keys to the precast panels. Integration of both of these detailing aspects will undoubtedly improve the performance of the Con-Struct system at ultimate conditions. Clearly, this also applies to the generic prefabricated steel box girder systems being investigated in this project.

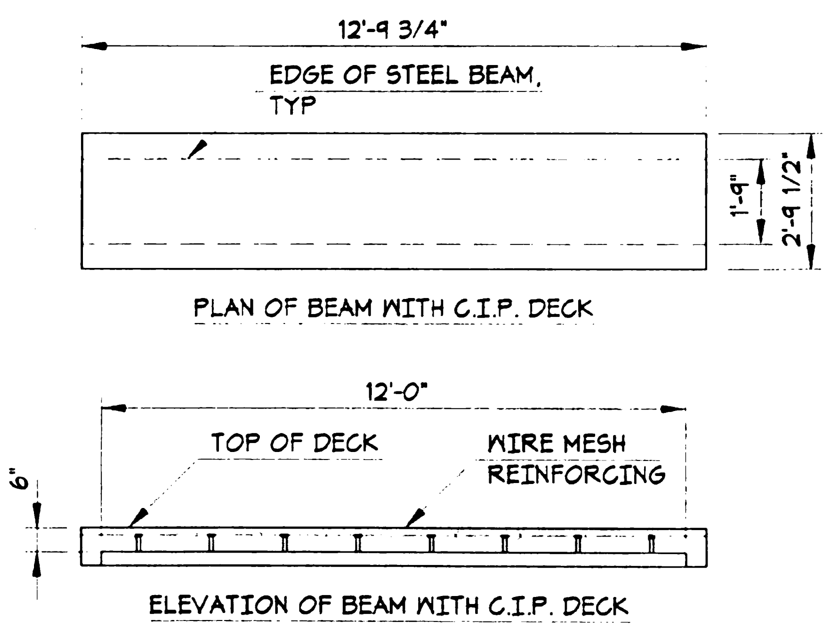

Figure 23. Test Unit with Cast-in-Place Concrete Deck (Nelson, 2006)

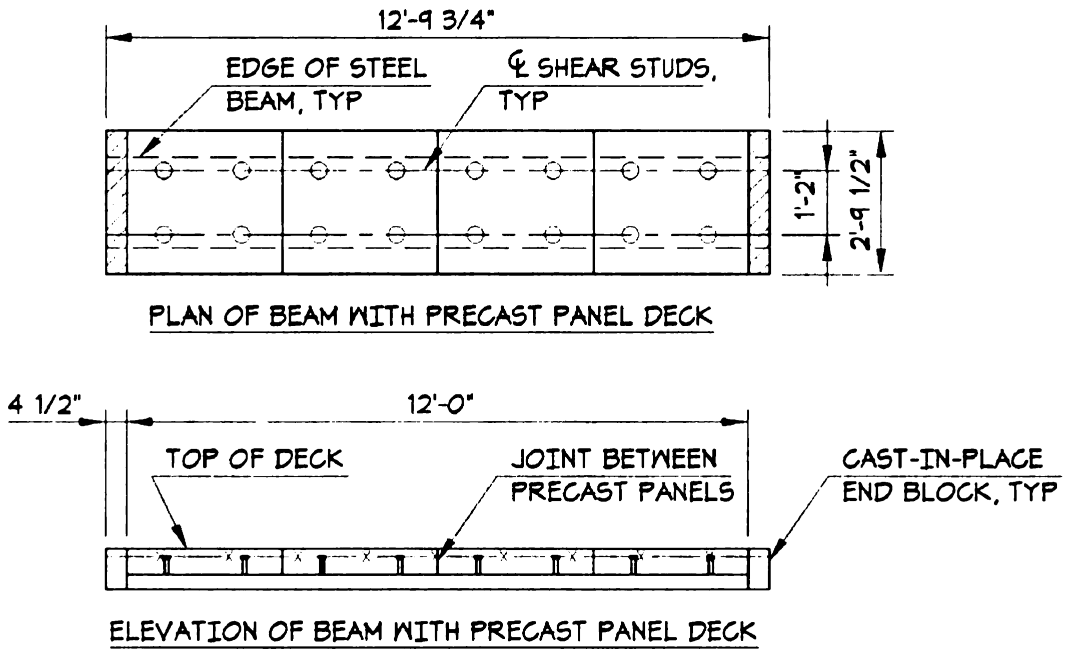

Figure 24. Test Unit with Precast Concrete Deck System (Nelson, 2006)

This space intentionally left blank

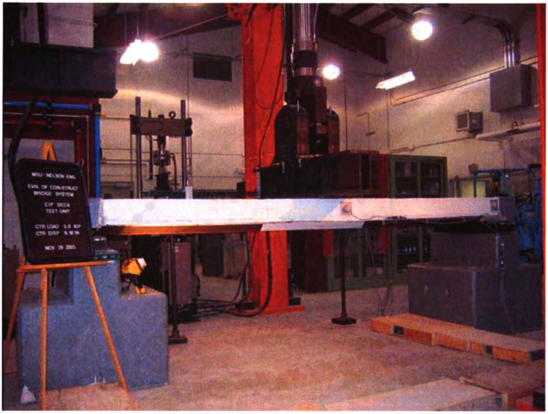

a) Overview

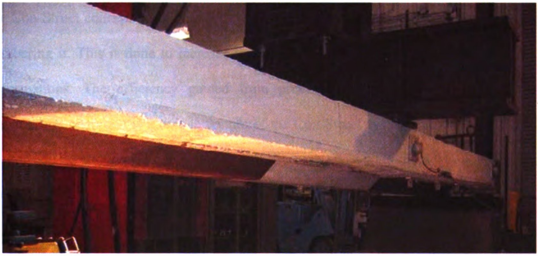

b) Underside View

Figure 25. General Test Setup Views – C.I.P. Test Unit

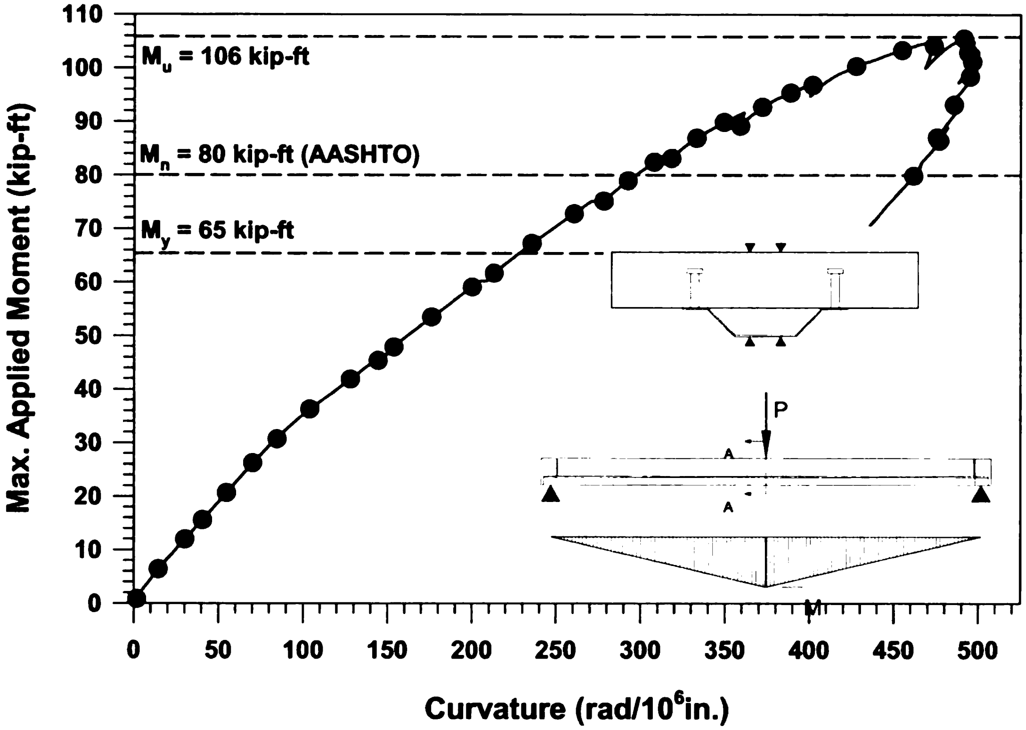

Figure 26. Moment vs. Curvature Response of C.I.P. Test Unit at Mid-Span

In addition to the use of a shallow cold-bent steel profile for the composite beam, the Con-Struct concept introduces prestressing to the steel beam during construction by cambering it. This is done to increase the yield moment capacity and offset dead load deformations. The efficiency gained from prestressing the steel plate during the construction operation is a unique feature of the Con-Struct system and one that should be considered for the general goals of this research project. It should be recognized, however, that the prestressing effect is really beneficial only up to the onset of yield in the critical section response for the system. Thus, benefits are to be gained while satisfying serviceability stress limits. Gains in ultimate strength will be minor since at full plastification of the steel section ultimate section capacity is more heavily controlled by the effective lever arm between tensile and compression forces and the location of the

plastic neutral axis. In addition, consideration should be given to the "longevity" of the prestressing benefits since creep effects in the concrete slab and stress relaxation of the prestressed steel plate will most likely reduce the initial stress conditions.

The experimental study also permitted evaluating the applicability of code guidelines to assess the capacity of composite sections and showed that the shallow composite girder system can be well predicted by conventional theory of steel-concrete composite structures.

4.2 Concept Evaluation and Selection

Based on the literature review (see Chapter 2), one goal of this task was to preliminarily evaluate prefabricated composite steel box systems to explore their advantages, disadvantages, possible improvements, and the development of new similar concepts.

Another goal of this task was to perform a preliminary study that would identify three to five concepts with high potential that would become the focus of this research project. All concepts are to be evaluated under a common set of structural, construction, and durability requirements. A ranking method was used to assess their potential.

With reference to Figure 1 and based on what has been learned thus far from the literature review presented in Chapter 2, a list of design alternatives based on permutations of different features can be generated. The variable parameters were the type of steel plate, the type of concrete deck, and the type of longtiduinal deck joint. The different options for each of these variables are listed next.

A) Steel Plate. From the literature review, the author believes that the inverted steel box solution will not be as effective as its developers envision. Thus, only the use of a "right-side-up" steel box will be considered. Four types of steel tub-plates will be considered based on their method of construction and implementation:

1) Pressed-formed or cold-bent – unstressed
2) Shop-welded – unstressed
3) Pressed-formed or cold-bent – prestressed
4) Shop-welded – prestressed

B) Concrete Deck. The literature review has shown advantages and disadvantages for different types of concrete decks and different solutions have been adopted for the prefabricated steel box systems proposed thus far. As such, the following *prefabricated* deck options, based on their construction method, will be considered as options:

1) Cast-in-place at shop/yard
2) Modular precast made continuous with passive wet longitudinal joints at shop/yard
3) Modular precast made continuous with passive wet longitudinal joints at shop/yard and prestressed at shop/yard before making composite with steel girder.
4) Hybrid – precast stay-in-place form with exposed reinforcement for a cast-in-place topping and closure pour at job site.

C) Longitudinal Deck Connection. As shown by the literature review, this detail is the one that presents the most options. Based on the design alternatives presented in

Section 2.7, the following are considered viable options for the system under consideration:

1) Grouted female-to-female shear keys
2) Grouted tongue-and-groove shear keys
3) Reinforced (confined or unconfined) shear keys blocks
4) Reinforced (confined or unconfined) female-to-female shear keys
5) Post-tensioned grouted female-to-female shear keys
6) Post-tensioned grouted tongue-and-groove shear keys
7) Welded plate grouted shear key blocks
8) Reinforced grouted moment key blocks
9) Post-tensioned grouted female-to-female moment keys
10) Post-tensioned grouted tongue-and-groove moment keys

In order to evaluate the potential design concepts that could develop from the various permutations of the different design options, a common set of performance criteria was used. The criteria is aimed at *qualitatively* ranking the performance of the individual design options listed above, i.e., steel plate, deck, and transverse deck connections, based on the judgment of the author. In addition, each of the criteria was assigned a weighting factor of importance on a scale of 1 to 3 with 1 being low, 2 being medium and 3 being high. The criteria and their weighting factors are given in Table 5.

Each of the design options was given a score for each of the criteria on a scale of 1 to 5, where 1 represented the lowest mark and 5 the highest. The tabulated results for each of the system components are presented in Table 6. The last column in this table shows the total "score" of the bridge component after factoring the score in each category by the importance factors in Table 5. The highest scores for each of the design components are shown in bold font.

Table 5. Design Parameter Selection Criteria and Importance Factor

Criteria ID	Description	Importance Factor
A	Cost Efficiency	3
B	Structural Efficiency	2
C	Design Versatility	1
D	Design/Analysis Ease	1
E	Construction Ease	3
F	Fatigue Performance	3
G	Durability & Corrosion Resistance	3
H	Replacement/Removal Ease	2

* Importance Factor: 1 = Low; 2 = Medium; 3 = High

This space intentionally left blank

Table 6. Scoring and Ranking of Design Options

Design Option	Criteria*								Score
Plate	**A**	**B**	**C**	**D**	**E**	**F**	**G**	**H**	
1	5	3	2	5	5	5			**58**
2	3	4	4	4	2	2			37
3	5	3.5	2.5	5	4.5	5			**58**
4	3	4.5	4.5	4	2	2			38.5
Deck	**A**	**B**	**C**	**D**	**E**	**F**	**G**	**H**	
1	5	4	4	5	4		3	3	**59**
2	4	4	3	4	5		3.5	3	**58.5**
3	3	5	4	3	4		4	2	54
4	3	4	3	2	3		3	3	46
Deck Connection	**A**	**B**	**C**	**D**	**E**	**F**	**G**	**H**	
1	5	2	2	5	5	5	5	5	**81**
2	5	2	2	5	4.5	5	5	5	**79.5**
3	4	3	3	4	4	4	3	4	66
4	4	3	3	4	4	4	3	4	66
5	3	4	4	3	3	5	4	3	66
6	3	4	4	3	2.5	5	4	3	64.5
7	3.5	3	3.5	3	4	2	3	4	58
8	3	3	3.5	4	4.5	4	3	4	65
9	2.5	4.5	4.5	2	3	5	4	3	65
10	2.5	4.5	4.5	2	2.5	5	4	3	63.5

*Evaluation: 1 = Low to 5 = High

5. ANALYTICAL EVALUATION

5.1 General

The objective of the analytical evaluation is to develop a suite of hierarchical finite element models to investigate issues related to structural performance, with particular attention to connection detailing and design. The different levels of model refinement supported each other to investigate system performance. The conducted analyses were:

A) **Stress Analysis of Bridge Component and System.** 3D finite element analyses of component and system to evaluate detailed performance of the prefabricated element.

B) **Global Parametric Analysis.** 3D finite element analyses of bridge systems to perform system parametric studies.

C) **Stress Analysis and Characterization of Connection Details.** 3D finite element analyses of connection details.

5.2. Stress Analysis of Bridge Components and System

The original goal of the research was to use 3D skeletal-type (frame element) models to perform system parametric studies to evaluate the need for any intermediate diaphragms and the load transfer demand and performance of deck connections. The use of full 3D finite element models was not considered appropriate for the parametric studies due to their computational expense and effort to develop. Thus, grillage models were initially envisioned for these studies. Despite this, both model types were created to evaluate their performance and decide which method to use. This section presents the development of both model types and a comparison of their performance.

For an initial check of compatibility between the grillage and 3-D FE models, simple plate models were created and moment responses were compared. To begin this comparison, two sets of models were created. One set of models were square plates, while the other set were rectangular plates with sides at a 2:1 ratio. Two loading conditions were considered. The first was a distributed load over the entire plate, while the second was a point load at the center of the plate. The bending moment distribution of each model was then compared in three different ways: at mid-span under both distributed and concentrated loads, and its transverse distribution under the concentrated load. The results of this comparison indicated a sufficient agreement between the two methods to move to a more sophisticated comparison. A graphical representation of the results can be seen in Appendix I. It should be noted that the loads and dimensions were arbitrarily chosen and that the results were normalized for clearer presentation. After this simple verification, the two modeling approaches were then applied to actual bridge models under consideration and compared.

5.2.1 Model Bridge Geometry

The bridge chosen for modeling was a two-lane bridge with a 50-ft span. It consisted of five girder/deck units, as shown in Figure 27. The geometry of the girder/deck units was developed by making use of the Excel optimization spreadsheet detailed in Section 3.8. However, the purpose of this exercise was not to find an optimum design, but rather to compare the two analysis models (i.e., grillage vs. 3D FE). The geometry of the girder/deck units used in the comparison is shown in Figure 18.

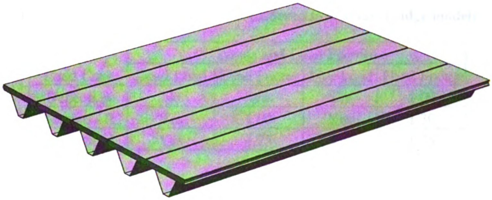

Figure 27. Bridge being modeled for analysis approach comparison

5.2.2 Model Bridge Loading

Loading for the bridge models was chosen according to the AASHTO LRFD Bridge Design Specifications [AASHTO, 1998]. Dead load and vehicular live load were considered. Dead load consisted of self-weight and barrier weight. The cross section of the barrier was that of a New Jersey Concrete Barrier as specified by the Federal Highway Administration (FHWA) [FHWA, 2006]. The vehicular live load consisted of the design lane load and the design truck load with an axle spacing of 14-ft (see Figure 17). Three different AASHTO limit states were evaluated, namely, live-load deflection, Service-II, and Strength-I. A summary of the limit states and associated loads and load factors is given in Table 7.

Table 7. Summary of limit states considered to evaluate bridge models

Load Case	Loads and Load Factors			
	Dead Load	Load Factor	Live Load	Load Factor
Deflection	No	n/a	Yes	1.00
Service - II	Yes	1.00	Yes	1.30
Strength - I	Yes	1.25	Yes	1.75

5.2.3 Grillage Model

A grillage model is a means of representing a structure with a series of beam elements that have been given properties appropriate for representing the stiffness, torsion and unit weight properties of the structure being modeled. Grillage models reduce the number of required elements and degrees of freedom, thereby reducing the number of equations that need to be solved to evaluate system response. Grillage models can be 2D or 3D. For this project a two-dimensional grillage model was created and analyzed, as detailed in this section.

5.2.3.1 Derivation of Grillage Member Properties

The grillage model followed the recommendations presented in Hambly (1991) and Barker and Puckett (1997). To completely capture the behavior of the bridge, several sections were chosen for grillage members to represent the bridge as shown in Figure 28.

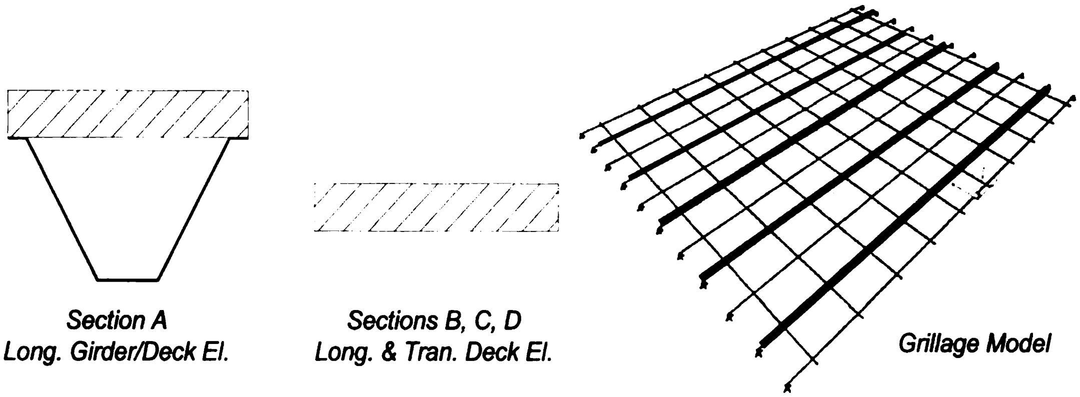

Figure 28. Schematic of grillage element cross-sections and grillage model

The longitudinal section representing the girder/deck units (see Figure 28) was termed section A. The section moment of inertia, I, was calculated for a section in which the concrete deck had been transformed to an equivalent width of steel using the modular ratio of the two materials. The torsion constant, J, was also calculated for a transformed section, but instead of changing the width, the height was modified. Then, the torsion constant for a thin walled hollow section was determined with equation (5-1) (Hambly, 1991)

$$J_t = \frac{4A^2}{\oint \frac{ds}{t}} \tag{5-1}$$

where A is the area enclosed by the center line of the walls, ds is the length of each individual wall and t is the wall thickness. This value is known as the pure torsion constant, or J_t. However, due to local deformations of the open box section, the pure torsion constant is not valid. Thus, an equivalent torsion constant that accounts for distortion, J_d, must also be found (Hambly, 1991). The process to obtain J_d follows.

The flexural rigidity of the individual sides of the box (see Figure 29) is obtained by applying equation (5-2) [Hambly, 1991]

$$D_a = \frac{E_a t_a^3}{12(1-\nu_a^{\ 2})} \tag{5-2}$$

where D is the flexural rigidity, E_a is the elastic modulus, t_a is the wall thickness and ν_a is Poisson's ratio; and the subscript a refers to side a (see Figure 29).

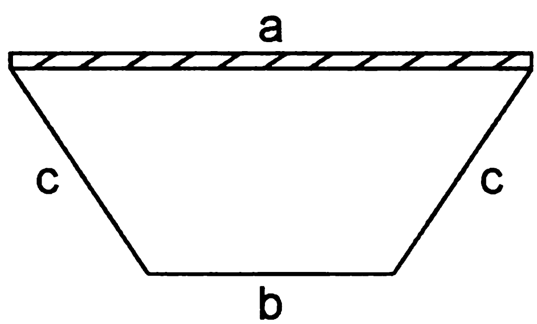

Figure 29. Nomenclature of box sides

After calculating the flexural rigidity of each side with equation (5-2) above, the out-of-plane shear in the bottom flange per unit torsional load, v, is given by equation (5-3) [Hambly, 1991]

$$v = \frac{\frac{1}{D_c}\left[(2a+b)abc\right] + \frac{1}{D_a}\left[ba^3\right]}{(a+b)\left[\frac{a^3}{D_a} + \frac{2c}{D_c}(a^2+ab+b^2) + \frac{b^3}{D_b}\right]} \tag{5-3}$$

where D_a, D_b and D_c and a, b and c are the flexural rigidities and the lengths of the walls in Figure 29, respectively.

Once v is calculated, the vertical deflection of one web per unit torsional load, δ_l, is given by equation (5-4) below:

$$\delta_1 = \frac{ab}{24(a+b)}\left\{\frac{c}{D_c}\left[\frac{2ab}{a+b} - v(2a+b)\right] + \frac{a^2}{D_a}\left[\frac{b}{a+b} - v\right]\right\}. \quad (5\text{-}4)$$

Next, a parameter, β, used in the analysis of beams-on-elastic-foundations (BEF), the theory from which the previous equations were derived, is calculated as shown in equation (5-5) [Hambly, 1991]

$$\beta = \left\{\frac{1}{EI_c\delta_1}\right\}^{0.25} \quad (5\text{-}5)$$

where I_c is the moment of inertia of the box girder cross-section.

Next a dimensionless distortion-induced deflection term, w, is obtained from a chart presented in Hambly (1991) and reproduced in Figure 30. For this example w was found to be equal to 1.0.

The final formula to find J_d is given in Equation (5-6) below:

$$J_d = \frac{a^2}{l^2}\frac{I_c(\beta l)^3}{1.6w} \quad (5\text{-}6)$$

The values of J_t and J_d are then combined to give the value of J used for the grillage member, J_{dt}, as shown in equation (5-7) [Hambly, 1991]. For further information and references on this method, the reader is referred Chapter 6.5 of Hambly (1991).

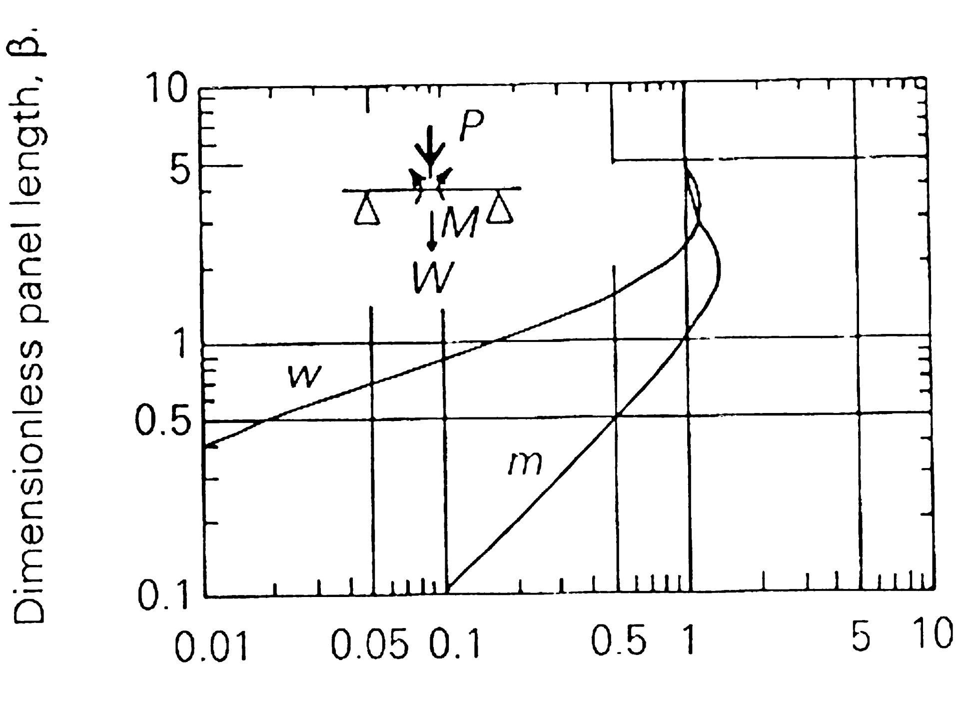

$$w = \frac{8EI_b\beta^3}{P} W \qquad m = \frac{4\beta}{P} M$$

Figure 30. Chart for distortion deflection parameter w for simply supported beams and box without cross-bracing or diaphragms (Hambly, 1991)

The final properties of the longitudinal girder/deck members are shown in Figure 31.

$$\frac{1}{J_{dt}} = \frac{1}{J_d} + \frac{1}{J_t}. \tag{5-7}$$

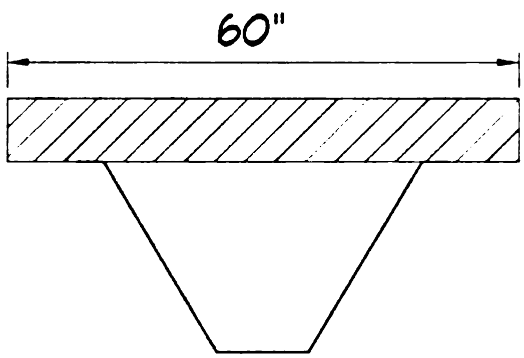

<u>Grillage Properties</u>

A = 85.9 in^2

E = 29,000 ksi

I = 10,598 in^4

J = 1,349 in^4

Figure 31. Section A geometry and associated grillage properties

Longitudinal deck elements of different widths were also included in the model to improve its accuracy. Sections B and C and their properties are given in Figure 32. The moment of inertia for these elements was found with equation (5-8) [Barker, 1997]:

$$I = \frac{bh^3}{12}. \tag{5-8}$$

The torsional constant was taken as twice the moment of inertia [Barker, 1997], or

$$J = \frac{bh^3}{6} \tag{5-9}$$

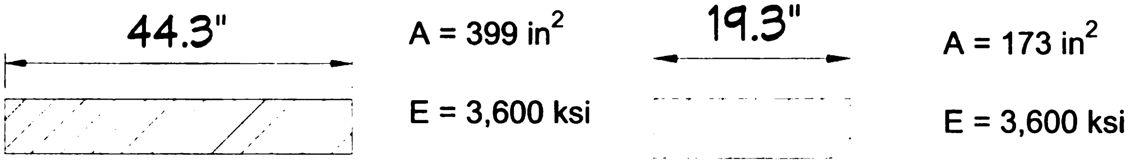

Figure 32. Section B and C geometry and associated grillage properties

Transverse grillage members represented the concrete deck. All transverse elements had the same cross section, which was labeled section D. Their properties were found in the same manner as for sections B and C, resulting in the values shown in Figure 33. Because the weight of the concrete deck was already included in the weight of the longitudinal members, the transverse deck elements were not assigned any self-weight. A summary of the properties for the grillage members is given in Table 8.

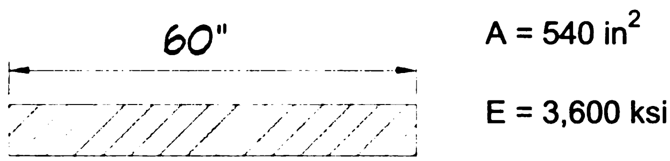

Figure 33. Section D geometry and associated grillage properties

Table 8. Summary of grillage member properties

Section Name	Description	Area (sq.in.)	Elastic Modulus (ksi)	Moment of Inertia (in.^4)	Torsion Constant (in.^4)
A	Long. Box Section	85.9	29,000	10,598	1,349
B	Long. Deck Section	399	3,600	2,693	5,385
C	Long. Deck Edge Section	173	3,600	1,346	2,693
D	Transverse Deck Section	540	3,600	3,645	7,290

5.2.3.2 Application of Loads

Vehicular lane load was applied by defining a tributary width for each longitudinal member and applying a distributed load of appropriate magnitude along the length of the member. Applying the concentrated truck loads required the determination of equivalent loads and moments to be applied to the existing members due to the tire locations not corresponding with the location of the grillage members. This was accomplished by creating a separate model of two beams intersecting at the location of the tire load and fixed at their ends, which coincided with points on the grillage model mesh. The truck load was applied at the intersection of the beams and the reaction forces (fixed-end forces) at the endpoints were obtained. These forces were then applied at their corresponding location on the master model. This approach is schematically shown in Figure 34. The grillage model was created and computed with the general finite element program SAP2000 (CSI, 2000). A figure of the completed grillage model, as well as its transverse moment response under the described loading, is shown in Figure 35. A discussion of the results and their comparison with those from a finite element continuum model is provided is Section 5.2.5.

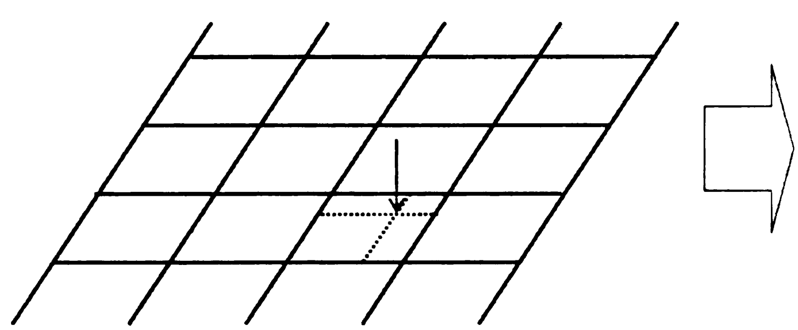

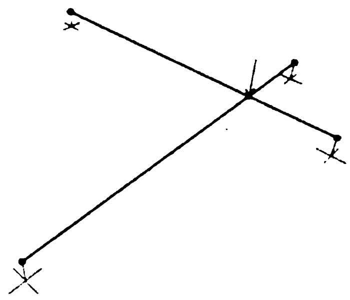

Figure 34. Application of wheel loads to grillage model

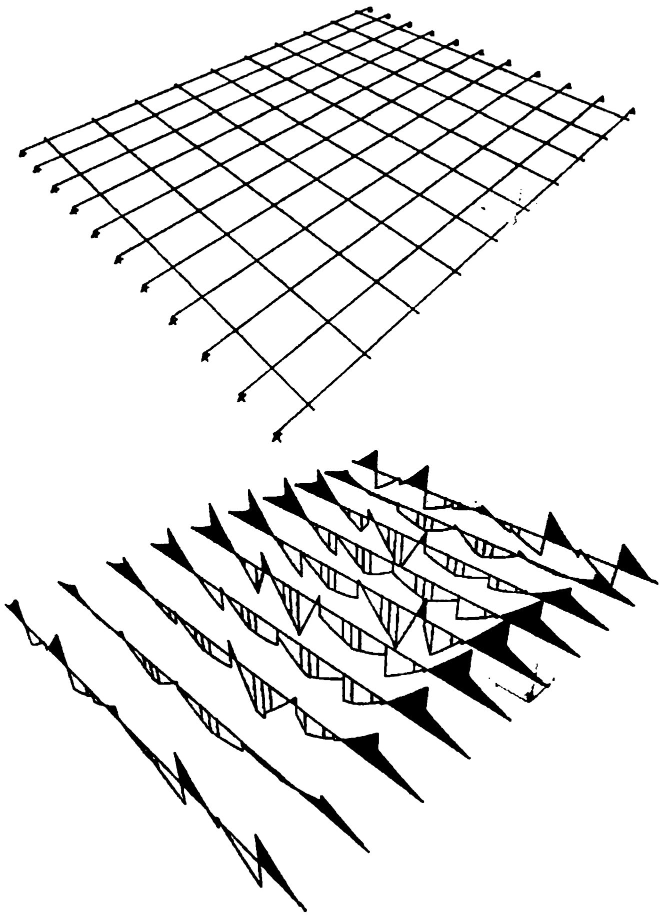

Figure 35. Completed grillage model and system transverse moment response

5.2.4 Three-Dimensional Finite Element Model

The 3-D finite element model was created completely of 4-noded shell elements (S4R, [Simulia, 2007]) – both deck and girder. The deck elements were positioned at the neutral axis of the actual deck to match the grillage model. The modeled geometry of the typical girder/deck unit is shown in Figure 36.

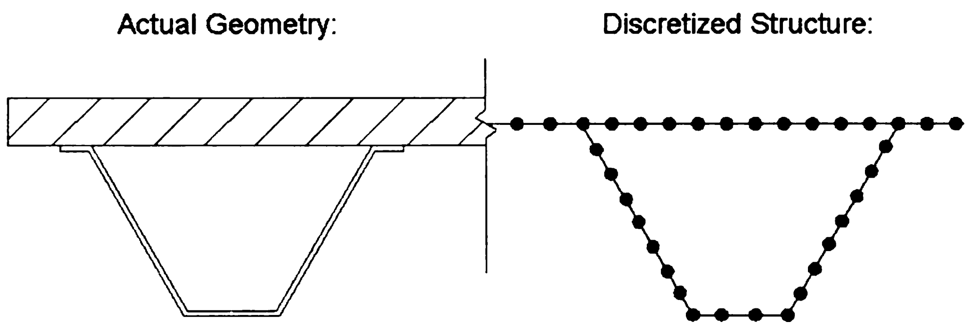

Figure 36. Girder modification in 3-D FEA model

In this analysis the deck is modeled as one continuous slab. This assumes full moment transfer at the joints, which may not be representative of actual behavior, depending on the type of joints that are used. However, because the same is true of the grillage model, this was not a problem for comparing the two modeling approaches. Yet, it is recognized that future models will need to address this issue (See Section 5.4). Also, the model assumes full shear interaction, meaning there is no relative slip between the deck and the girders which again is compatible with the grillage analysis. The completed 3-D FEA model and von Mises stress contours on the underside of the bridge can be seen in Figure 37.

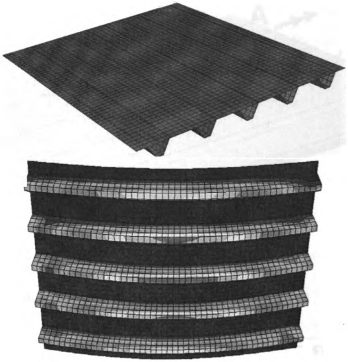

Figure 37. Completed 3-D FEA model and von Mises stress contours

5.2.5 Comparison of Models

The grillage and continuum models were first compared with only the design lane load applied. The response quantities chosen for comparison were the transverse moment forces along a line coincident with what would potentially be a longitudinal joint between girder units, as shown in Figure 38. The transverse moment demand for both strength and service conditions along line A-A (see Figure 38) is shown in Figure 39. It can be seen that the finite element response is smoother than the grillage output, which is to be expected due to the finer resolution of the nodes in comparison with grillage intersections. However, the models are considered to compare favorably. All other joint lines were also checked, and the results compared similarly.

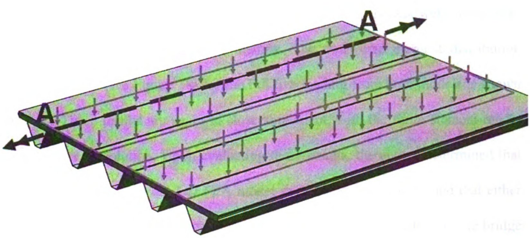

Figure 38. Location of forces chosen for comparison

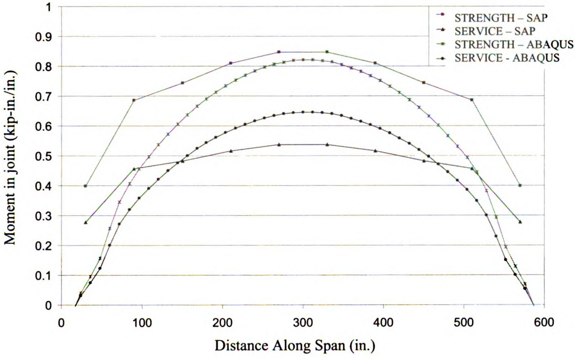

Figure 39. Comparison of analysis tools on full scale bridge model (lane load only)

After the initial verification had been established, both models were updated to incorporate the AASHTO design truck loading. The transverse moment distribution along joint line A-A (see Figure 38) for the full live loading from both models is shown in Figure 40. These results are again in close agreement, with the finite element model showing a greater resolution. Upon evaluating these results, the author determined that both the grillage model and the 3-D FEA model gave coinciding results, and that either could provide accurate representation of the forces in the joints, as well as in the bridge system as a whole. It follows that either model could be used for parametric studies of the system. While the original research plan was to use the grillage model for parametric studies due to its low computational demand, running the 3-D FEA model only took 1-2 minutes longer than running the grillage model. Yet, as noted in the comparison of results, the FEA model provides better resolution. Additionally, the FEA models were easier to create due to the use of the program's (Simulia, 2007) graphical user interface. For these reasons, the author decided to supersede the grillage model and use 3-D continuum FEA models with shell elements not only for the detailed analyses, but for parametric studies as well.

This space intentionally left blank

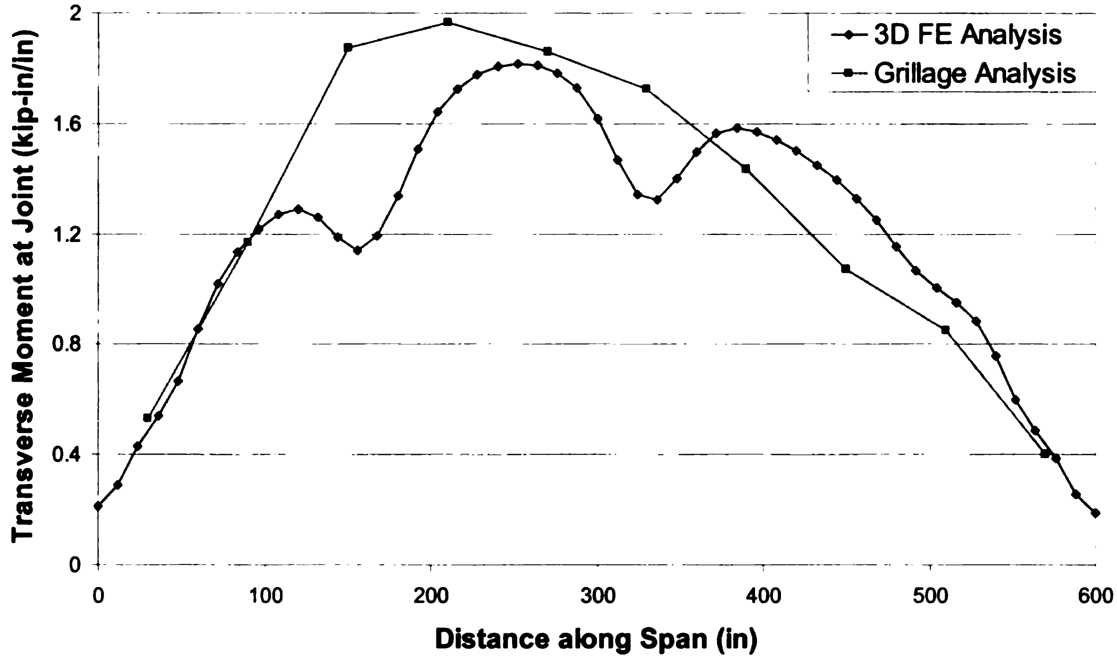

Figure 40. Comparison of analysis tools (full AASHTO loading)

5.2.6 Verification of Models Using Experimental Data

As detailed in Section 4.1, previous research performed by the author provided experimental data that directly correlated to the system being studied (Burgueño and Pavlich, 2006). Hence, this data could be used to verify that the models of the box-girder system were producing results that match what happens in experimental situations. General information on the Con-Struct test units and the conducted experiments was given in Section 4.1 and complete information can be found in (Burgueño and Pavlich, 2006).

In the aforementioned project, a prototype of the Con-Struct System – the concept that motivated the present study – was tested at Michigan State University's Civil Infrastructure Laboratory. The cross-section dimensions of the Con-Struct test girder are shown in Figure 22.

The test setup for the experimental testing program is shown in Figure 41. The test was a simple three point bending test on a girder with a span of 12 ft. Continuous displacement and applied load measurements were recorded during the test. The displacements were measured at the girder mid-span by linear potentiometers. The applied load was measured with a load cell in the actuator.

The load displacement response from the girder with a cast-in-place deck is shown in Figure 42. From the graph it can be seen that the maximum applied load achieved during the test was approximately 35 kips. The maximum displacement of the 12 ft girder was approximately 2 inches. The response can be separated into two portions, an assumed linear portion, and a non-linear portion. The linear of the portion is assumed, as it is not perfectly linear. This assumed linear portion of the response is from a load of 0 kips up to a load of 12.5 kips. The 12.5 kip point was chosen as the end of the linear portion because after this point the slope of the load displacement response in each of the successive load increments has a different, smaller slope. Between loads of 0 and 12.5 kips the slope remains approximately constant. It is this pseudo-linear portion of the response that was to be modeled using a full 3D finite element model.

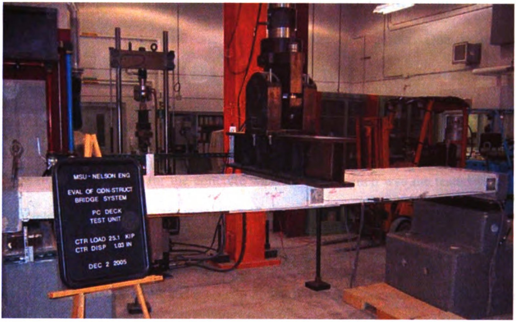

Figure 41. Experimental Test Setup

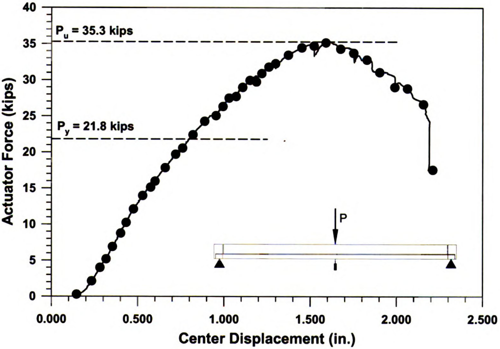

Figure 42. Experimental Load Displacement Response of Cast-in-Place Con-Struct System

The 3D FE model of the Con-Struct system was generated by creating two parts: one representing the deck, and one representing the steel girder. Due to its thin dimensions, the tub was modeled with shell elements. The deck was modeled with solid elements. Details are shown in Table 9. The dimensions of the modeled girder matched exactly with the dimensions of the actual girder (see Figure 22 and Figure 23). The modulus of elasticity used for the concrete was 4576 ksi, which was the tested value of the concrete used in the experiment based on uniaxial break tests of specimens taken at the time of casting. Properties for the concrete and steel are given in Table 10.

The 3D model also utilized a no-slip constraint at the concrete-steel interface i.e., full shear interaction. This assumption is considered adequate to assess service performance of composite steel box bridge systems. Nonetheless, since failure in the tested cast-in-place Con-Struct beam units (see Section 4.1) was controlled by the shear interaction, incorporation of partial shear interaction between the surfaces of the concrete deck and the top steel flanges through ABAQUS's contact and surface interaction modeling options might be considered for future modeling efforts. As this type of failure was not directly applicable to the system being studied, it was ignored in this project. The 3D model can be seen in Figure 43. A general view of the displacement contours on the developed 3D finite element model is shown in Figure 44.

Table 9. Elements Used in Con-Struct 3D FE Model

Part	Material	Shell Thickness (in)	Element Type	Hourglass Control	Reduced Integration	Element Size (in)
Deck	Concrete	n/a	C3D8R	Active	Active	4.5
Tub	Steel	0.375	S4R	Active	Active	6

Table 10. Material Properties used in 3D FE model

Material	Elastic Modulus (ksi)	Poisson's Ratio	Unit Weight (kips/in^3)
Concrete	4,576	0.2	8.68 E-5
Steel	29,000	0.3	2.83 E-4

Figure 43. Assembled 3D Model

Figure 44. Finite Element Model of Con-Struct System in Flexure.
(Contours Represent Vertical Displacement)

Comparative results of the load displacement response are shown in Figure 45. This plot shows the assumed linear range of the experimental data only, to appropriately compare with the linear elastic FE model. The nonlinear behavior of the system was not of interest in this project and thus no effort was spent trying to calibrate an FE model with the nonlinear experimental data.

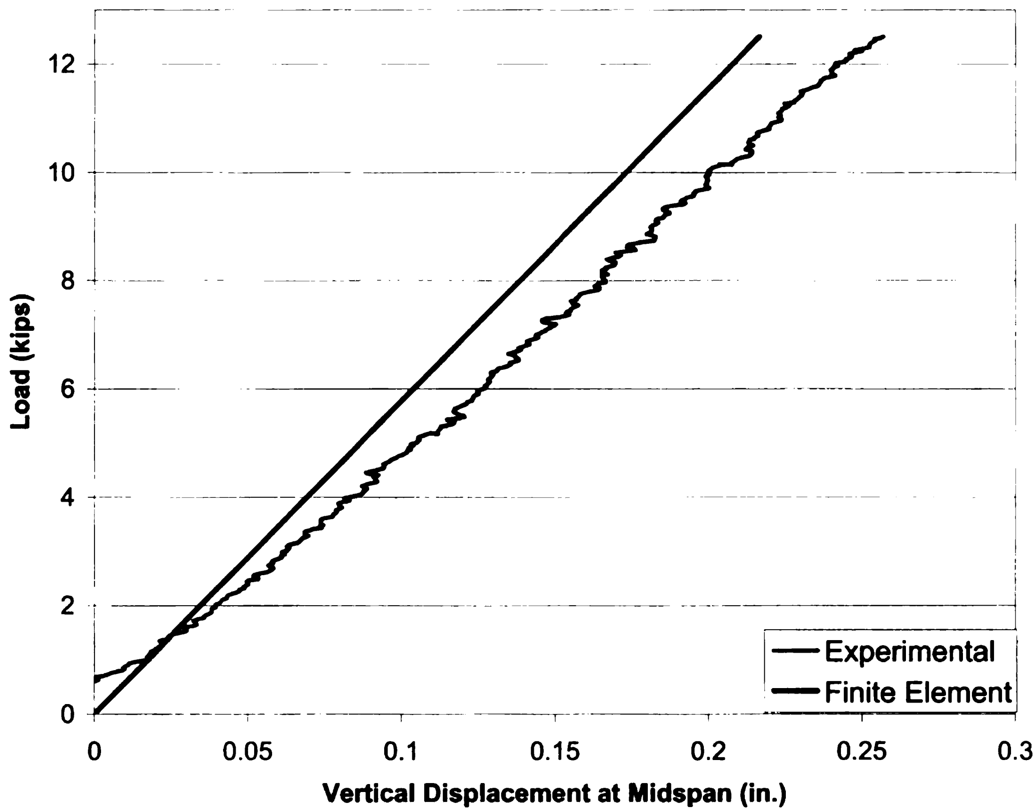

Figure 45. Load Displacement Results of Experimental Model vs. FE Model

The experimental data in Figure 45 has been shifted to correct for nonlinearities at the beginning of the loading, such as settlement of the elastomer pads at supports as well as settling of the loading element. The shift was calibrated so that the two sets of data would be at the same value of displacement when the load was one kip. From the figure it is possible to see that the results from the FE model were stiffer than the experiment. The maximum displacement value of the FE model was 0.216 inches, while the experimental model had a maximum displacement of 0.256 inches. This could be attributed to further settlement and/or compression of the end supports, and slip at the girder/deck interface. Additionally, it is well known that the finite element method typically gives results that are stiffer than reality. However, the present study cannot fully clarify which, if any of the listed effects are causing the slight discrepancy.

5.3 Global Parametric Analysis

To evaluate the behavior of feasible bridge systems built with the prefabricated girder/deck units under consideration, a parametric study was performed. In the study, the parameters under evaluation were: (1) span length, (2) girder spacing, and (3) existence/location of intermediate diaphragms. The proposed case matrix for the parametric studies is given in Table 11. All the bridges studied carried two design lanes of traffic, with one design truck in each (See Section 3.3). The material properties and limit states can be found in Sections 3.2 and 3.4, respectively.

The study was performed in order to investigate three separate responses: (1) transverse load distribution, (2) transverse moment demands along longitudinal joints, and (3) longitudinal moment demands along longitudinal joints. These responses of interest are schematically shown in Figure 46.

This space intentionally left blank

Table 11. Case Matrix for Global Parametric Analyses

Case #	Span Length (ft)	Girder Spacing (ft)	Diaphragm
1	50	4	None
2	50	6	None
3	50	8	None
4	75	6	None
5	75	6	1/2 pt
6	75	8	1/2 pt
7	100	6	None
8	100	6	1/3 pts
9	100	8	None
10	100	8	1/3 pts
11	100	10	None
12	100	10	1/2, 1/4pts

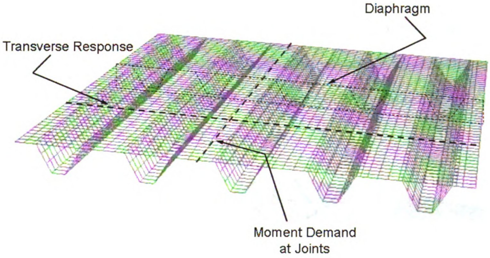

Figure 46. Response measures of interest in parametric studies

A parameter of interest not included in the above cases is the type of longitudinal joint used in a given bridge. While joint types will certainly influence system behavior, they are not included in the parametric studies because modeling of their behavior is difficult and computationally expensive. Thus, the author chose to study the effect of joint type and behavior through a reduced set of selective case studies (see Section 5.4). The parametric studies will then focus on overall behavior assuming that full moment continuity has been achieved through the longitudinal joint.

5.3.1 Creation of 3D FE Models

To improve computational efficiency, the models generated in the matrix shown in Table 11 were created using shell elements. More specifically, the ABAQUS (Simulia, 2007) element S4R was used. This is defined by ABAQUS as "a 4-node doubly curved thin or thick shell, [with] reduced integration, hourglass control, [and] finite membrane strains". In addition, the deck was considered to be one continuous slab. This assumption can be considered valid if it can be shown that the longitudinal joints can be held closed under service loads by a reasonable amount of prestressing. This check is performed in Section 5.4. A sample bridge model can be seen in Figure 47.

Figure 47. Typical Bridge Model Using Shell Elements

As seen in Figure 47, the bridge models have end-blocks, and some models (see Table 11), such as the model in the figure, have diaphragms. The end-blocks were modeled with shell elements, and were assigned a thickness of 24 inches. The material used was concrete. The diaphragms were also modeled using shell elements. They were made of steel, and assigned a thickness of 0.5 inches. Steel was chosen for the diaphragms to reduce weight. However, concrete diaphragms could also be used in practice. The end-blocks were then simply supported, creating the boundary conditions for the bridge. The sizes of the different elements vary. The original element size was 6 inches for deck and girder elements. End-block and diaphragm responses were not being studied, and consequently they were composed of a coarser 12 inch mesh. However, after running some analyses it was found that the deck and end-block meshes needed to be as fine or finer than the girder mesh to prevent the girders from passing through the deck and end-blocks. Therefore, the mesh size of the deck and end-block elements was reduced to 4 inches. The final selection of elements is detailed in Table 12.

Table 12. Element Data for Parametric Models with Shell Deck Elements

Part	Material	Shell Thickness (in)	Element Type	Hourglass Control	Reduced Integration	Element Size (in)
Deck	Concrete	9	S4R	Active	Active	4
Tub	Steel	0.375	S4R	Active	Active	12
Diaphragm	Steel	0.5	S4R	Active	Active	4
End Block	Concrete	24	S4R	Active	Active	4

5.3.2 Selection of Model Geometries

In order to obtain realistic and usable geometries for the sample bridges used in the parametric study, the initial dimensions were selected by making use of the Excel spreadsheet developed for preliminary system analysis (see Section 3.8). The combinations of span and spacing defined in Table 11 were entered into the optimization spreadsheet, and the preliminary dimensions that were obtained have been listed in Table 13. These models were then created and analyzed using ABAQUS. The results of these analyses were then compared against AASHTO specifications for midspan deflection and maximum tub stress to check their feasibility. This comparison can be found in Table 14.

Table 13. Original Geometries Used for Models in Parametric Study

Model No.	Span/Spacing		Diaphragm	Section Depth (in)	Equivalent Depth (in)	Tension Flange (in)	Compression Flange (in)	Number of Girders	Spacing (in)
1	50'	4'	none	19.5	24	10	4	12	47
2		6'	none	20.5	25	10	4	8	70.5
3		8'	none	21.5	26	10	4	6	94
4	75'	6'	none	31.5	36	13	4	8	70.5
5		6'	1/2 pt.	31.5	36	13	4	8	70.5
6		8'	1/2 pt.	33	37.5	13.5	4	6	94
7	100'	6'	none	41.5	46	16.5	4	8	70.5
8		6'	1/3 pt.	41.5	46	16.5	4	8	70.5
9		8'	none	43.5	48	17.5	4	6	94
10		8'	1/3 pt.	43.5	48	17.5	4	6	94
11		10'	none	45.5	50	20	4	5	112.8
12		10'	1/4,1/2 pt.	45.5	50	20	4	5	112.8

This space intentionally left blank

Table 14. Results of ABAQUS Analysis on Original Geometries

Model No.	Span/Spacing		Results (ABAQUS) Max. Tub Stress (ksi)	Results (ABAQUS) Midspan Deflection (in)	Predicted (Excel) Max. Tub Stress (ksi)	Predicted (Excel) Midspan Deflection (in)	AASHTO Limits Max. Tub Stress (ksi)	AASHTO Limits Midspan Deflection (in)
1	50'	4'	23.5	0.695	19.7	0.728	50	0.750
2		6'	31.1	0.861	25	0.718	50	0.750
3		8'	35.2	1.95	30	0.722	50	0.750
4	75'	6'	33.8	1.44	27.7	1.11	50	1.125
5		6'	32.3	1.22	27.7	1.11	50	1.125
6		8'	38.1	1.34	32.8	1.10	50	1.125
7	100'	6'	32.1	1.66	29.4	1.48	50	1.500
8		6'	29.3	1.56	29.4	1.48	50	1.500
9		8'	34.8	1.84	34.3	1.46	50	1.500
10		8'	32.2	1.73	34.3	1.46	50	1.500
11		10'	42.6	1.84	35.8	1.36	50	1.500
12		10'	39.2	1.69	35.8	1.36	50	1.500

As Table 14 indicates, many of the geometries obtained by using the spreadsheet optimization were inadequate, despite incorporation of the AASHTO criteria into the spreadsheet. This could be due to several things, but the most likely cause, as determined by the author, is an inability of the AASHTO distribution factors to accurately model the true load distribution. The reason for skepticism toward these distribution factors is their inherent vagueness – the same equation is used for both shear and bending for interior and exterior beams. In addition, the only factors considered are number of lanes and number of beams. These observations seem to indicate that minimal time has been spent developing distribution factors for the system being studied here, and this is reflected in their inaccuracies, as observed in this study.

To make the parametric study more practical, the bridges were redesigned so that they would meet the AASHTO criteria for stress and for deflection. In addition, for the 75-ft span and the 100-ft span models a "standard geometry" was chosen to be used for several different bridge models. This was done in order to show that a single girder geometry could have the versatility to be used in a variety of situations. The updated geometries are shown in Table 15, and the corresponding system responses are shown in Table 16.

Table 15. Modified Geometries to Meet AASHTO Specifications

Model No.	Span/Spacing		Diaphragm	Section Depth (in)	Equivalent Depth (in)	Tension Flange (in)	Compression Flange (in)	Number of Girders	Spacing (in)
1	50'	4'	none	19.5	24	10	4	12	47
2		6'	none	23	27.5	10	4	8	70.5
3		8'	none	26	30.5	12	4	6	94
4	75'	6'	none	36	40.5	13	4	8	70.5
5		6'	1/2 pt.	36	40.5	13	4	8	70.5
6		8'	1/2 pt.	36	40.5	13.5	4	6	94
7	100'	6'	none	44	48.5	16.5	4	8	70.5
8		6'	1/3 pt.	44	48.5	16.5	4	8	70.5
9		8'	none	50	54.5	17.5	4	6	94
10		8'	1/3 pt.	50	54.5	17.5	4	6	94
11		10'	none	50	54.5	18.5	4	5	112.8
12		10'	1/4,1/2 pt.	50	54.5	18.5	4	5	112.8

Table 16. Results of ABAQUS Analysis on Modified Geometries

Model No.	Span/Spacing		Results (ABAQUS) Max. Tub Stress (ksi)	Results (ABAQUS) Midspan Deflection (in)	AASHTO Limits Max. Tub Stress (ksi)	AASHTO Limits Midspan Deflection (in)
1	50'	4'	23.2	0.667	50	0.750
2		6'	26.9	0.670	50	0.750
3		8'	26.9	0.635	50	0.750
4	75'	6'	27.5	0.951	50	1.125
5		6'	30.2	0.857	50	1.125
6		8'	34.8	1.07	50	1.125
7	100'	6'	29.5	1.45	50	1.500
8		6'	26.8	1.38	50	1.500
9		8'	28.5	1.28	50	1.500
10		8'	28.8	1.12	50	1.500
11		10'	36.3	1.48	50	1.500
12		10'	34.8	1.32	50	1.500

5.3.3 System Response

Once it had been verified that the models for the study fit within AASHTO parameters for stress and deflection, the response at the joints was analyzed. Specifically, the three responses investigated were: transverse moment response along a transverse path across the bridge, transverse moment response along a theoretical longitudinal joint, and longitudinal moment response along a theoretical longitudinal joint (see Figure 46). A graphical representation of these responses for individual bridges, as well as a depiction of measurement locations, can be found in Appendices II-XIII. The vertical lines in these plots represent the location of the tires from the design truck(s). The paths were chosen by selecting a line passing through the areas of the deck with the highest magnitude of the moment under consideration (located under the design truck tires). For a visual representation of the system response, see Figure 48 and Figure 49.

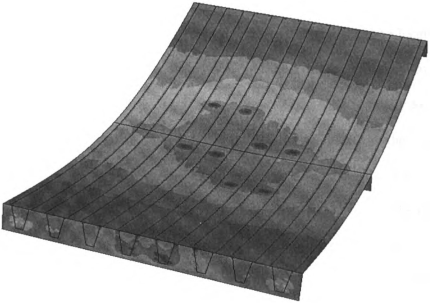

Figure 48. Typical Deformed Shape and Moment Distribution. (Contours Represent Longitudinal Moment)

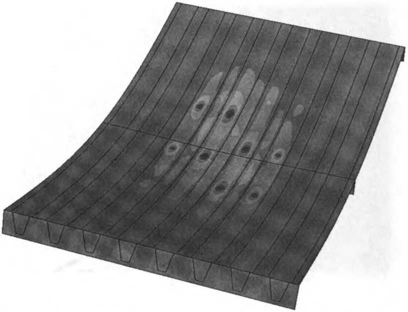

Figure 49. Typical Deformed Shape and Moment Distribution. (Contours Represent Transverse Moment)

To display the system responses graphically, a number of plots were generated which show system response over a specified path. These paths were chosen to show the most extreme forces that would be experienced by the bridge. The location of the paths varied slightly from model to model, and thus all paths are shown in the Appendices. In addition, Figure 50 shows where these paths were typically found.

While the plots of individual bridges have been relegated to the Appendices, several comparisons between models will be provided here. First the data for the 50' span bridge models are shown in Figure 51, Figure 52, and Figure 53. The data for the 75' span bridge models are shown in Figure 54, Figure 55, and Figure 56. Finally, the data for the 100' span bridge models are shown in Figure 57, Figure 58, and Figure 59.

A summary of the forces represented in Figure 51-Figure 59 is shown below in Table 17.

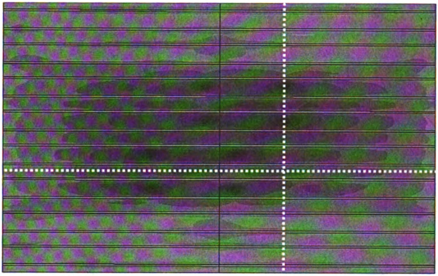

a) Plan View

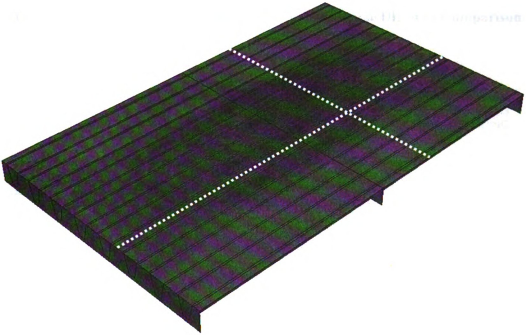

b) Isometric View

Figure 50. Typical Location of Paths.
(Contours Represent Transverse Moment)

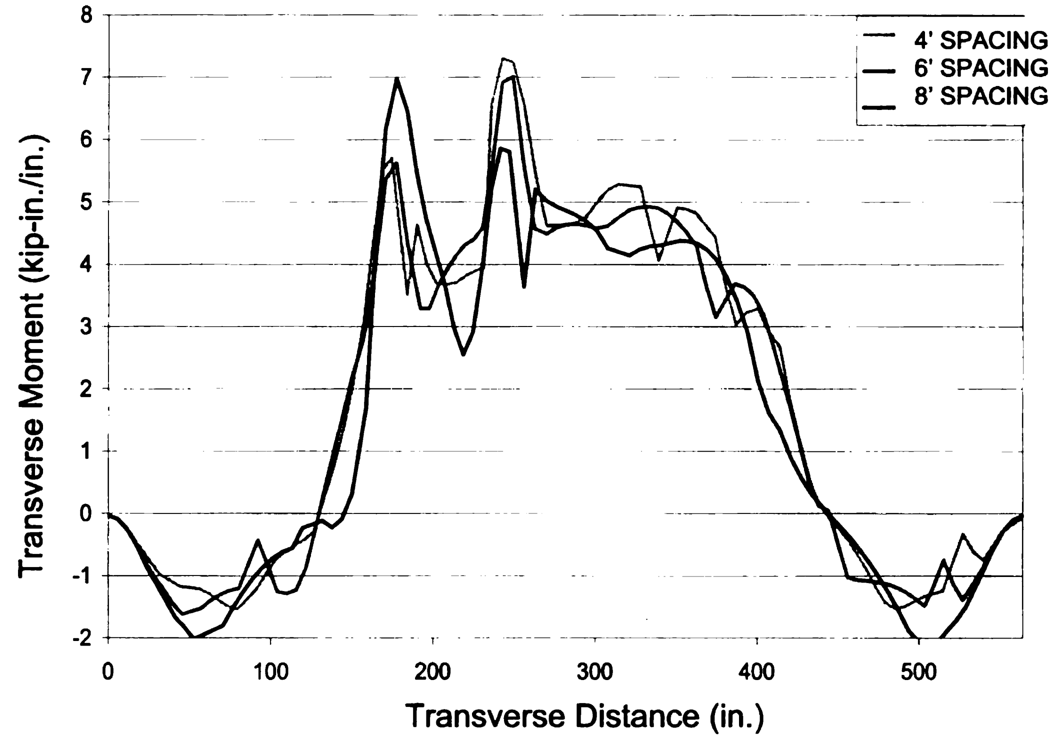

Figure 51. 50' Span: Transverse Moment v. Transverse Distance Comparison

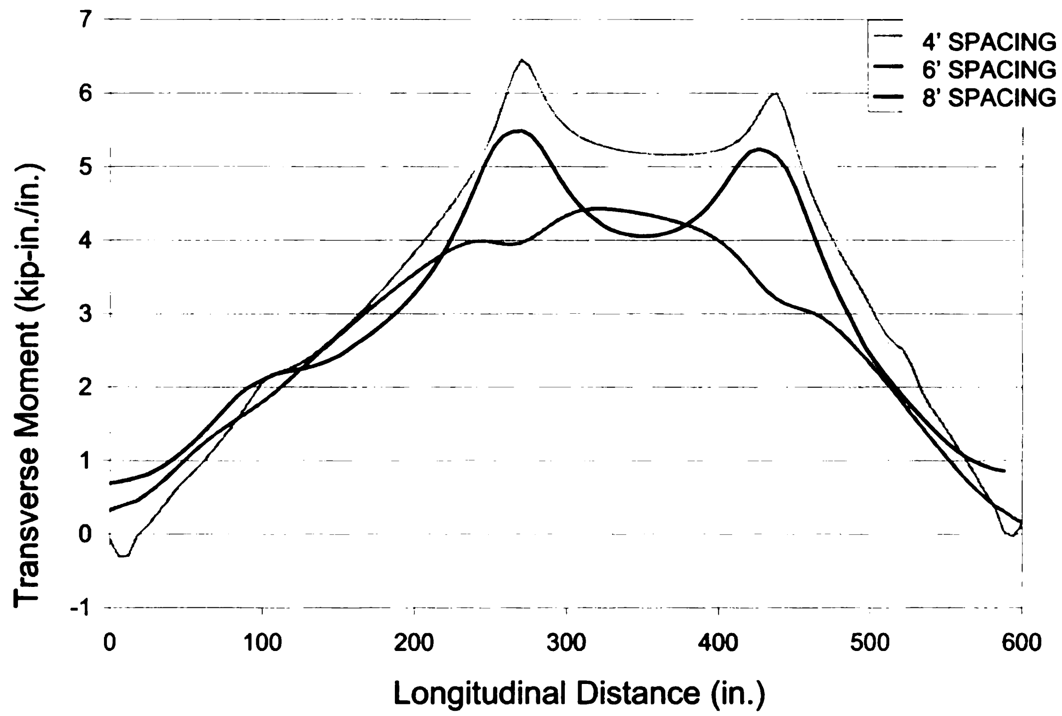

Figure 52. 50' Span: Transverse Moment v. Longitudinal Distance Comparison

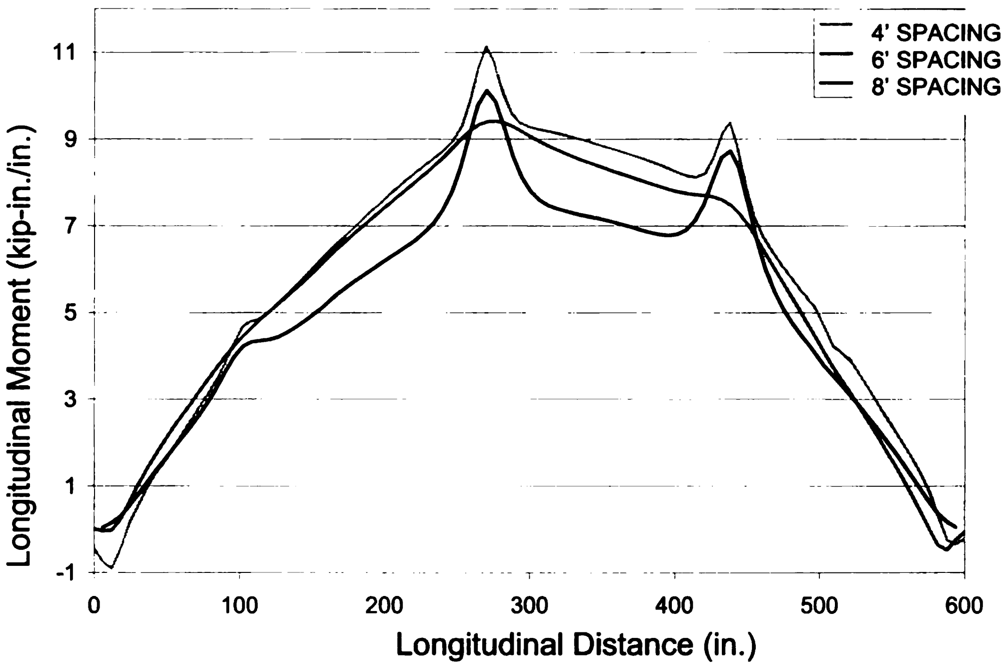

Figure 53. 50' Span: Longitudinal Moment v. Longitudinal Distance Comparison

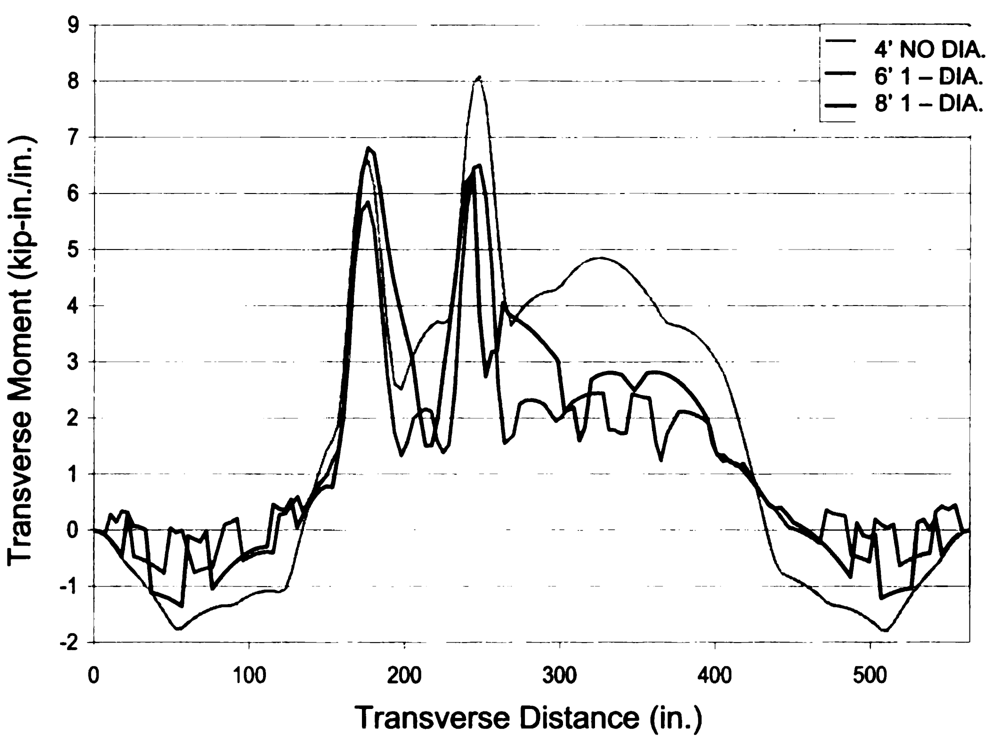

Figure 54. 75' Span: Transverse Moment v. Transverse Distance Comparison

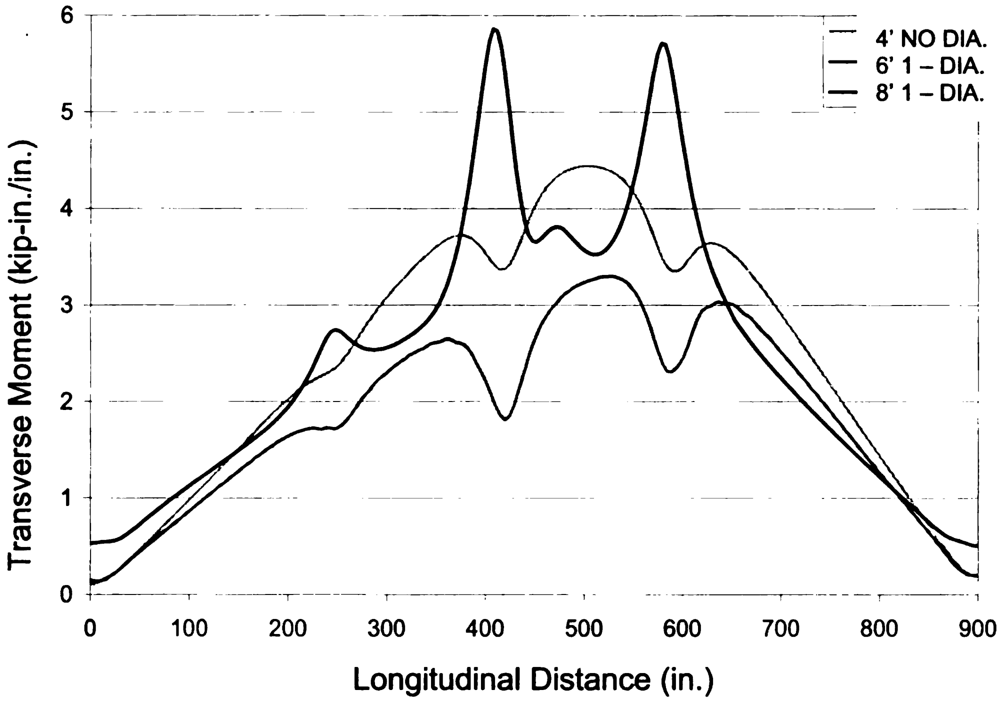

Figure 55. 75' Span: Transverse Moment v. Longitudinal Distance Comparison

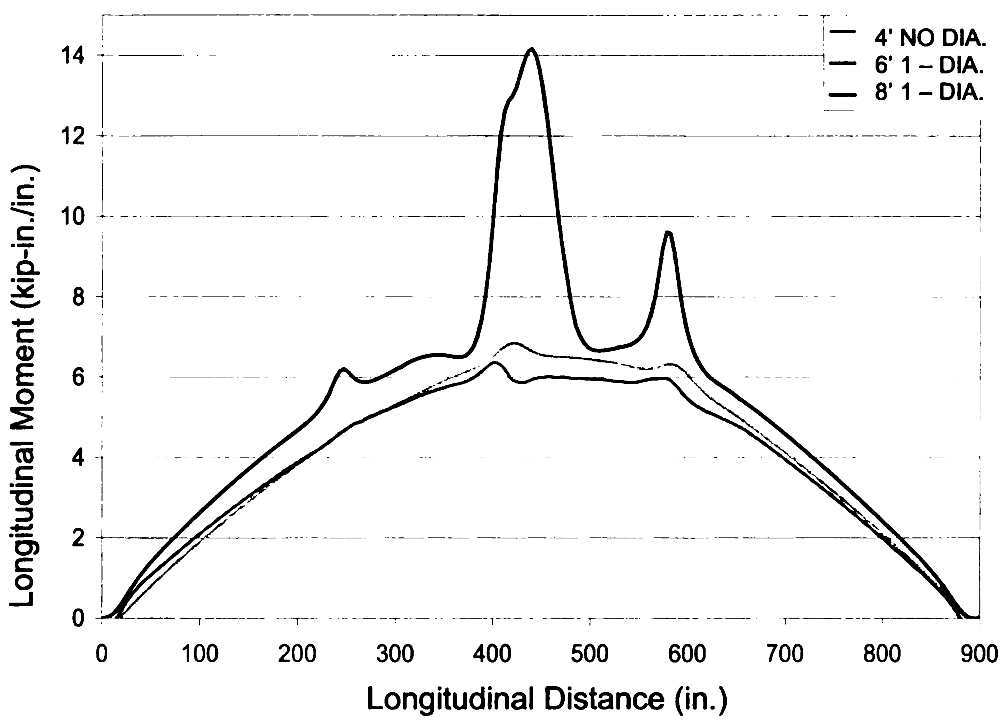

Figure 56. 75' Span: Longitudinal Moment v. Longitudinal Distance Comparison

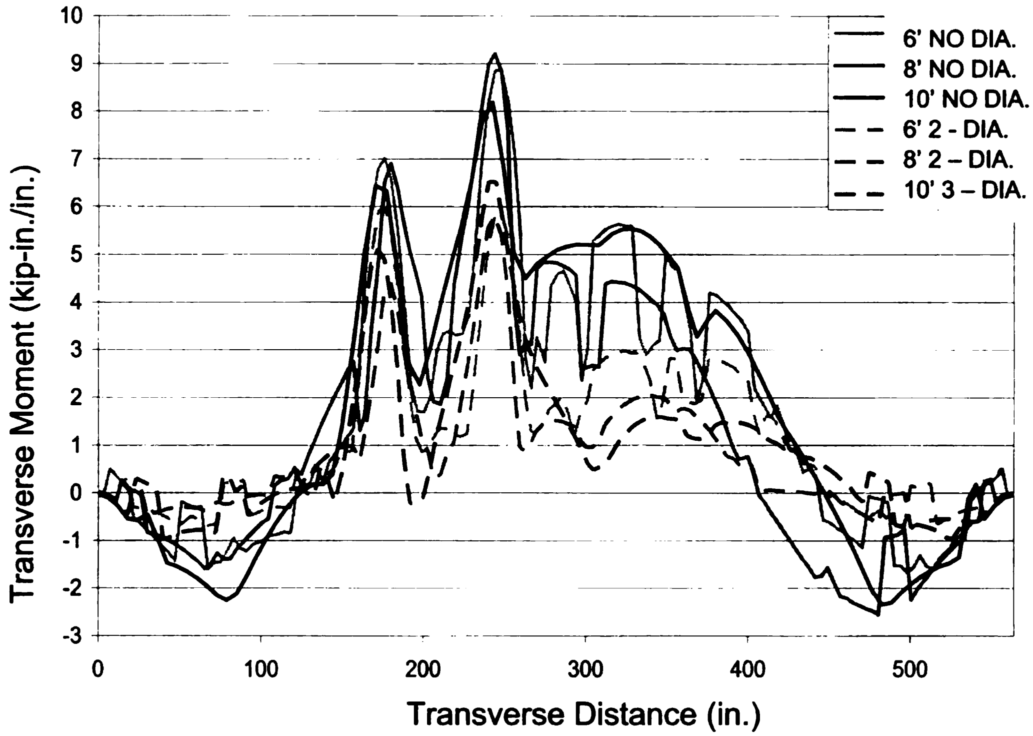

Figure 57. 100' Span: Transverse Moment v. Transverse Distance Comparison With and Without Diaphragms

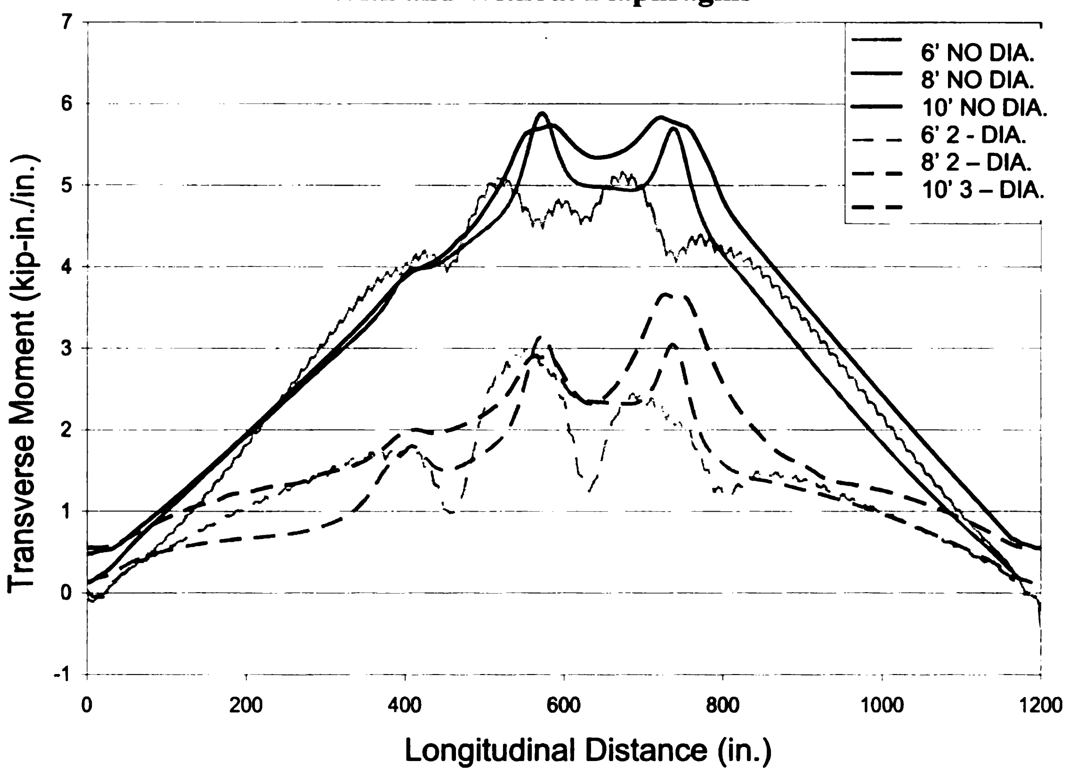

Figure 58. 100' Span: Transverse Moment v. Longitudinal Distance Comparison With and Without Diaphragms

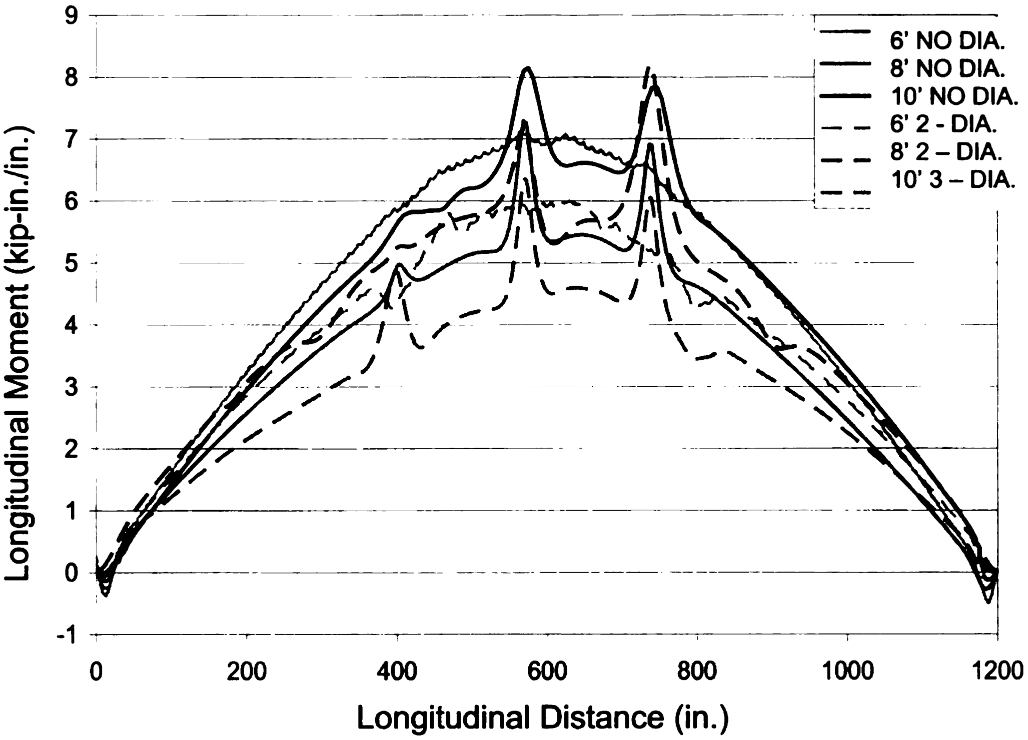

Figure 59. 100' Span: Longitudinal Moment v. Longitudinal Distance Comparison With and Without Diaphragms

Table 17. Summary of Maximum Forces in Bridge Models

Bridge No.	Max. Tran. Moment (kip-in/in)	Max. Tran. Moment at Joint (kip-in/in)	Max. Long. Moment at Joint (kip-in/in)
1	7.30	6.46	11.13
2	7.01	4.43	9.42
3	6.98	5.49	10.11
4	8.08	4.44	6.84
5	6.50	3.30	6.37
6	6.81	5.86	14.17
7	8.88	5.16	7.12
8	6.00	2.99	6.02
9	9.21	5.88	7.30
10	5.81	3.15	6.36
11	8.18	5.84	8.15
12	6.52	3.66	8.19
Avg.	7.27	4.72	8.43
Max.	9.21	6.46	14.17

5.3.4 Discussion of Results

The results presented in Section 5.3.3 show some interesting trends. A discussion of these trends and possible explanations will be offered here. First, the transverse moment response along the transverse paths will be discussed. These graphs show a trend to spike at positions where design tire loads are applied. The magnitude of the moment increases slightly on average as the span increases, but the increase is small. As shown in Table 17, the maximum transverse moment force that was developed in any of the models was 9.21 kip-in/in.

The transverse moment response along a longitudinal path (meant to represent the location of a joint) provided the most intriguing results. As seen in Figure 52, Figure 55, and Figure 58, certain models showed a *decrease* in the magnitude of the transverse moment at points in line with the wheel loads. This is at odds with conventional logic. Careful inspection of the schematics showing where the forces were extracted (Appendix II - Appendix XIII) reveal that in the models showing the decrease in magnitude, the wheel load falls between two girders. However, when the wheel load falls in a location above a girder, the predicted increase in transverse moment occurs. The author believes this phenomenon is caused by the girders absorbing much of the force due to their increased rigidity in comparison with the deck. The maximum transverse moment developed was 6.46 kip-in/in. This is lower than the maximum found along the transverse path, indicating that in these simulations the maximum transverse moment does not occur at a joint. This supports the theory that the girders attract load with their large torsional rigidity. However, the maximum transverse moment along the transverse path (9.21 kip-in/in) should be kept in mind for design purposes, as the wheel loads' locations will vary during live traffic.

The longitudinal moment along the longitudinal path shows a typical moment diagram for a distributed load with spiked increases under the wheel loads. The longitudinal moment does not appear to be affected by the placement of the wheel loads over the girders. One notable anomaly in the data can be seen in Figure 56. Here the increase in moment under the wheel load is extremely pronounced. Once again, this can be explained by looking at the schematic of the bridge in Appendix VII. The figure clearly shows the longitudinal path crossing very near to the wheel loads. This close proximity to the wheels creates a more pronounced increase. This fact should again be carefully considered by a designer. Trucks could certainly drift in their lane, or change lanes and in doing so drive over a joint. Therefore, the maximum longitudinal moment developed (14.17 kip-in/in) should be used for design.

Another trend in the data that is decisively shown in Figure 54, Figure 57, Figure 58, and Figure 59 is the effect of diaphragms on design forces. In every case the moment magnitudes are reduced by the presence of diaphragms. However, the reductions are most notable when considering transverse moment. Although there are also decreases in longitudinal moment, they are not as prominent. Correspondingly, if moment demands are of concern to the designer, the addition of diaphragms may be a viable way to reduce forces.

5.4 Stress Analysis and Characterization of Connection Details

5.4.1 General

The final step in the hierarchical suite of analyses outlined at the beginning of this chapter was to evaluate the performance of longitudinal joints between the prefabricated girder/deck units through detailed 3D stress analyses. This step involved the largest and most complex FE models as it required three-dimensional simulation of the connection detail and the forces being transferred using computationally expensive solid elements. This section describes the modeling procedure, validation, and results that are relevant to this project.

5.4.2 Approach

The author conceptualized different options to realize the longitudinal joints of the concrete deck flanges. While specific design options were outlined, they fall within the following categories:

1) Cast-in-place reinforced concrete joints
2) Shear keys (keyed, grouted or reinforced with steel dowels)
3) Post-tensioned shear keys/joints

From the three main joint categories, cast-in-place reinforced concrete joints (type 1) are designed as a full moment connection joint and thus expected to behave accordingly. Thus, no special analytical evaluation is considered to be required for this connection type. In addition, system performance with this type of connection detail was covered through the parametric studies (see Section 5.3).

Non-post-tensioned shear keys (type 2) that are not designed to transfer moments are not permitted according to the AASHTO LRFD specifications. Rather, a minimum post-tensioning force is specified. Thus, characterization of connection type 3, of the list above, was considered to be of most relevance to this project. Therefore, the research effort concentrated on studying the behavior of post-tensioned shear key joints to evaluate their load transfer efficiency and to determine the transverse post-tensioning level required for adequate performance. In addition, successful modeling of this connection type can allow for modeling of the shear key connection (type 2) as a special case where the transverse post-tensioning level is not enough to provide significant moment transfer across the joint.

Finite element simulation of post-tensioned shear key/joints requires modeling disconnected girder/deck units that are in contact only at the joints of the concrete deck. This is achieved in finite elements through contact and interaction modeling. Successful modeling of interaction problems is difficult. Thus, the next sections present a summary of the efforts taken to ensure that the contact and interaction modeling options to be used in the joints were applied properly.

5.4.3 Evaluation of Contact Interaction Modeling

5.4.3.1 Evaluation Rationale

Once 3D FE modeling had been chosen as the method for analyzing the system at the global level (see Section 5.2.5), the author opted to pursue 3D FE modeling of longitudinal joints at the local level. The difficulty in this undertaking is accurately modeling the contact interaction between the surfaces of the joint. To model the contact interaction in ABAQUS, both normal and tangential behavior of the interacting surfaces must be specified. In the direction normal to the surfaces, the constraint-enforcement method chosen was the default type, and the pressure-overclosure relationship chosen was "hard" contact. These selections were made based on recommendations in the ABAQUS user's manual (Simulia, 2007). It was specified in the contact property that separation of nodes was allowed after they had come into contact.

For the tangential behavior of the interacting surfaces, a friction formulation needs to be chosen. Originally the rough friction formulation was used, which does not allow any slip once surfaces come into contact. However, a warning message generated by ABAQUS advised that the penalty friction formulation should be used, and thus it was adopted. Based on some findings from similar modeling efforts, a friction coefficient of 0.5 was conservatively chosen.

Although the interaction property is well documented in ABAQUS, the author chose to perform several checks in order to verify that the interaction property used in the model was functioning as desired. Details of the evaluation measures follow.

5.4.3.2 Qualitative Evaluation

To properly represent the behavior of the joint, the contact property needed two characteristics. First, when nodes come into contact, the interaction property needs to prevent them from passing through each other. Second, if the nodes lose the pressure pressing them together, the model needs to allow them to separate. Verifying that these two behaviors were occurring was the aim of this first evaluation.

The model created to perform this check consisted of two simply supported cubes with pressure applied inward on the outer face of each block, as shown in Figure 60. The motivation for choosing this setup was to create a situation where the blocks would come into contact, and then separate. This first objective was achieved, as shown in Figure 61. Loading was then applied to the top of the cubes in order to achieve a separation at the bottom of the interface, as an actual loaded joint would behave. This is shown in Figure 62. The separation was achieved, as shown in Figure 63.

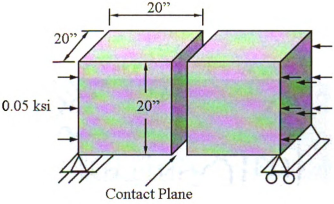

Figure 60. Schematic of Cube Contact Model with Pressure Applied Normal to the Contact Plane

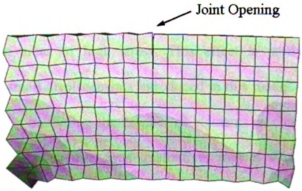

Figure 61. Cube model showing separation of nodes

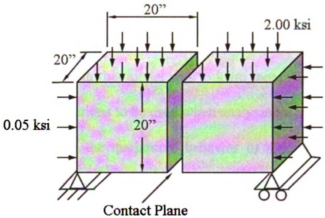

Figure 62. Schematic of Cube Contact Model with Pressure Normal to the Contact Plane and Vertical Pressure

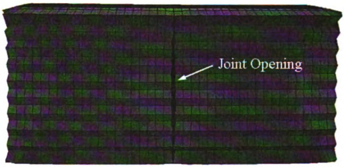

Figure 63. Bottom view of top-loaded model showing separation of nodes under load

As Figure 61 and Figure 63 show, these models exhibited major deformations at the element level in areas of high stress. This effect is partly due to graphical representation of the small displacements introduced in this model. This problem could have been remedied by increasing the number of elements or changing to a quadratic element. However, this evaluation was qualitative; thus it was instead decided to evaluate a model with a geometry closer to that of a bridge deck. As shown in Figure 64 and Figure 65, the model was modified to use flatter parts which more closely approximate deck slabs.

The objective with this model was to learn more about creating an accurate way of modeling the connections to be used when analyzing a joint with no moment transfer, as well as to observe the qualitative behavior of a joint modeled with the contact interaction. The results of this analysis can be seen in Figure 66.

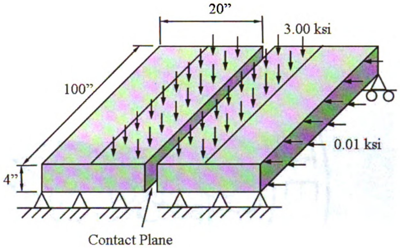

Figure 64. Schematic of Updated Model with More Accurate Geometry

This space intentionally left blank

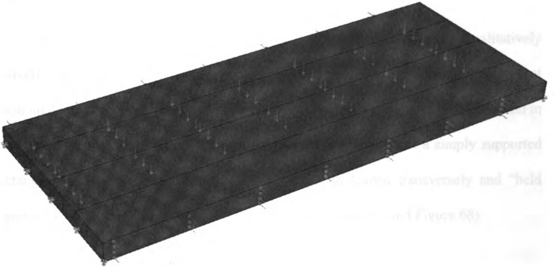

Figure 65. Updated Model with More Accurate Geometry

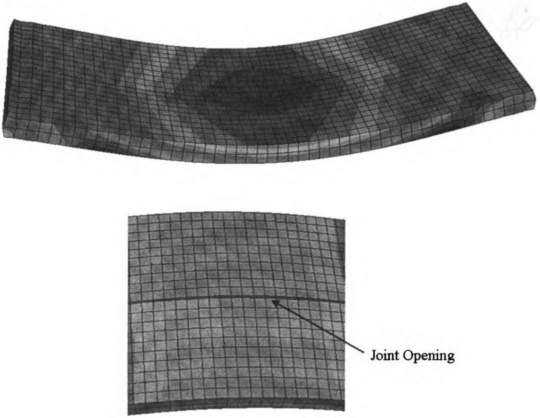

Figure 66. (a) Top view of deformed shape of model in Figure 65 and (b) Bottom view of model in Figure 65 showing node separation

5.4.3.3 Quantitative Evaluation

Once it was observed that the interaction property was behaving qualitatively correctly, a series of quantitative evaluations were performed in order to ensure that these qualitative observations were in fact correct, and not merely a misrepresentation in the post-processor. The first model used for this check consisted of a simply supported rectangular beam divided in two sections at mid-span loaded transversely and "held together" by a longitudinal post-tensioning force (see Figure 67 and Figure 68).

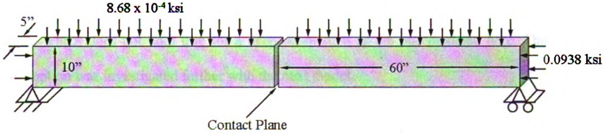

Figure 67. Schematic of Rectangular Beams Used for Quantitative Evaluation

Figure 68. Model of rectangular beams

To calibrate the model, hand calculations were performed to choose the magnitude of post-tensioning required for zero longitudinal stress at the bottom fiber of the beam at mid-span. This level of post-tensioning was chosen in order to check that the interface would remain closed as theoretically predicted. The FE simulation showed that the beam did remain closed under loading as shown in Figure 69. In Figure 69 the stress is very close to zero at the bottom fiber (1.0037 ksi, compressive). This matches with theoretical predictions.

A stress profile was then determined from beam theory, and compared with the results of the ABAQUS model. This comparison is shown in Figure 70. The results showed close agreement (<5% error) with the theoretical calculations, except at the extreme fibers, where there was greater error. However, the author believes that the FE model is actually correct, because beam theory assumes that plane sections remain plane, which does not hold true for a deep beam such as the one modeled here. This assumption was investigated further with the next model.

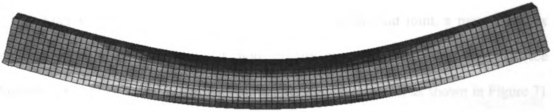

Figure 69. Deformed rectangular beam model showing no separation at midspan (Contours Represent Longitudinal Stresses)

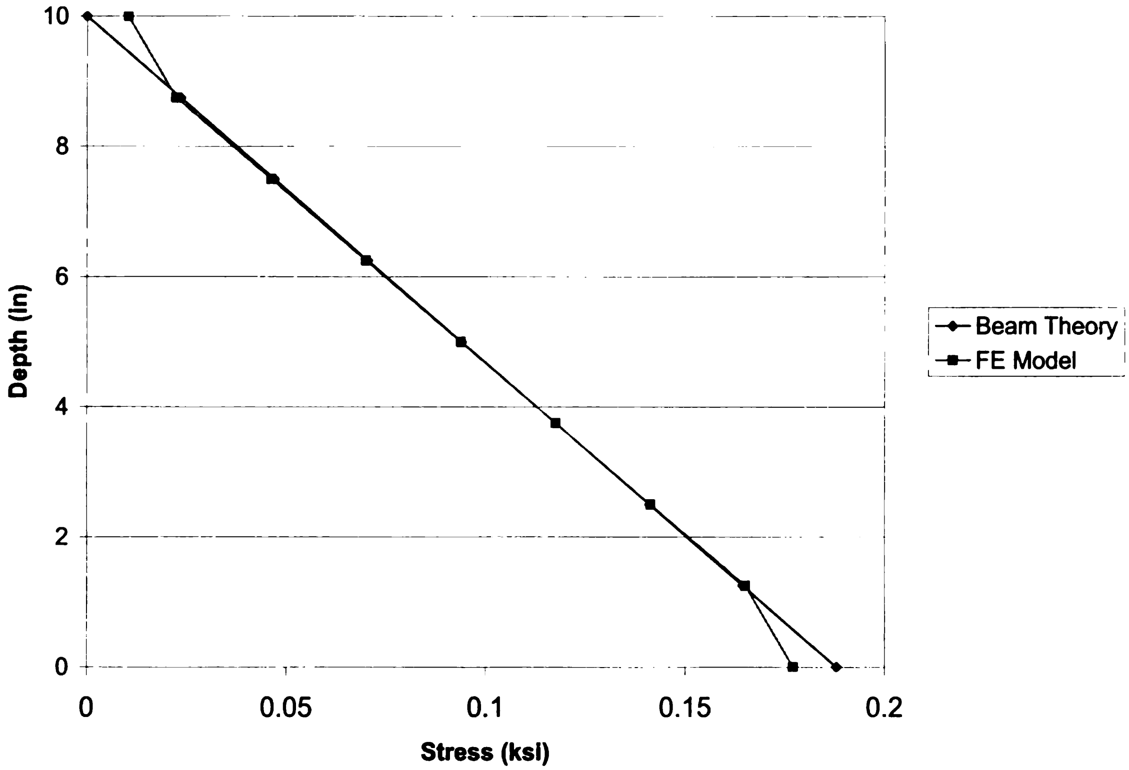

Figure 70. Stress profile in rectangular beam model

After verifying the accuracy of a model with a flat butt joint, a more complex male-to-female joint geometry that more closely resembled joint types 2 or 3 (see Section 5.4.2) in an actual bridge superstructure was investigated, as shown in Figure 71 and Figure 72. This model was subjected to a post-tensioning force and vertical loading similar to the rectangular beam with the flat butt joint. However, in this model the post-tensioning was proportioned so that the entire joint would remain in compression. This kept the joint closed, as shown in Figure 73. When this model was analyzed, it matched closely with predicted longitudinal stress values, again with the exception of the extreme fibers. These results are shown in Figure 74. As previously mentioned, this discrepancy was believed to be caused by shear deformations due to the relatively thick beams being modeled. To check that the departure from theoretical predictions at the extreme fibers were being caused by shear deformation and not a numerical problem caused by modeling the joint, a beam was modeled with the same dimensions as the beam shown in Figure 67, but without a joint. These results, shown in Figure 75, also showed the nonlinear stress profile exhibited in Figure 70 and Figure 74. This indicates that this nonlinearity is due to shear deformation and is not related to a modeling issue.

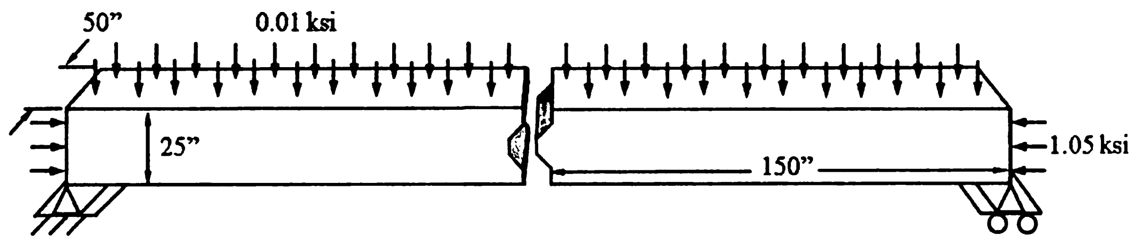

Figure 71. Schematic of Male-to-Female Joint Model

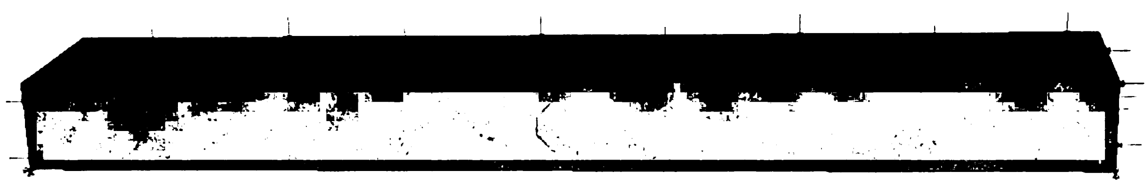

Figure 72. ABAQUS Model with Male-to-Female Joint

Figure 73. FE Model of Male-to-Female Joint (Contours Represent Longitudinal Stress)

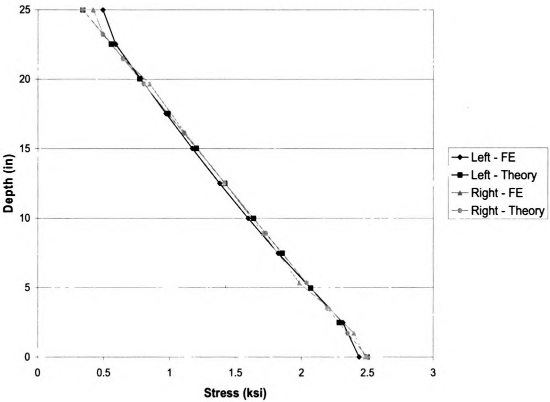

Figure 74. Comparison of longitudinal stress in FE model

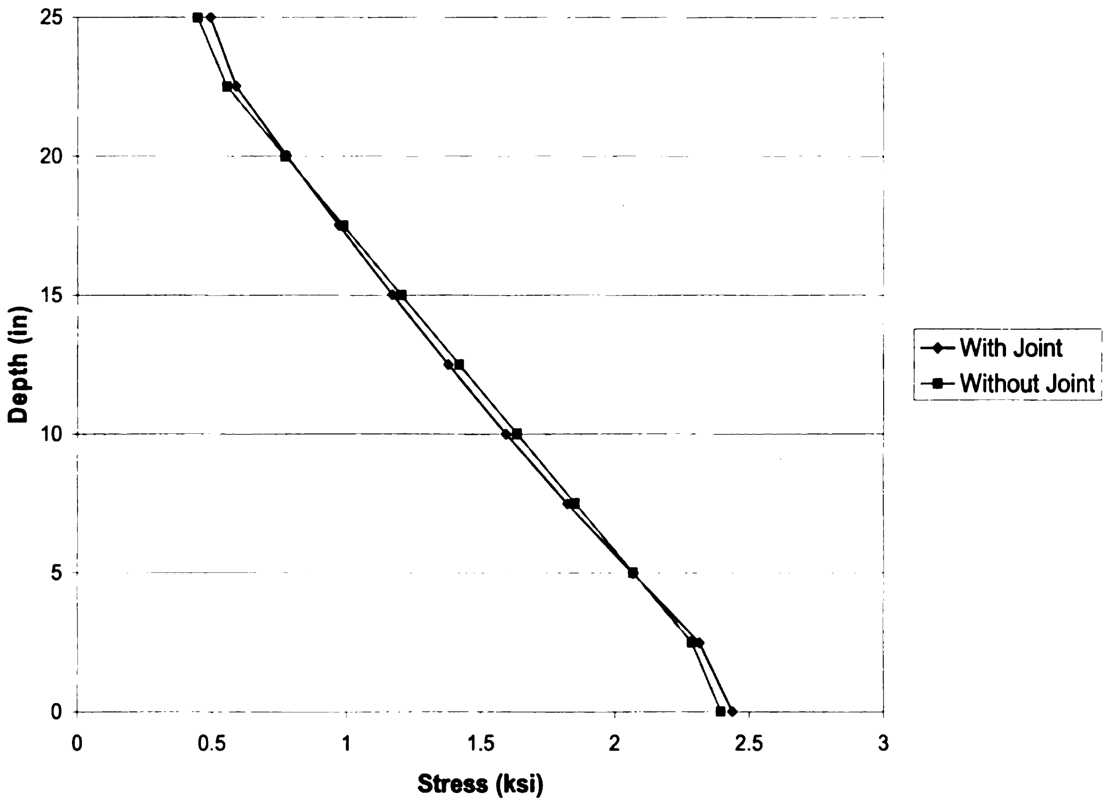

Figure 75. Comparison of longitudinal stresses in models with and without joint

After completing these checks, the author is satisfied that the method for modeling the interaction property is adequate. The results of these models agree with predicted results and the physical behavior coincides with what is expected. Therefore, a similar model can be used to assess the behavior of the longitudinal joints in the prefabricated composite steel box girder system and determine the level of post-tensioning required for proper system performance.

5.4.4 Model Characterization

Having established the functionality of the contact interaction when modeling joints, the author began modeling a typical joint geometry that could be used in an actual bridge. The goal is to show that joints can be kept closed with a reasonable amount of post-tensioning. This will be done by performing a global analysis with detailed joint modeling in order to establish the post-tensioning force required to maintain closure of the joints under AASHTO service loading. If joint closure can be maintained, a full moment connection model can be assumed to carry out parametric studies.

To verify that the deck was acting as a continuous slab, and hence could be analyzed using a single shell-element deck, two FE models were created with solid-element decks and shear-key type joints. Model 1 was a 50-ft bridge with double girder units, each individual girder spaced at 4 ft. Model 2 was a 100-ft bridge with single girder units and a girder spacing of 8 ft.

The joints were modeled to represent a typical shear key joint (type 2 or 3 from Section 5.4.2). The FE representation of such a joint can be seen in Figure 76. Although the FE model incorporates one male and one female side of the joint, in practice both flanges would likely be female, with a grouted key running through the void created by the two female flanges.

Globally, the models (particularly the 100-ft model) were very large and extremely cumbersome computationally. Therefore, it was advantageous to reduce the model using symmetry. With a symmetric geometry and an anti-symmetric loading, the model was cut in half at mid-span, and given a shear-mechanism boundary condition. A completed model is shown in Figure 77.

By checking the system response under different levels of post-tensioning, the minimum amount of post-tensioning required can be determined. Therefore, multiple combinations of varying post-tensioning levels and loading conditions were prescribed. A matrix of these combinations is presented in Table 18. Finally, the element types and sizes can be found in Table 19.

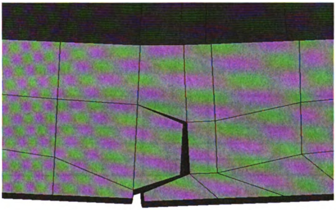

Figure 76. FE Model of Shear Key Joint Opening Under Loading

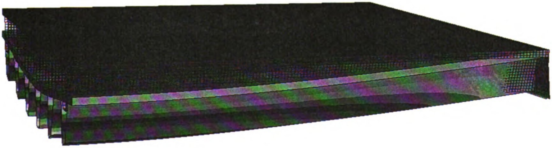

Figure 77. FE Model of Bridge Model 9.
(Contours Represent Longitudinal Stress)

Table 18. Case Matrix of Post-Tensioning Levels and Loading Conditions

Load Case	Post-Tensioning (ksi)	Loading Condition (AASHTO)
1	0.25	Service II
2	0.225	Service II
3	0.2	Service II
4	0.175	Service II
5	0.15	Service II
6	0.125	Service II
7	0.25	Strength I
8	0.225	Strength I
9	0.2	Strength I
10	0.175	Strength I
11	0.15	Strength I
12	0.125	Strength I

Table 19. Element Data for Full Models with Solid Deck Elements

Part	Material	Shell Thickness (in)	Element Type	Hourglass Control	Reduced Integration	Element Size (in)
Deck	Concrete	n/a	C3D8R	Active	Active	4.5
Tub	Steel	0.375	S4R	Active	Active	6
End Block	Concrete	24	S4R	Active	Active	4

5.4.5 System Response

5.4.5.1 General

The results of these analyses were favorable for this system. Three areas of interest were evaluated in order to determine the viability of using shear-key joints in a prefabricated system such as the one being studied. They were:

- Longitudinal Stress in Steel Tubs
- Deflection Profile
- Joint Opening

These parameters were derived for the two models with joints, and then compared to a model that was identical in geometry, except the segmental deck had been replaced with a deck slab which was continuous over the width of the bridge. This approach aimed to show that a prefabricated system could function similarly to a superstructure with a traditional cast-in-place deck.

5.4.5.2 Interpretation of Results

Figure 78 shows the location of the measurements taken to evaluate the responses listed in Section 5.4.5.1. The first parameter studied was longitudinal stress in the steel tubs. The stress in each tub was extracted at mid-span, in the middle of the bottom (tension) flange. The second parameter studied was the vertical deflection of the bridge deck. The deflection at each node along the deck surface at mid-span was recorded. The third parameter studied was the joint opening along the span of the bridge. To obtain this data, the lateral coordinate of each node along either side of the joint was extracted, and the difference of the two was taken to be the joint opening. Hence, the value reported here represents the lateral distance between nodes, not the true distance between the two. Since there is minimal vertical differential between the nodes, this difference is negligible. To see the naming convention used to define each individual joint, see Figure 78.

Also presented in the graphs of joint opening is an "acceptability threshold" imposed by the author. See Section 3.7 for details on the derivation of the acceptability threshold.

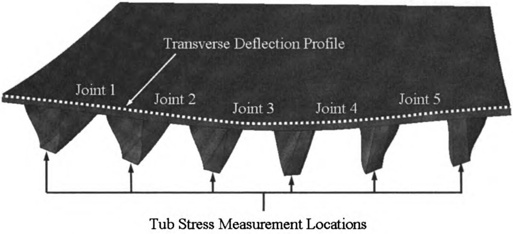

Figure 78. Parameters Studied in Models with Joints

5.4.5.3 50-ft Bridge Model

The FE model used to analyze the 50-ft bridge is shown in Figure 79. The dimensions of the girders are those of bridge model 1 of the parametric study. These dimensions can be found in Table 15. The deformed shape is also presented in Figure 80.

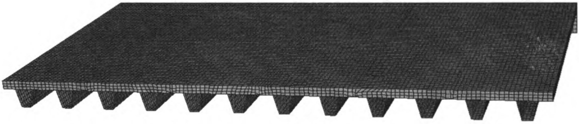

Figure 79. FE Model with Solid Deck Elem ents and Joints Representing Model # 1

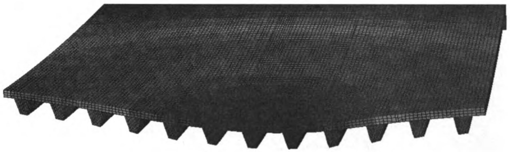

**Figure 80. Deformed Shape of Model in Figure 79.
(Contours Represent Vertical Displacement)**

As shown in Figure 81 and Figure 82, the stress in the tubs is largely unaffected by post-tensioning levels. The variation between the models with prefabricated decks is very small (less than 1 ksi). However, some of the tubs in the model with a continuous deck have stresses that differ greatly when compared with the corresponding tubs in the segmental models. The charts show a much more uniform distribution of stress across the width of the bridge when there is a continuous deck. However, the critical central tubs that experience the highest stress do not see a significantly higher stress with the segmental deck. Therefore, using prefabricated girder units does not diminish performance when compared with a continuous-slab bridge of the same dimensions.

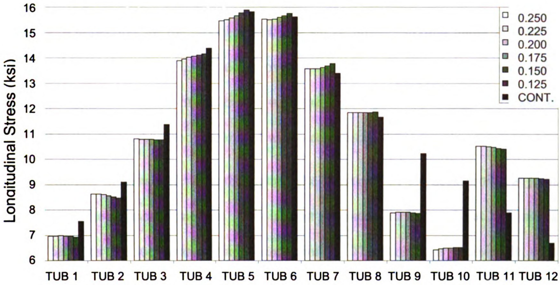

Figure 81. Longitudinal Stress Variation by Girder (50-ft Model, Service Loading)

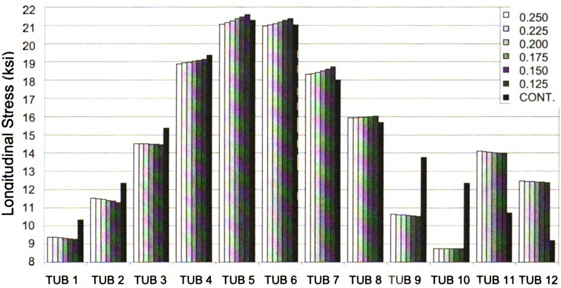

Figure 82. Longitudinal Stress Variation by Girder (50-ft Model, Strength Loading)

The deflection profile of the bridge deck is plotted in Figure 83 and Figure 84. As indicated by the graphs, it is again noticeable that the load is better distributed by the continuous slab deck. However, similarly to the longitudinal stresses, the maximum values of deflection do not differ significantly in the segmental model. The increase in maximum deflection for the model with 0.250 ksi of post-tensioning under AASHTO Service II loading is about 0.025 inches over that of the model with a continuous slab. The increase in deflection of the model with the lowest post-tensioning, 0.125 ksi, is about 0.050 inches over that of the model with a continuous slab.

Another important trend in this data is the "kinking" of the deck profile at joint locations in the segmental models. This is most prominent in Figure 84 at 282 inches and 376 inches (the locations of Joint 3 and Joint 4). This kinking is undesirable, as it indicates the bridge superstructure is functioning as individual pieces and not one unified entity. This behavior occurs when the post-tensioning is 0.150 ksi or lower under service loading, and when the post-tensioning is 0.200 ksi or lower under strength conditions. Although this kinking may be tolerable under strength loading, it should be prevented under service conditions.

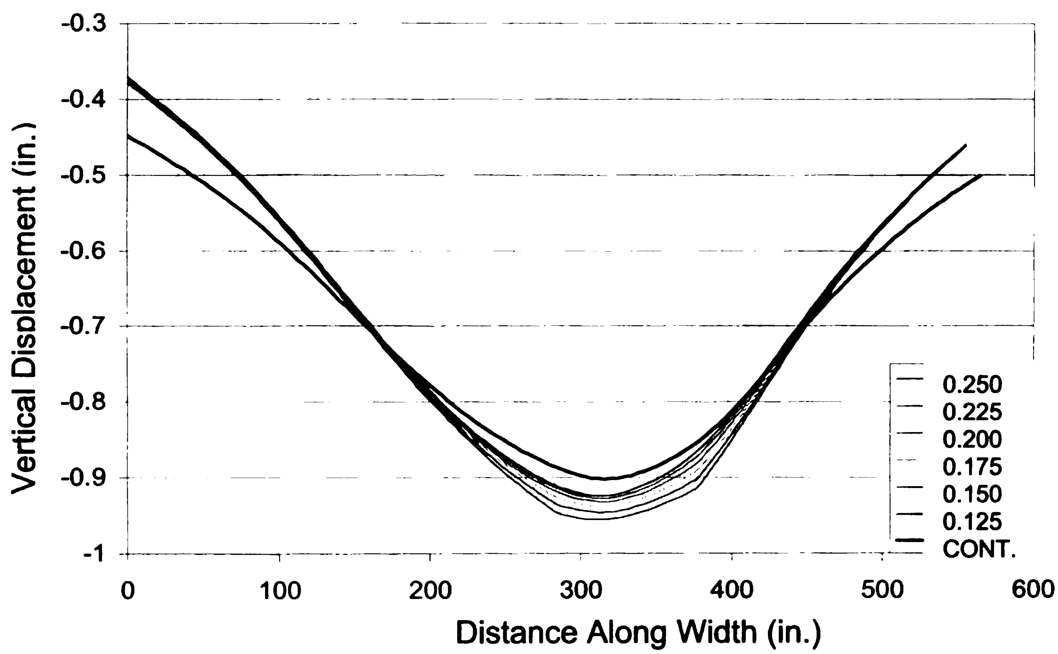

Figure 83. Transverse Profile of Vertical Displacement at Midspan Under Varying Post-tensioning Levels (50-ft Model, Service Loading)

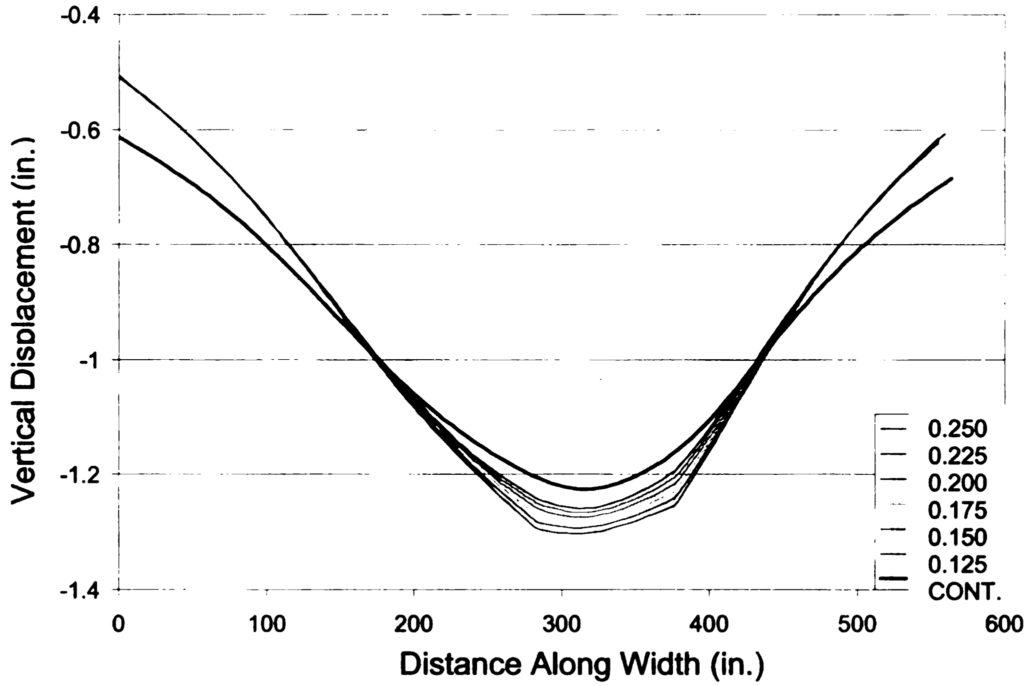

Figure 84. Transverse Profile of Vertical Displacement at Midspan Under Varying Post-tensioning Levels (50-ft Model, Strength Loading)

For the 50-ft span bridge, only Joint 3 and Joint 4 show significant opening, and as such only the opening of those joints has been presented. Plots of the joint opening along the span can be found in Figure 85 - Figure 88. As the plots show, the "acceptability threshold" developed by the author was only exceeded under strength loading conditions at Joint 4. In this circumstance, models with a post-tensioning level of 0.200 ksi or lower do not meet the maximum opening criteria.

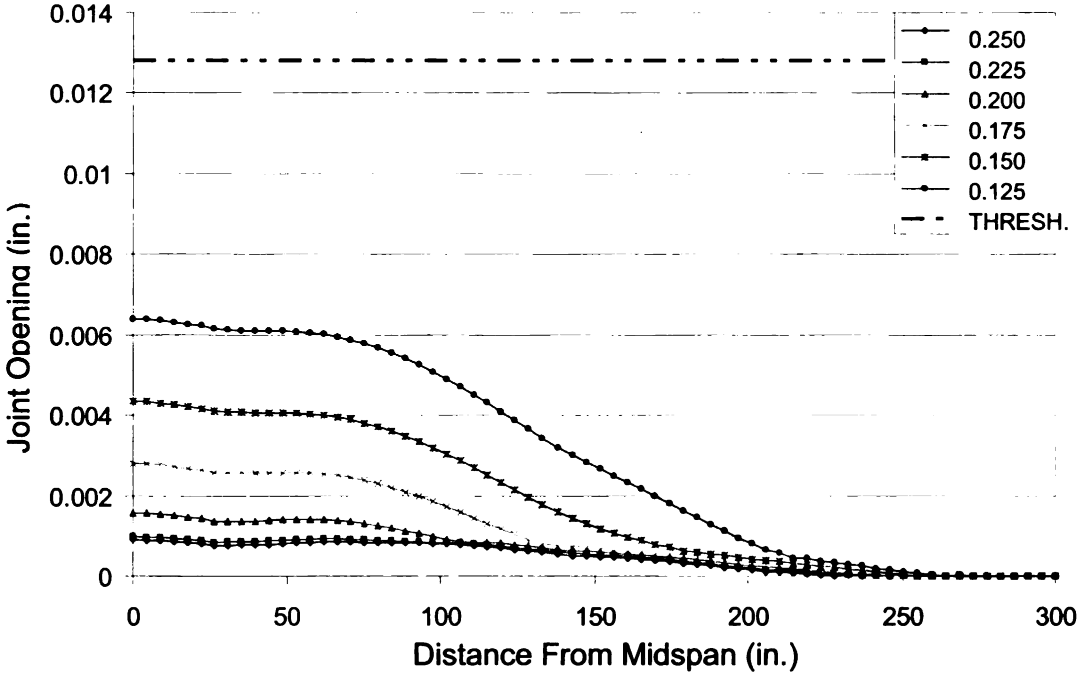

Figure 85. Joint 3 Opening Along Span (50-ft Model, Service Loading)

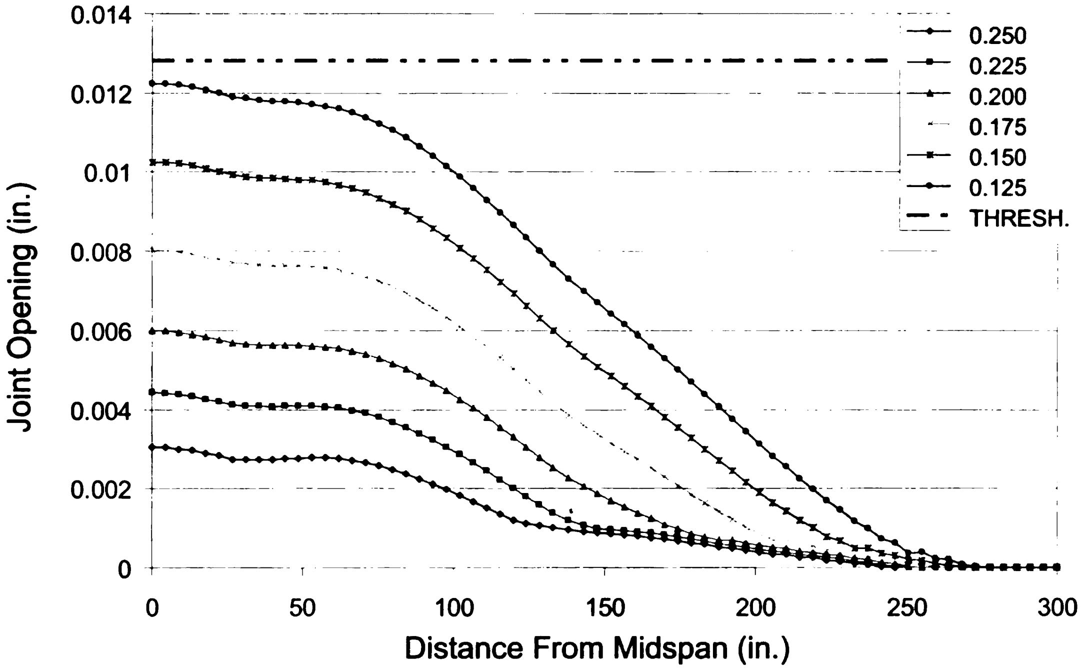

Figure 86. Joint 3 Opening Along Span (50-ft Model, Strength Loading)

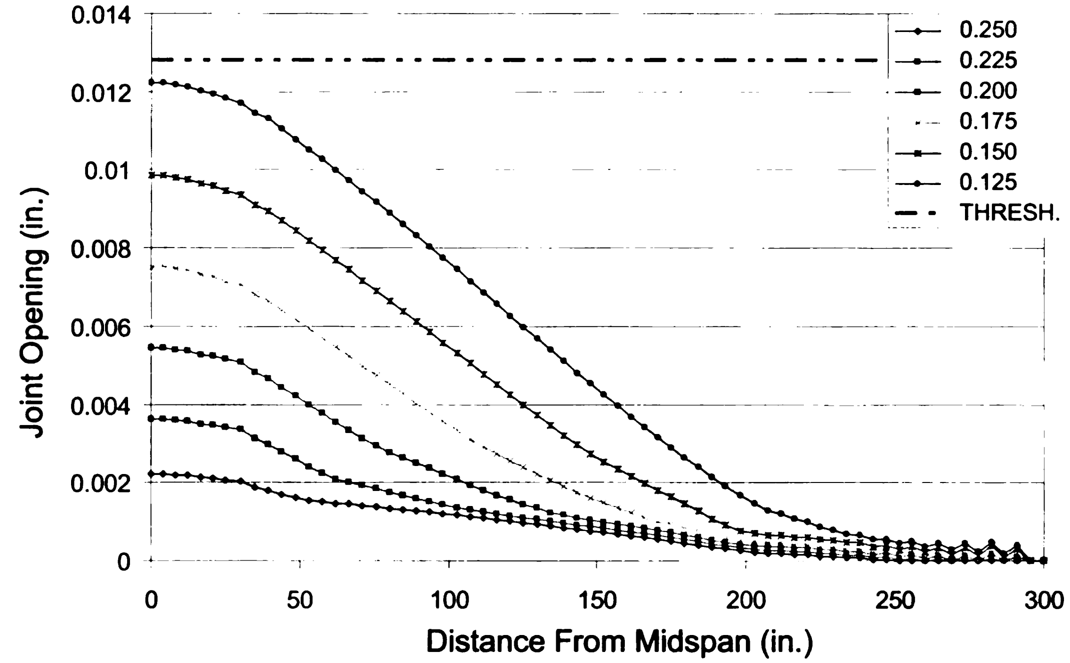

Figure 87. Joint 4 Opening Along Span (50-ft Model, Service Loading)

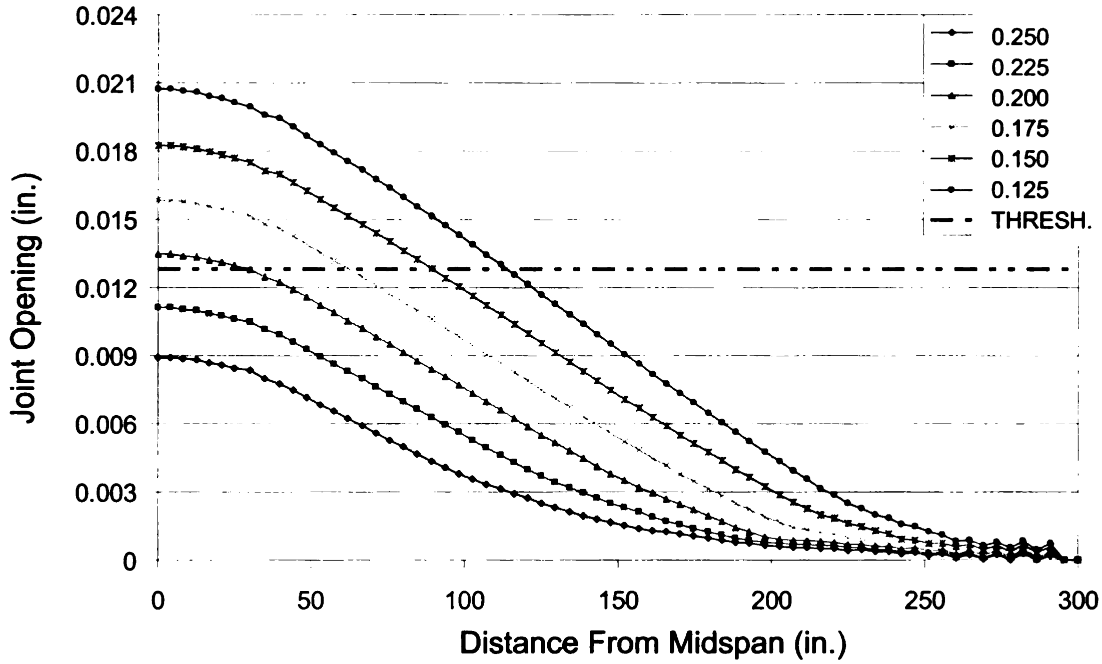

Figure 88. Joint 4 Opening Along Span (50-ft Model, Strength Loading)

5.4.5.4 100-ft Bridge Model

The FE model used to analyze the 100-ft bridge is shown in Figure 89. The dimensions of the girders are those of bridge model 9 of the parametric study, found in Table 15. The deformed shape is also presented in Figure 90.

The same parameters studied with 50-ft model were again evaluated for the 100-ft model. The first parameter was longitudinal stress in the steel tubs. As shown in Figure 91 and Figure 92, the stress in the tubs is largely unaffected by post-tensioning levels. As was the case in the 50-ft bridge, the variation between the models with prefabricated decks is very small (less than 1 ksi). Consequently, the same conclusions drawn in Section 5.4.5.3 can be drawn here: the segmental bridge does not distribute load as well, but the maximum stresses increase only slightly.

Figure 89. FE Model with Solid Deck Elements and Joints Representing Model # 9

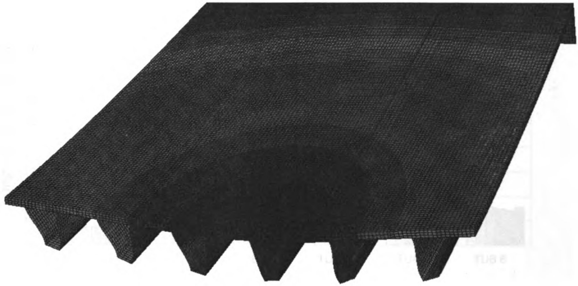

Figure 90. Deformed Shape of Model in Figure 89.
(Contours Represent Vertical Displacement)

The second parameter studied was vertical deflection of the deck surface, as shown in Figure 93 and Figure 94. An important trend in this data is the "kinking" of the deck profile at joint locations in the segmental models. This is most prominent in Figure 94 at 282 inches and 376 inches (the locations of Joint 3 and Joint 4). This kinking is undesirable, as it indicates the bridge superstructure is functioning as individual pieces and not one continuous structure. This behavior occurs when the post-tensioning is 0.175 ksi or lower under service loading, and in all cases under strength conditions. This kinking is thought to be undesirable under service loading and should be avoided.

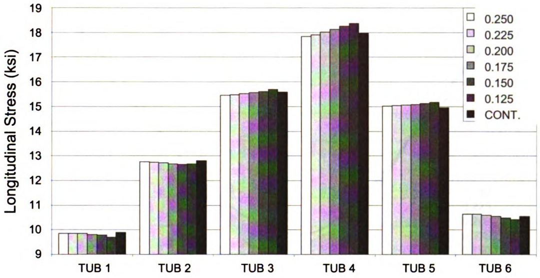

Figure 91. Longitudinal Stress Variation by Girder (100-ft Model, Service Loading)

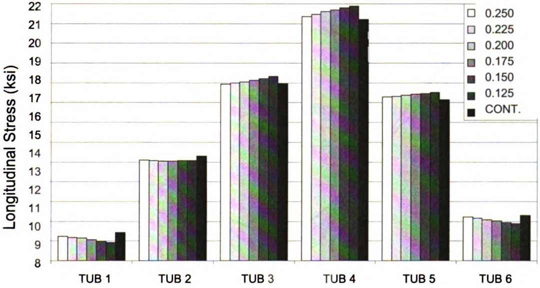

Figure 92. Longitudinal Stress Variation by Girder (100-ft Model, Strength Loading)

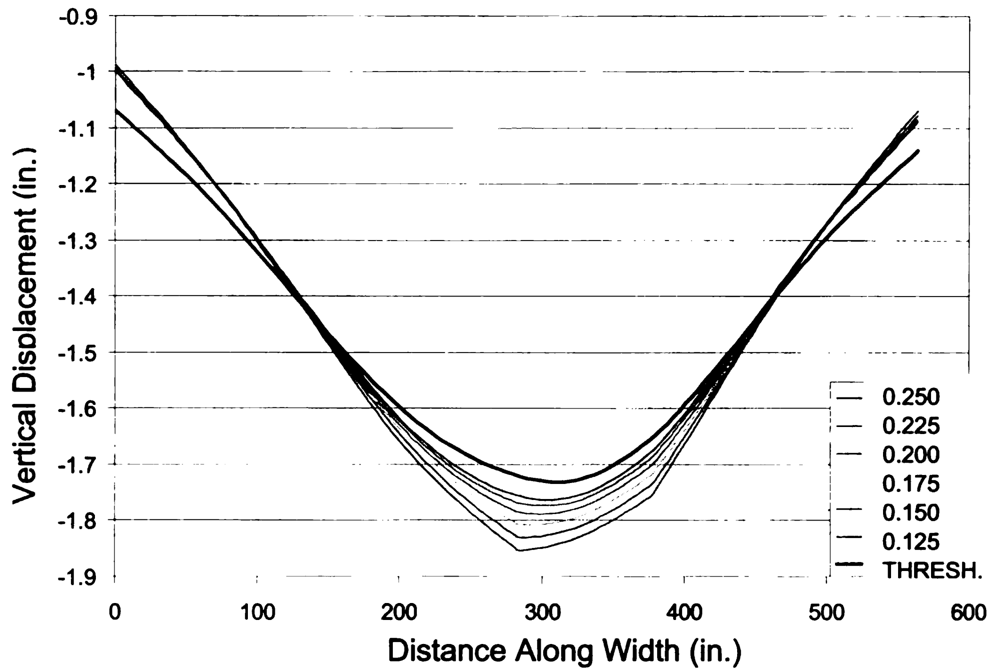

Figure 93. Transverse Profile of Vertical Displacement at Midspan Under Varying Post-tensioning Levels (100-ft Model, Service Loading)

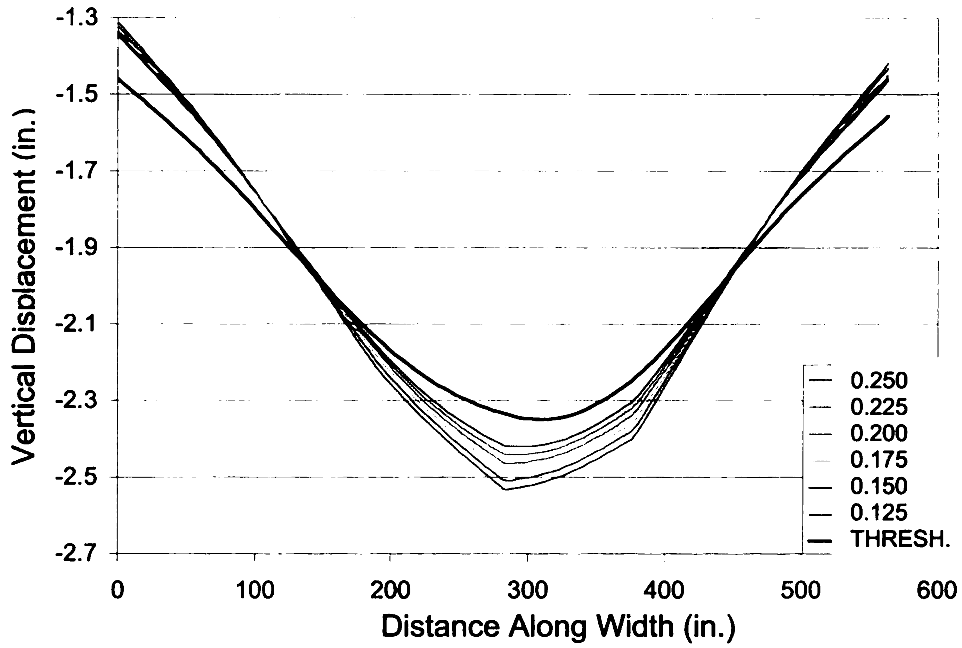

Figure 94. Transverse Profile of Vertical Displacement at Midspan Under Varying Post-tensioning Levels (100-ft Model, Strength Loading)

The third parameter studied was the joint opening along the span of the bridge. The joint naming scheme is shown in Figure 78. In the 100-ft model, Joints 2, 3, and 4 showed significant opening. Plots of the joint opening along the span can be found in Figure 95 - Figure 100.

As the plots show, the threshold is exceeded under service loading conditions at Joint 3 and Joint 4. However, models with a post-tensioning level of 0.175 ksi or higher always meet the maximum opening criteria under service loading. In contrast, strength loading causes all models to exceed the criteria at Joint 4, and all but the 0.250 ksi post-tensioning at Joint 3. Again, this criteria applies more directly to service loading than to strength loading, so this analysis indicates that 0.175 ksi should be sufficient for post-tensioning a 100-ft span bridge such as the one modeled here. Joint 2 never opens far enough to exceed the criteria. Finally, it should be kept in mind that this criteria is simply a guideline from the author, not an official standard.

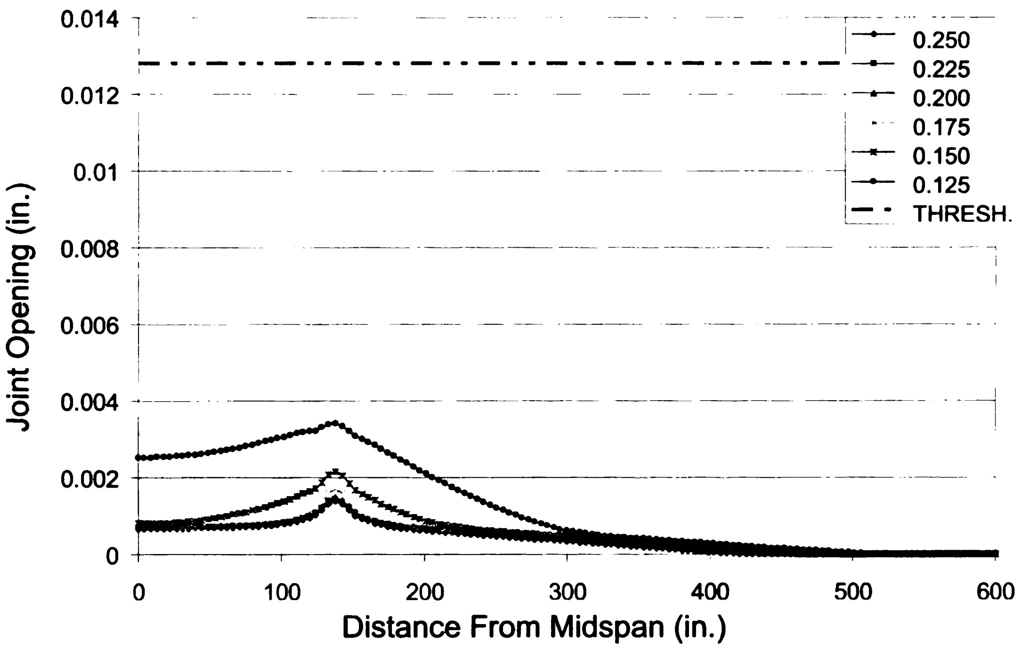

Figure 95. Joint 2 Opening Along Span (100-ft Model, Service Loading)

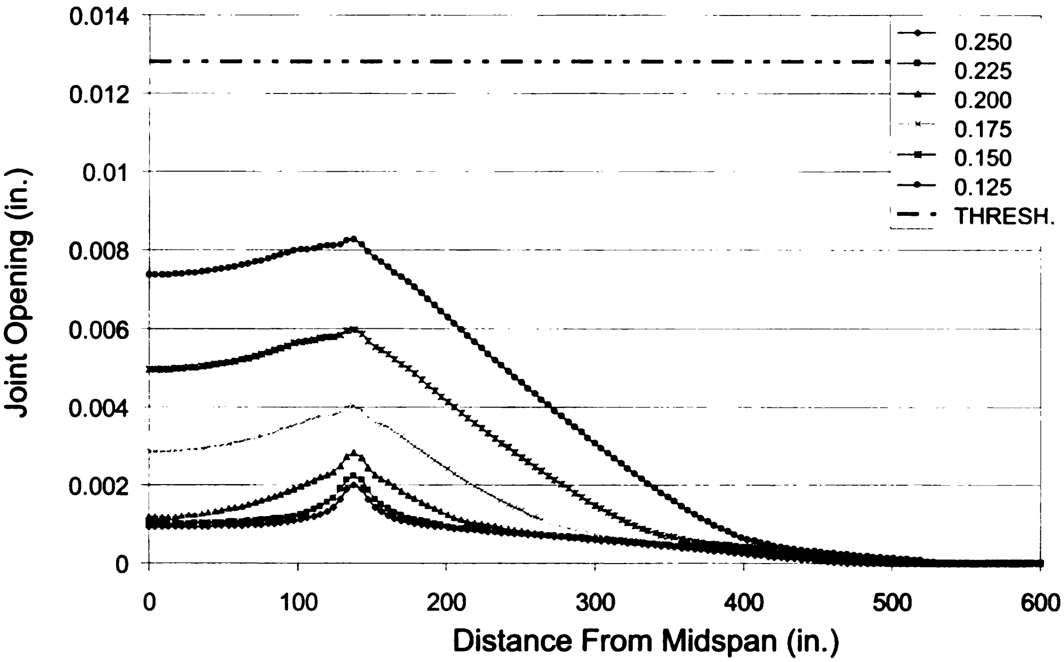

Figure 96. Joint 2 Opening Along Span (100-ft Model, Strength Loading)

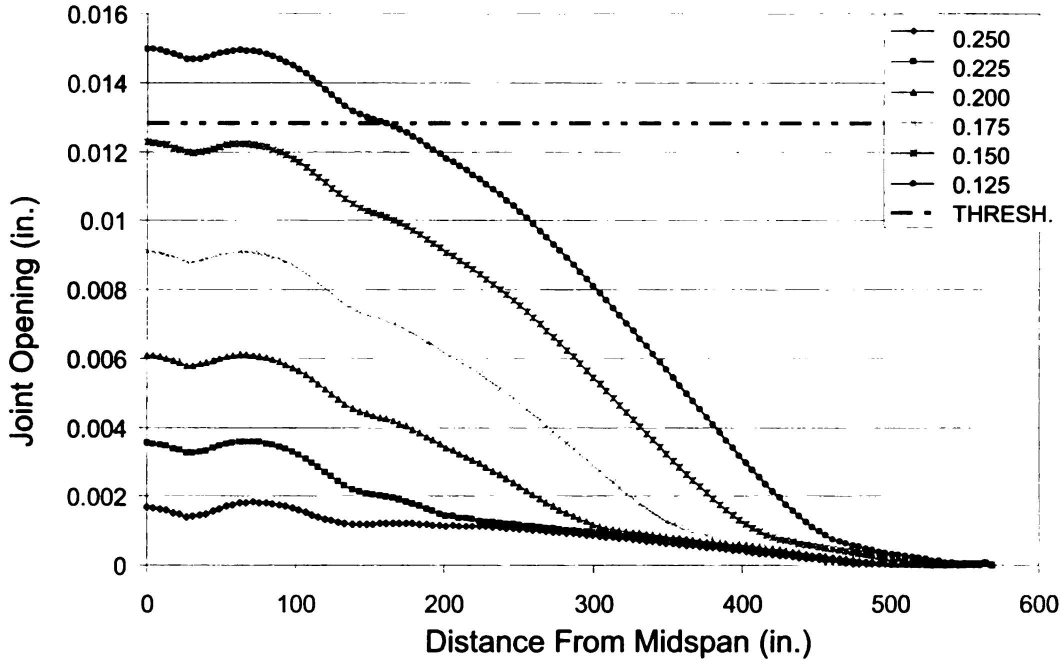

Figure 97. Joint 3 Opening Along Span (100-ft Model, Service Loading)

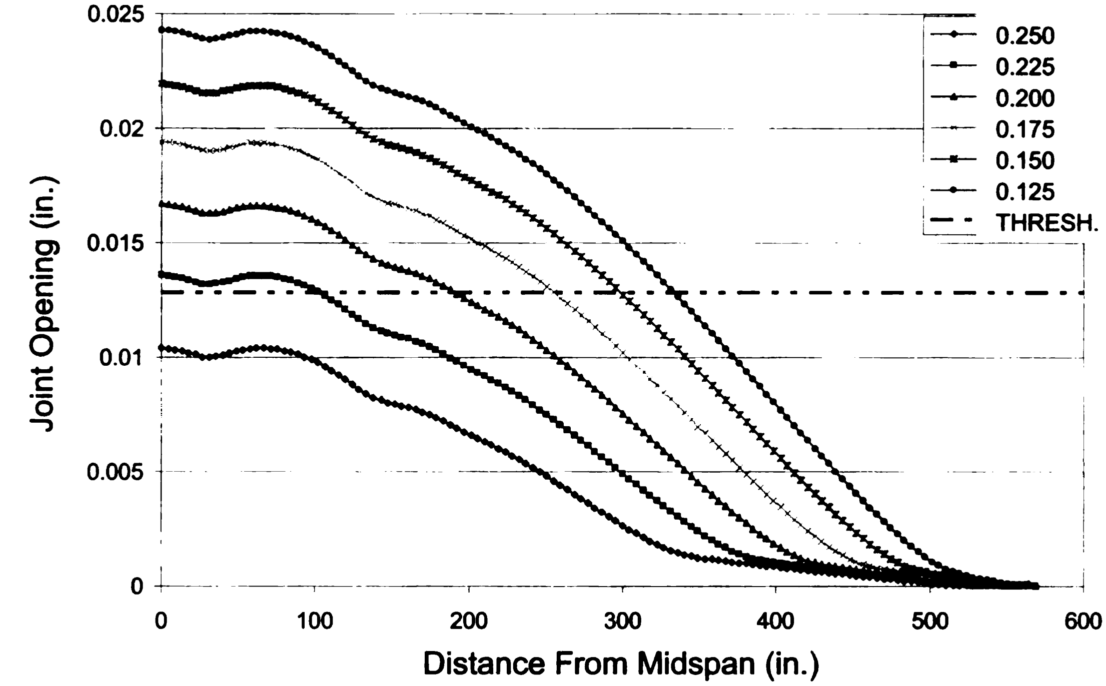

Figure 98. Joint 3 Opening Along Span (100-ft Model, Strength Loading)

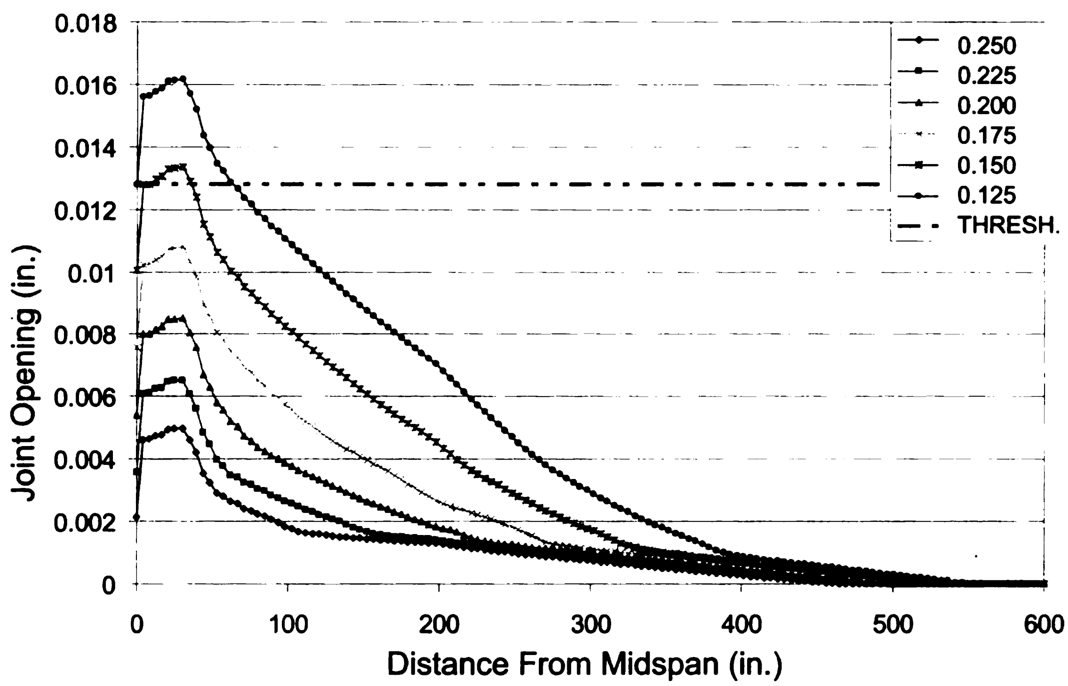

Figure 99. Joint 4 Opening Along Span (100-ft Model, Service Loading)

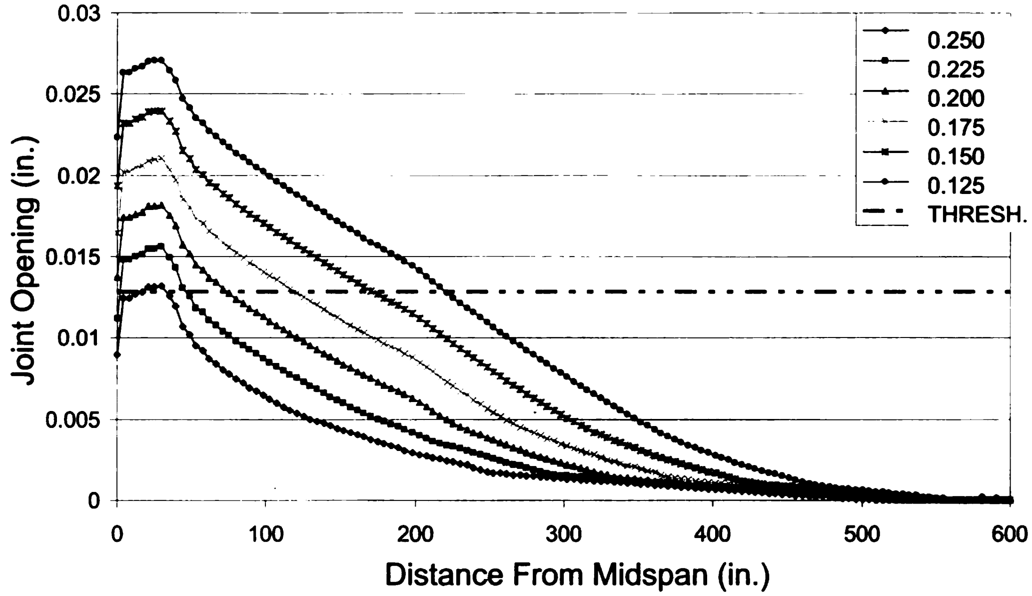

Figure 100. Joint 4 Opening Along Span (100-ft Model, Strength Loading)

5.5 Vibration Characteristics

The last task performed using the two FE models with solid deck elements was to determine the fundamental frequencies and mode shapes of these bridge systems. This was performed in ABAQUS using a linear perturbation step that was capable of running an eigenvalue analysis on the system mass matrix. Since Section 5.4.5 showed that continuity could be established with adequate post-tensioning, the dynamic analyses were performed on the models with continuous slabs. This avoided computational difficulties that arise out of modeling the base state of a segmental model.

The first three bending mode shapes were extracted, eliminating other mode shapes that were not of concern (i.e., transverse/longitudinal stretching). The first three fundamental frequencies for the 50-ft bridge model and the corresponding mode shapes are presented in Table 20 and Figure 101-Figure 103, respectively.

Table 20. Fundamental Frequencies of the First Three Bending Mode Shapes, 50' Bridge Model

Bending Mode	Fundamental Frequency	
	rad/time	cycles/time
Mode 1:	28.450	4.5280
Mode 2:	48.714	7.7530
Mode 3:	68.467	10.897

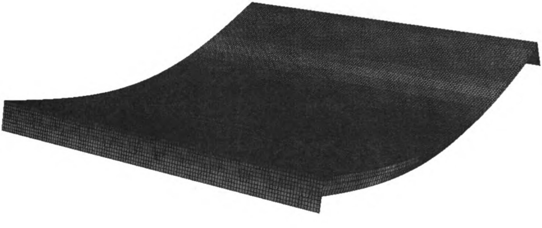

Figure 101. Bending Mode Shape 1, 50' Bridge Model

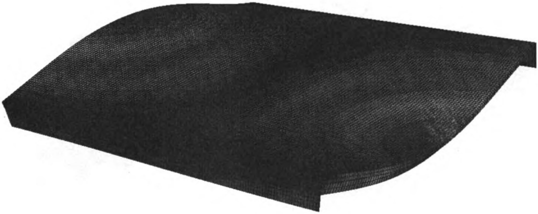

Figure 102. Bending Mode Shape 2, 50' Bridge Model

Figure 103. Bending Mode Shape 3, 50' Bridge Model

As the above figures show, the three bending mode shapes correspond to the first longitudinal bending mode, followed by the first two transverse bending modes. This is the qualitative expected result. To better visualize the bending behavior in Mode 2 and Mode 3, bridge cross-sections are provided in Figure 104 and Figure 105.

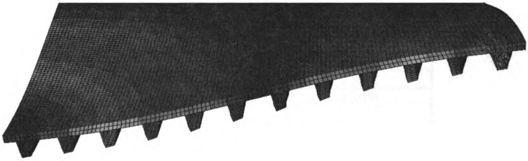

Figure 104. Bending Mode 2 Cross-Section

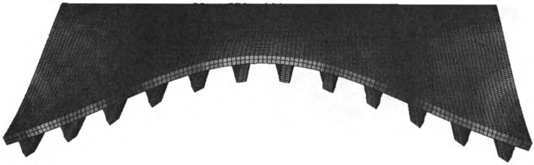

Figure 105. Bending Mode 3 Cross-Section

Qualitatively, the results of the dynamic analysis on the 100-ft model yielded the similar results. However, the value of the frequencies decreased significantly. The first three mode shapes, and the corresponding fundamental frequencies for the 100-ft bridge model are presented in Figure 106-Figure 108 and Table 21, respectively.

Table 21. Fundamental Frequencies of the First Three Bending Mode Shapes, 100' Bridge Model

Bending Mode	Fundamental Frequency	
	rad/time	cycles/time
Mode 1:	16.312	2.5962
Mode 2:	28.679	4.5644
Mode 3:	45.434	7.2310

Figure 106. Bending Mode Shape 1, 100' Model

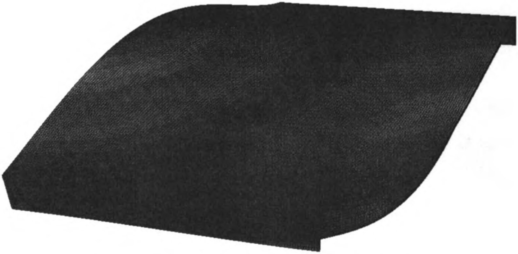

Figure 107. Bending Mode Shape 2, 100' Model

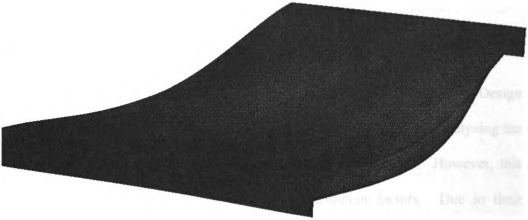

Figure 108. Bending Mode Shape 3, 100' Model

6. CONCLUSIONS AND RECOMMENDATIONS

6.1 Observations

The simplified analysis method presented in the AASHTO LRFD Design Specifications (AASHTO, 1998) were found to be generally applicable for analyzing the prefabricated composite steel box girder bridges studied in this work. However, this method seems to be lacking when it comes to distribution factors. Due to their geometry, box girders distribute load differently that traditional steel I-shape girders, or bulb-shape girders that are often used in highway bridges. Hence, their distribution factors require additional research. However, it appears that minimal research has gone into the development of distribution for these bridges, as evidenced by the single "blanket" equation to describe the distribution of both moment and shear demands to interior and exterior girders alike. Therefore, it is recommended that a refined analysis is always performed to accompany an AASHTO analysis of a composite box girder bridge system.

The grillage method is a well-established simplified method for analyzing bridge structures. By idealizing a structure into a set of beam elements, the number of degrees of freedom in a system can be greatly reduced. This subsequently reduces the number of equations that need to be solved in order to complete a system analysis, which in turn reduces computation time. However, with the increase in computing technology, running more refined three-dimensional finite element analyses with continuum-type elements no longer significantly increases computation time. In addition, when compared with grillage models, an experienced user can create complex continuum-type finite element models with relative ease. Therefore, it is recommended that when performing analytical evaluations similar to the type performed in this project, the finite element method should be used in lieu of the grillage method.

6.2 Recommendations for Design

The results of the parametric analysis in Section 5.3 indicate that at the global level, the composite steel box girder system can easily be designed in a way that will allow it to perform within the AASHTO specifications for stress and deflection. As seen in the figures and tables of Section 5.3.3, adequate designs have been developed for a range of spans and girder spacings. In addition, several of the span/spacing combinations have been satisfied using the same girder, indicating that a single girder could be versatile enough to be manufactured in bulk and used in a variety of situations. The frequency analyses that were performed (see Section 5.5) also returned acceptable results. Therefore, the design should be controlled by ensuring satisfactory behavior of the joints.

In Section 5.4, the joint behavior was investigated. First, the prefabricated segmental bridges were compared with another bridge model which was identical, with the exception that the segmental deck was replaced with a continuous slab. This was done to study the continuity that could be achieved with a transversely post-tensioned longitudinal joint as the connection element between the prefabricated girder/deck units. The AASHTO LRFD Bridge Design Specifications require these type of joints to be provided with a minimum of 0.250 ksi pressure of transverse post-tensioning (after all losses). As seen in Section 5.4, the prefabricated bridges were able to achieve continuity close to that of the continuous slab bridge with post-tensioning stress values lower than the AASHTO specified level. Stress and deflection profiles remained largely unchanged between the segmental models and the continuous models. However, when the level of post-tensioning drops too low (below 0.150 ksi in the 50-ft model, below 0.175 ksi in the 100-ft model) a kinking behavior occurs at the joints, which is undesirable. Hence, a post-tensioning level which is equal to or greater than these values should be specified.

As described in Section 5.4.4.2, a benchmark limit to judge the adequacy of the joint closure was proposed by the author, based on the AASHTO LRFD Bridge Design Specifications for crack opening in a reinforced concrete structures. It was recommended that this limit should not be exceeded under service conditions at the longitudinal deck joints connecting the prefabricated girder/deck bride units. Using this guideline, the transverse post-tensioning level should not fall below 0.175 ksi for the 100-ft model. All post-tensioning levels studied passed this criterion for the 50-ft bridge.

Summarizing the analysis results, the 50-ft bridge is controlled by kinking behavior at the joints. This occurs at a post-tensioning level of 0.150 ksi, which is then considered the minimum design value for this span length. The 100-ft bridge model is controlled by both kinking behavior and joint opening. These both become unacceptable at post-tensioning levels of 0.175 ksi. This level should be the minimum design value for these bridges of this length. These results are logical in that the transverse post-tensioning stress level required to maintain an emulative reinforced concrete joint increases with span length.

In summary, this study has confirmed that prefabricated steel/concrete composite girder/deck units connected together with transversely post-tensioned longitudinal deck joints are a safe and viable option for rapid bridge construction. The parametric studies indicated that adequate performance can be obtained for short spans ranging from 50 to 100 feet. Transverse diaphragms can improve load distribution and thus lower the moment demands on individual girder/deck units. However, cost-benefit assessment of the added time and fabrication costs related to the addition of the diaphragms compared to the improved efficiency gained must be evaluated. The vibration characteristics of the system indicated that the fundamental frequencies fall within acceptable limits. For the short spans over which the prefabricated steel/concrete composite sections are considered, transverse post-tensioning levels required by the AASHTO code, as well as levels significantly lower than the required minimum, will provide full emulative behavior of the joint. While the results from this investigation indicate that lower post-tensioning stress levels may be adequate, it should be mentioned that the current study has not considered concrete volume effects on the post-tensioning force and its influence on joint behavior. These considerations should be done before a reduced post-tensioning level from that recommended by AASHTO can be fully justified.

6.3 Recommendations for Future Work

To further the state-of-the-art in this field, several items for future work are possible. The work in this project has allowed evaluation of the prefabricated bridge concept only through numerical simulations, yet there are many aspects of the modeling and theory behind the simulation that need to be verified. The analytical models used to assess the global behavior of the bridge system should be trusted to a high degree of accuracy. However, the detailed 3D stress models used to evaluate joint behavior should be confirmed experimentally. Although great effort was taken to validate the contact interaction used in the finite element models of the joints, experimental testing could reveal issues that the numerical studies have missed. Thus, experimental verification of the system and connection behavior that parallel the analytical evaluation conducted in this study is recommended.

It is proposed that any experiment used to verify the work done in this project be designed to address and confirm the following findings from the project:

1) Component Stiffness: The numerical models should closely match with experimental results. However, longitudinal shear slip, nonlinear deformations, and other factors could affect the system response.

2) Joint Behavior: The analytical models in the project showed that adequate joint closure could be achieved with the levels of post-tensioning that were specified. The actual joint openings should be checked experimentally. Further, the performance of these types of joints under fatigue loading and volume concrete changes should be experimentally assessed.

3) System Response: The analytical models indicated that a kinking occurs at low post-tensioning levels. The actual limits of post-tensioning required for adequate behavior should be verified. Thus, system-level experiments that permit evaluation of joint behavior under realistic loading simulation and load distribution effects on multiple girders need to be performed.

APPENDICES

Appendix I. Comparison of Analysis Tools

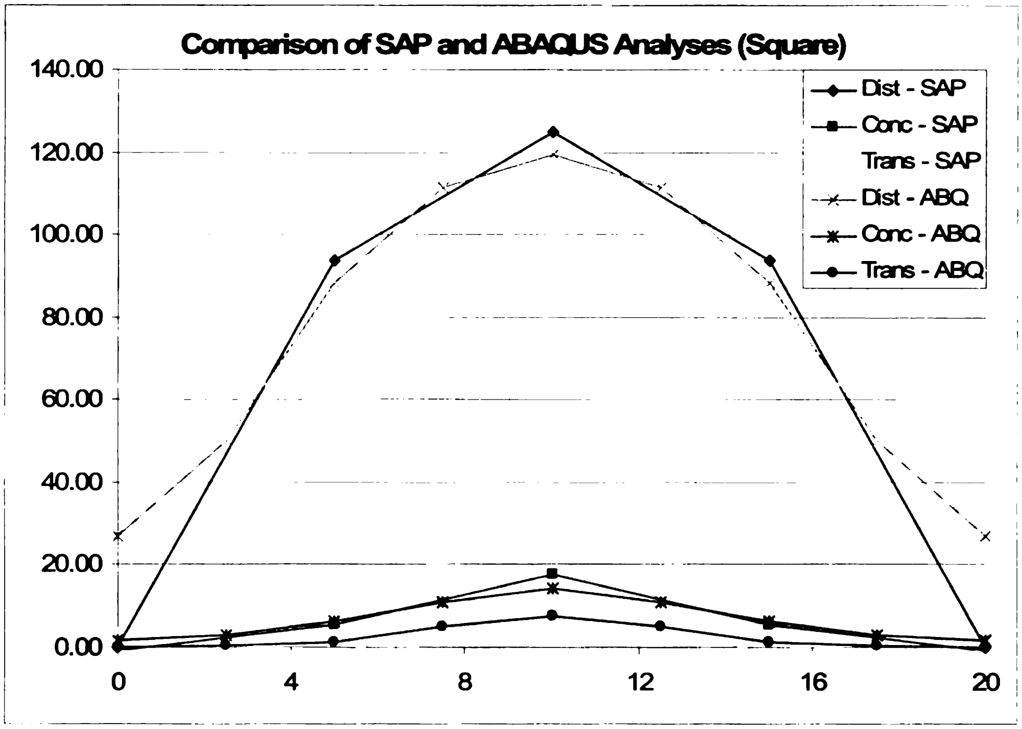

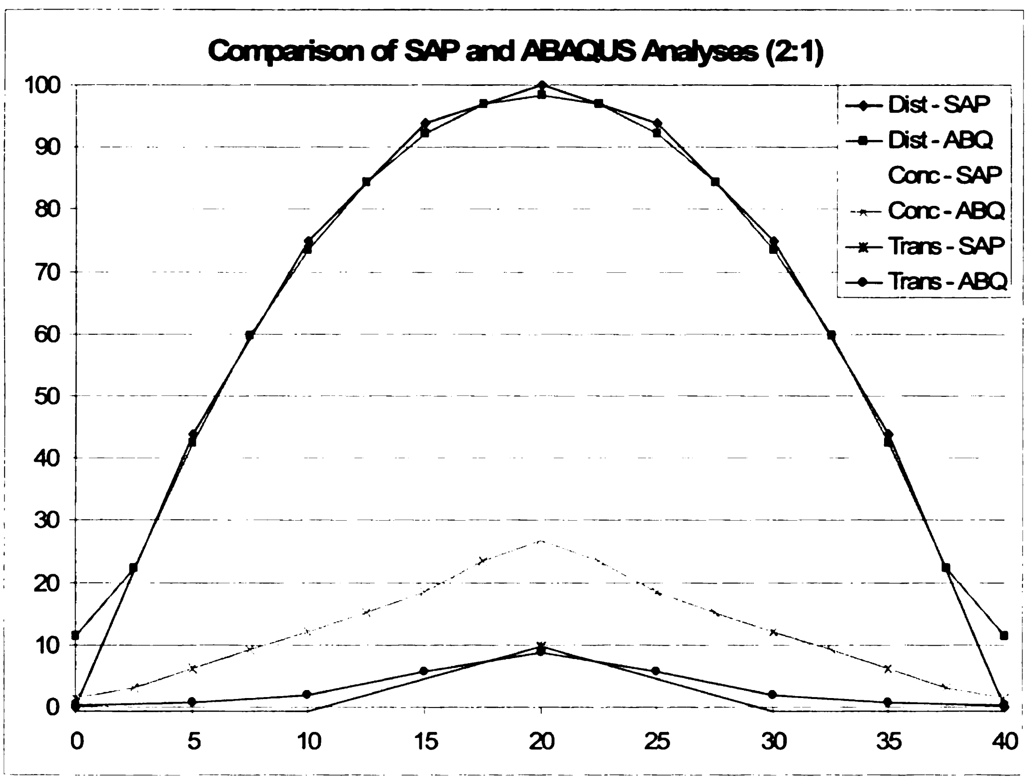

Appendix II. Bridge Case 1: FE Models Responses

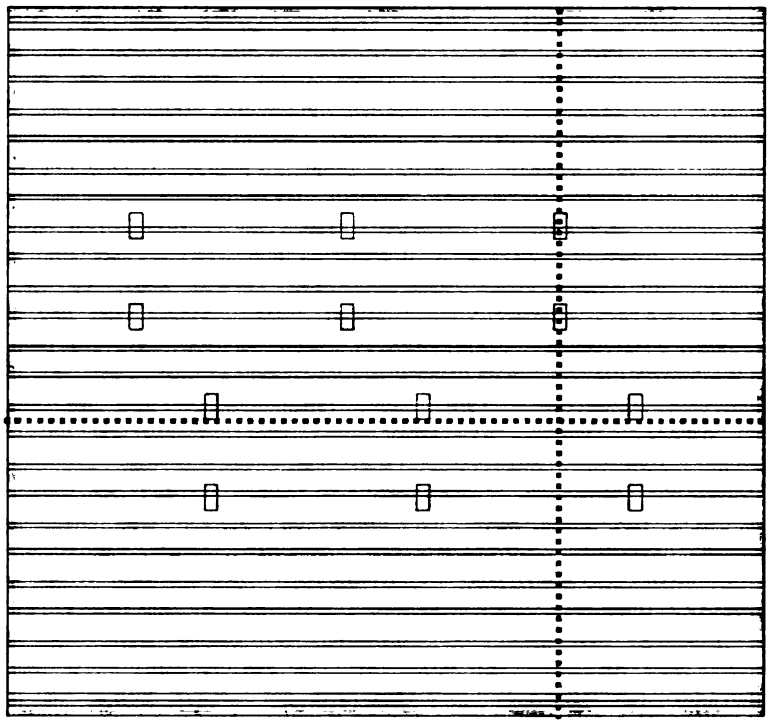

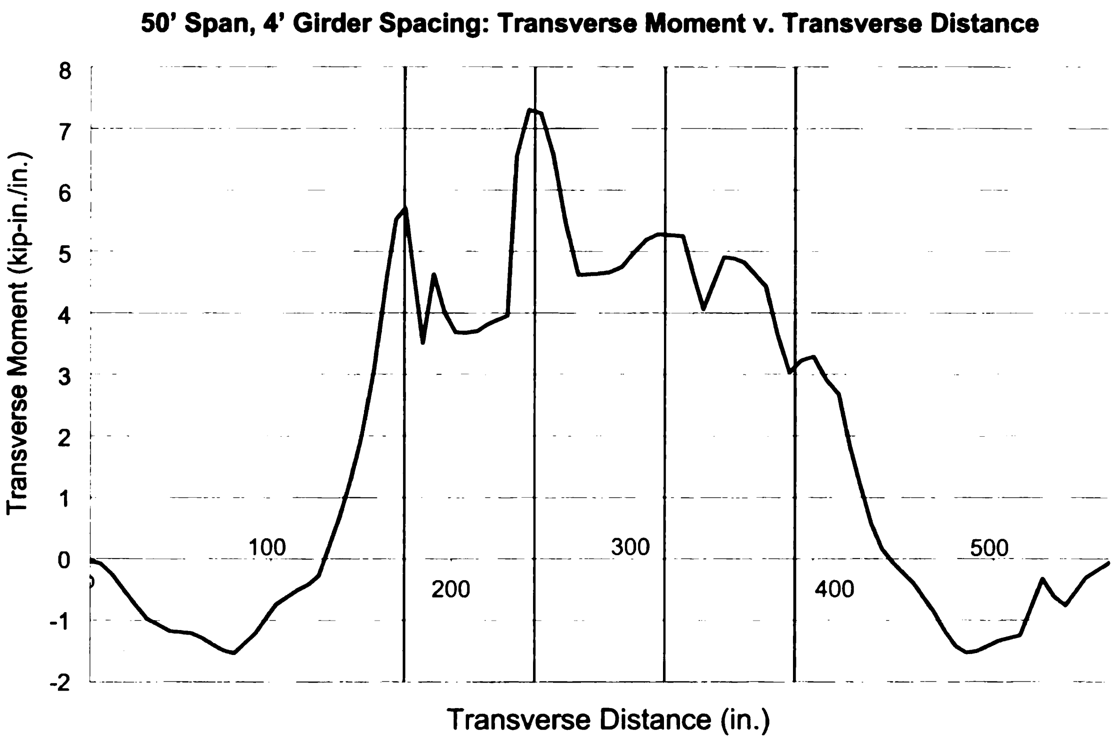

50' Span, 4' Girder Spacing: Transverse Moment v. Longitudinal Distance

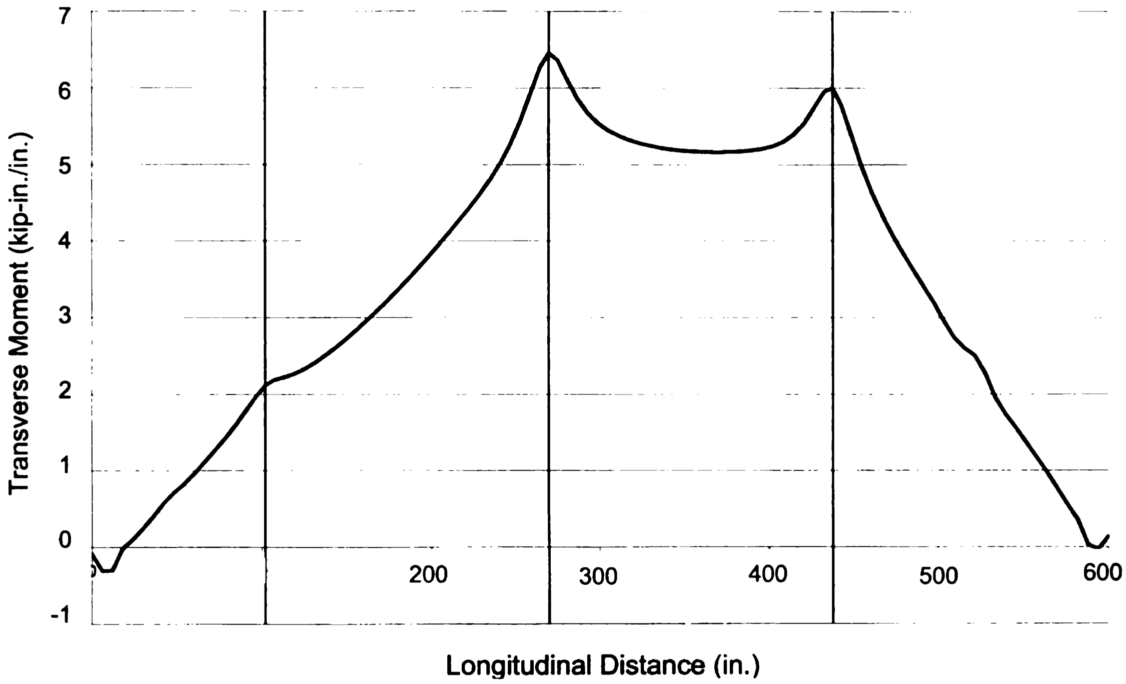

50' Span, 4' Girder Spacing: Longitudinal Moment v. Longitudinal Distance

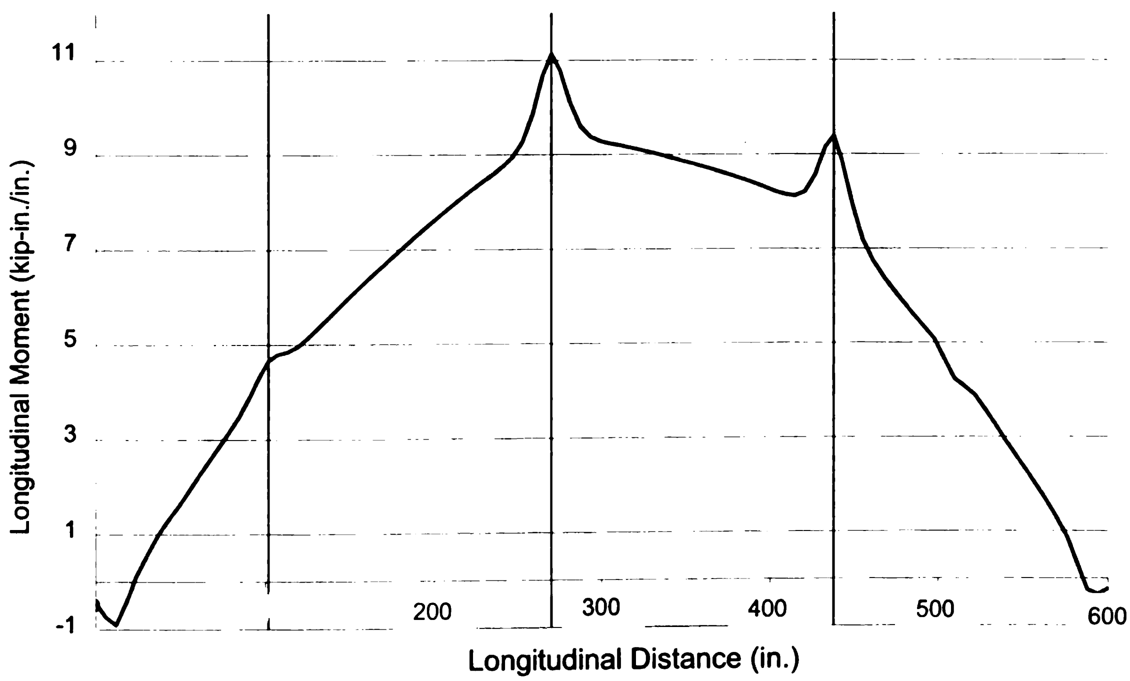

Appendix III. Bridge Case 2: FE Models Responses

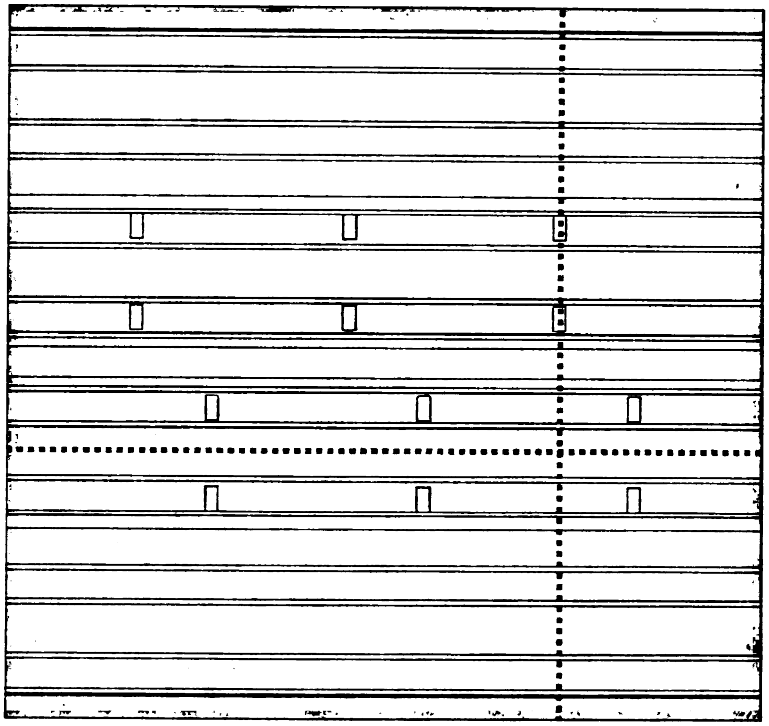

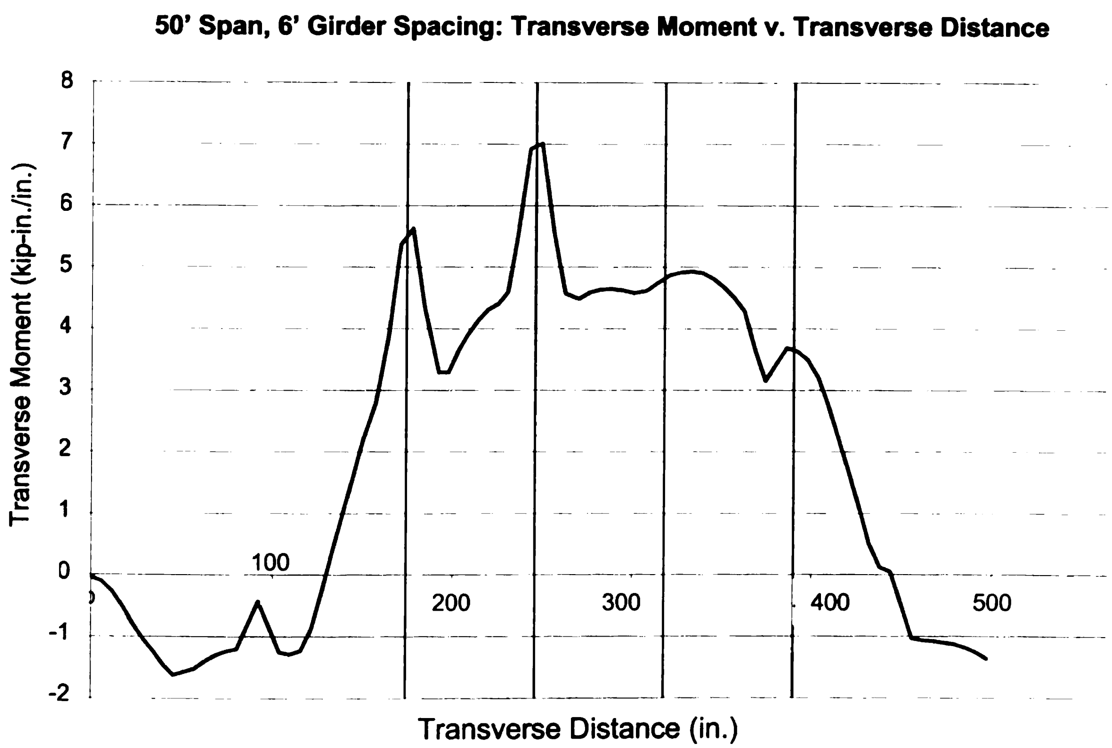

50' Span, 6' Girder Spacing: Transverse Moment v. Longitudinal Distance

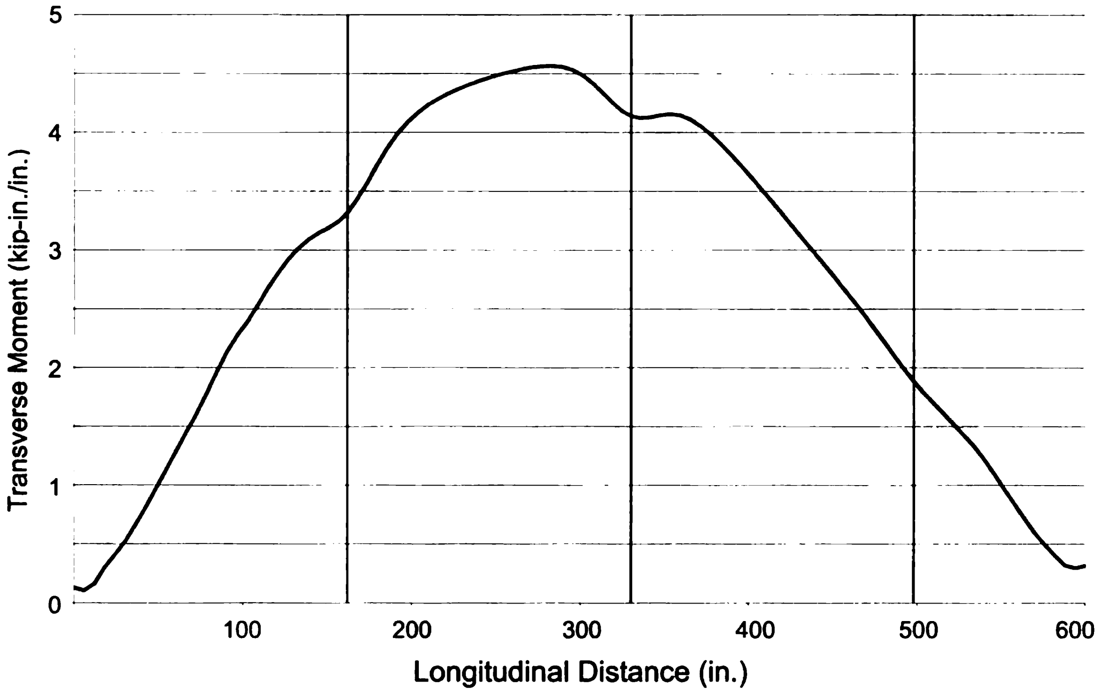

50' Span, 6' Girder Spacing: Longitudinal Moment v. Longitudinal Distance

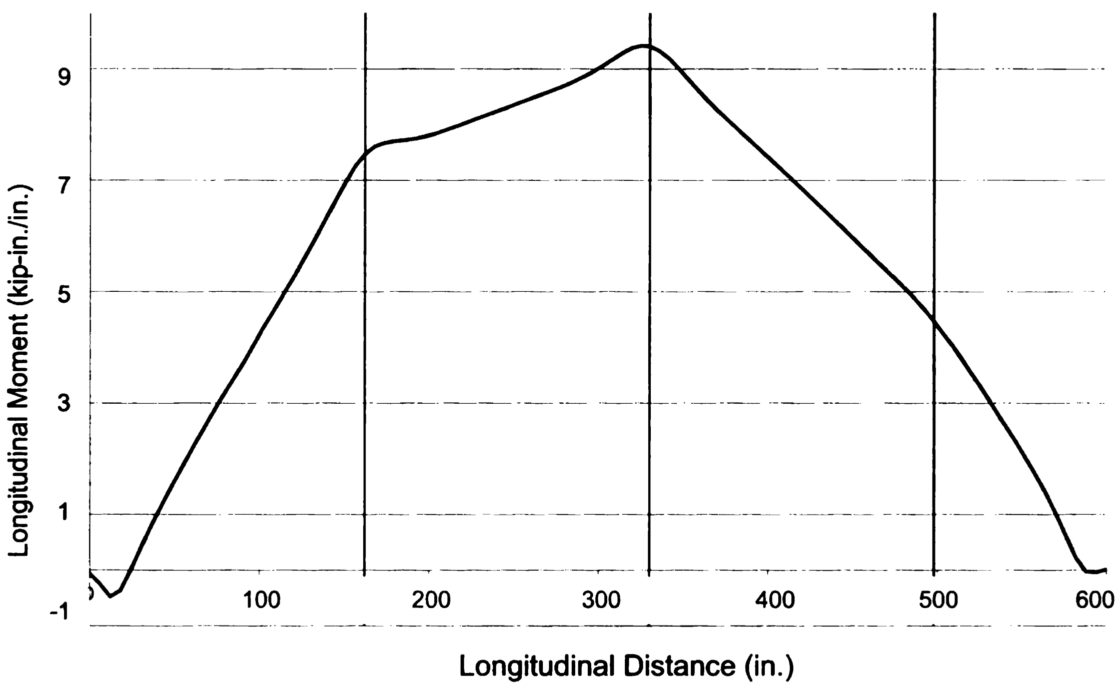

Appendix IV. Bridge Case 3: FE Models Responses

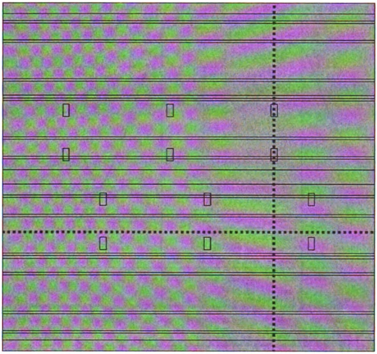

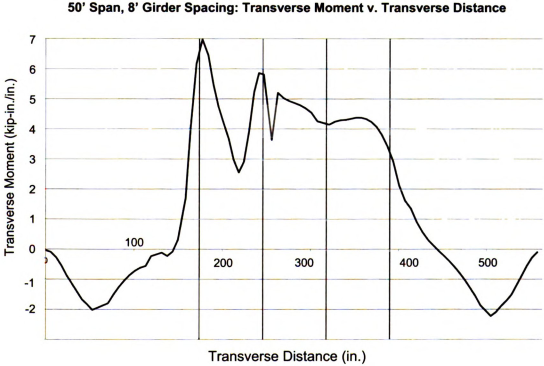

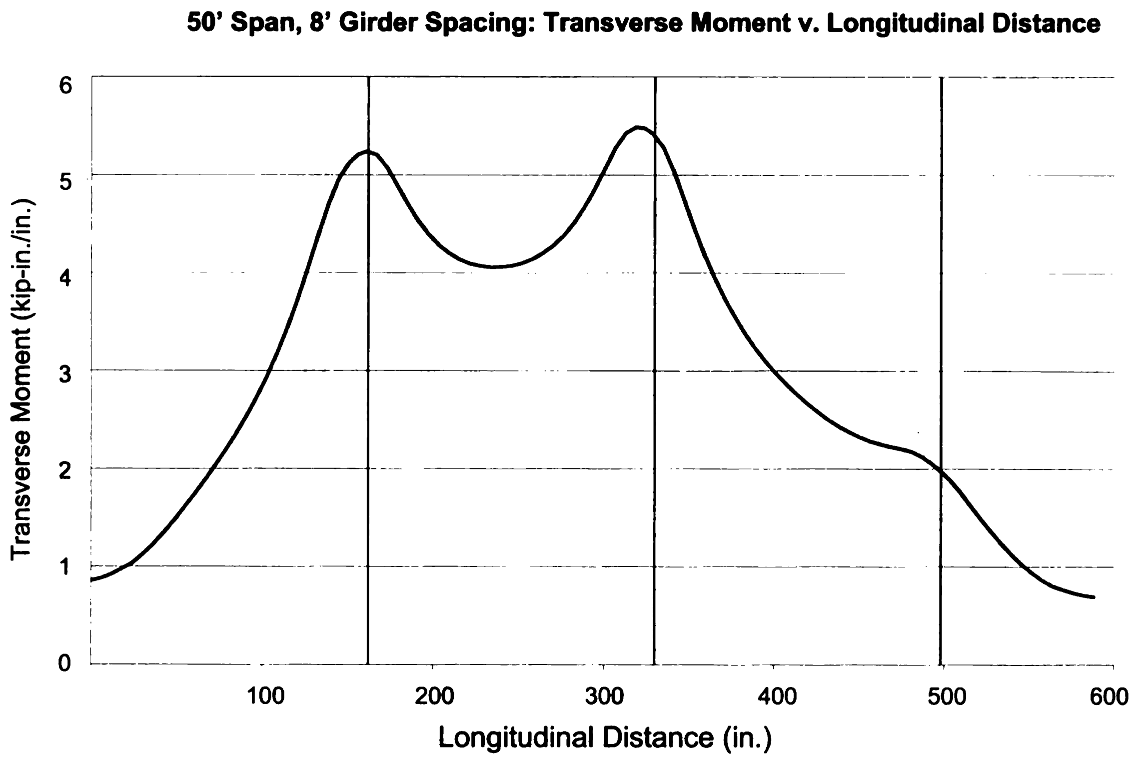
50' Span, 8' Girder Spacing: Transverse Moment v. Longitudinal Distance
Transverse Moment (kip-in./in.)
0
1
2
3
4
5
6
100
200
300
400
500
600
Longitudinal Distance (in.)

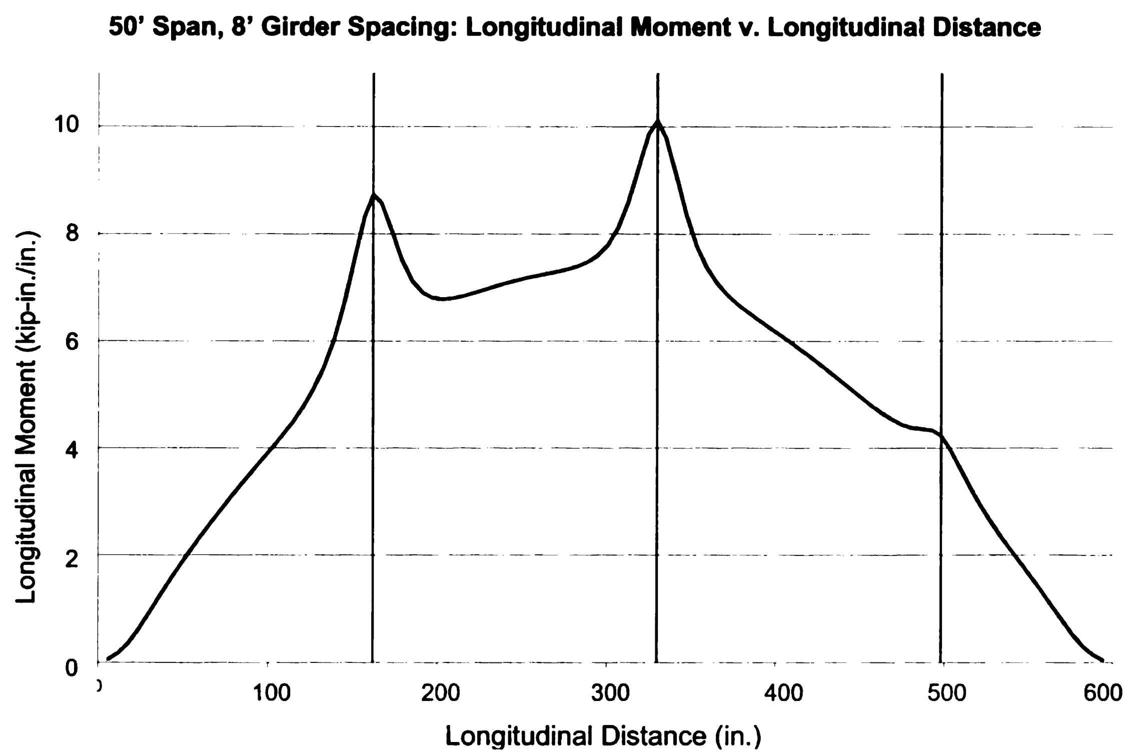
50' Span, 8' Girder Spacing: Longitudinal Moment v. Longitudinal Distance
Longitudinal Moment (kip-in./in.)
0
2
4
6
8
10
100
200
300
400
500
600
Longitudinal Distance (in.)

Appendix V. Bridge Case 4: FE Models Responses

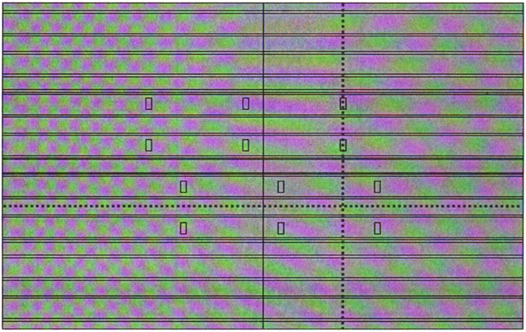

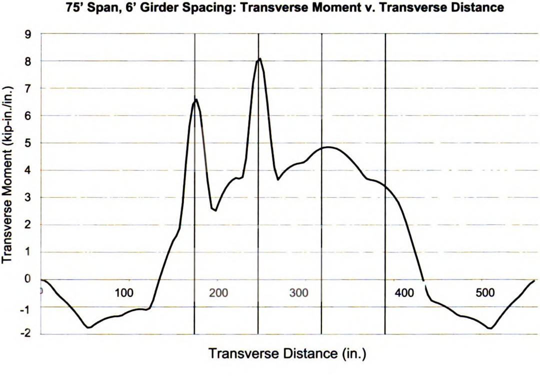

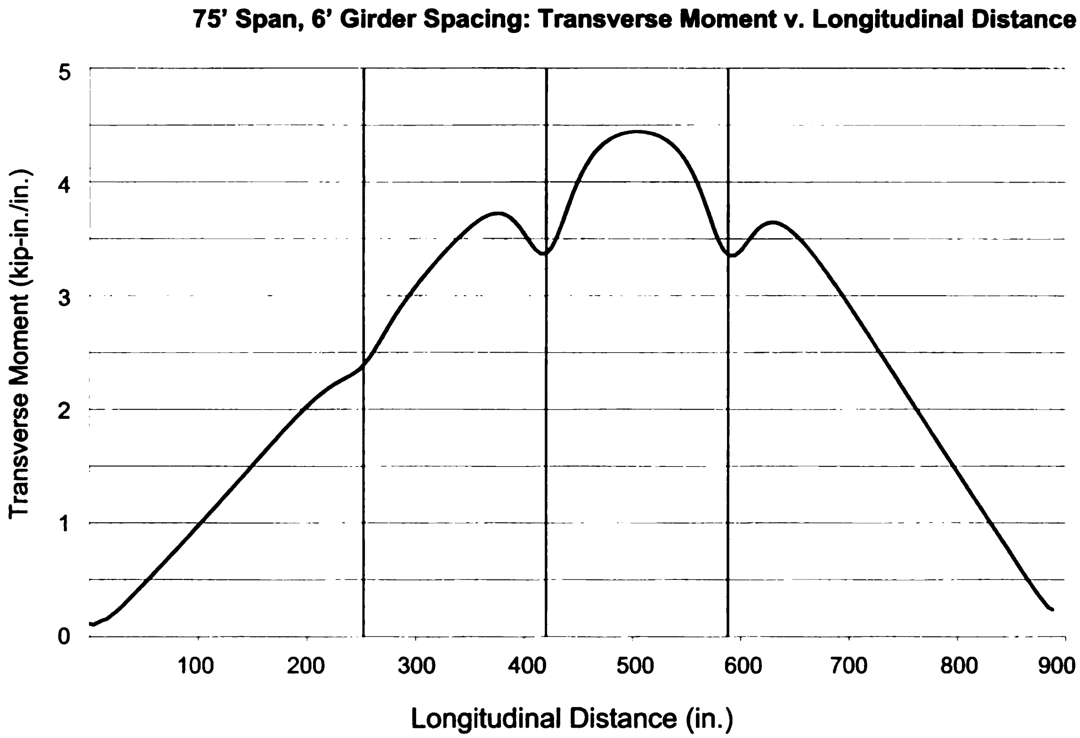

75' Span, 6' Girder Spacing: Transverse Moment v. Longitudinal Distance
Transverse Moment (kip-in./in.)
0
1
2
3
4
5
100
200
300
400
500
600
700
800
900
Longitudinal Distance (in.)

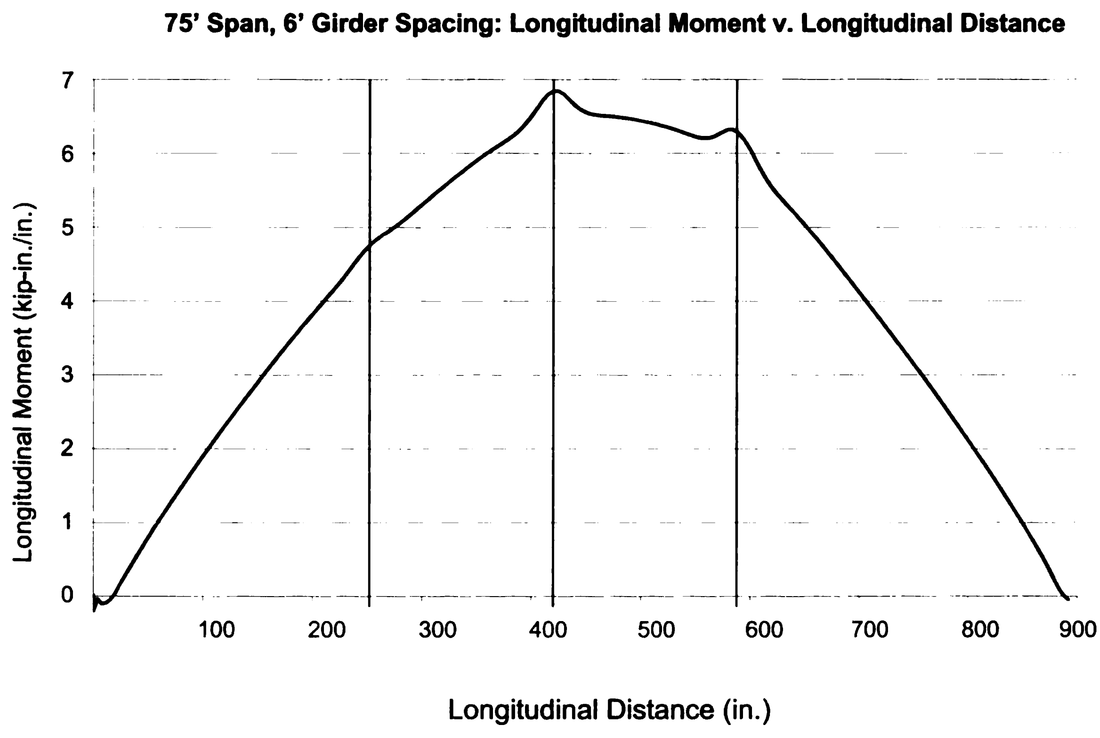

75' Span, 6' Girder Spacing: Longitudinal Moment v. Longitudinal Distance
Longitudinal Moment (kip-in./in.)
0
1
2
3
4
5
6
7
100
200
300
400
500
600
700
800
900
Longitudinal Distance (in.)

Appendix VI. Bridge Case 5: FE Models Responses

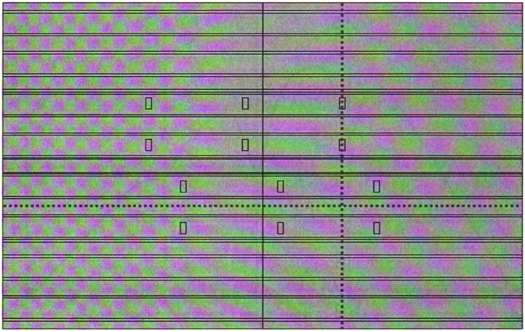

75' Span, 6' Girder Spacing, One Diaphragm: Transverse Moment v. Transverse Distance

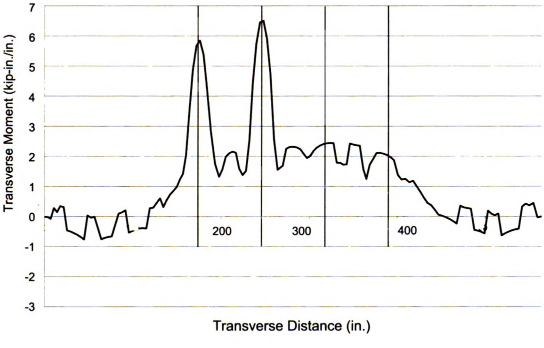

75' Span, 6' Girder Spacing, One Diaphragm: Transverse Moment v. Longitudinal Distance

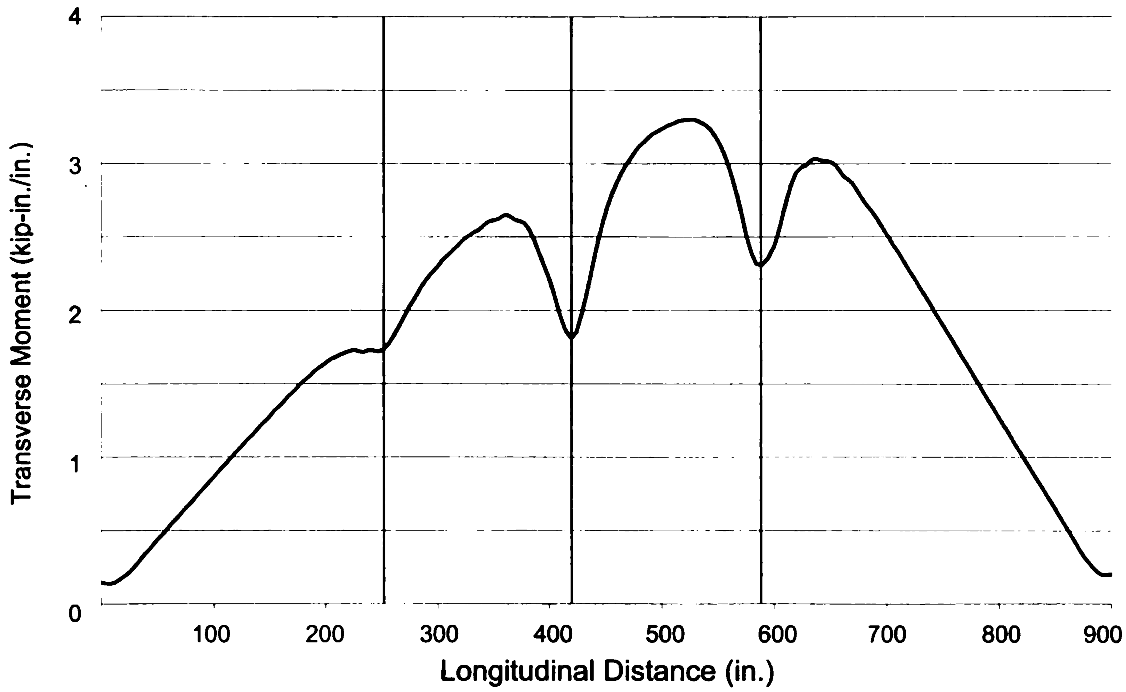

75' Span, 6' Girder Spacing, One Diaphragm: Longitudinal Moment v. Longitudinal Distance

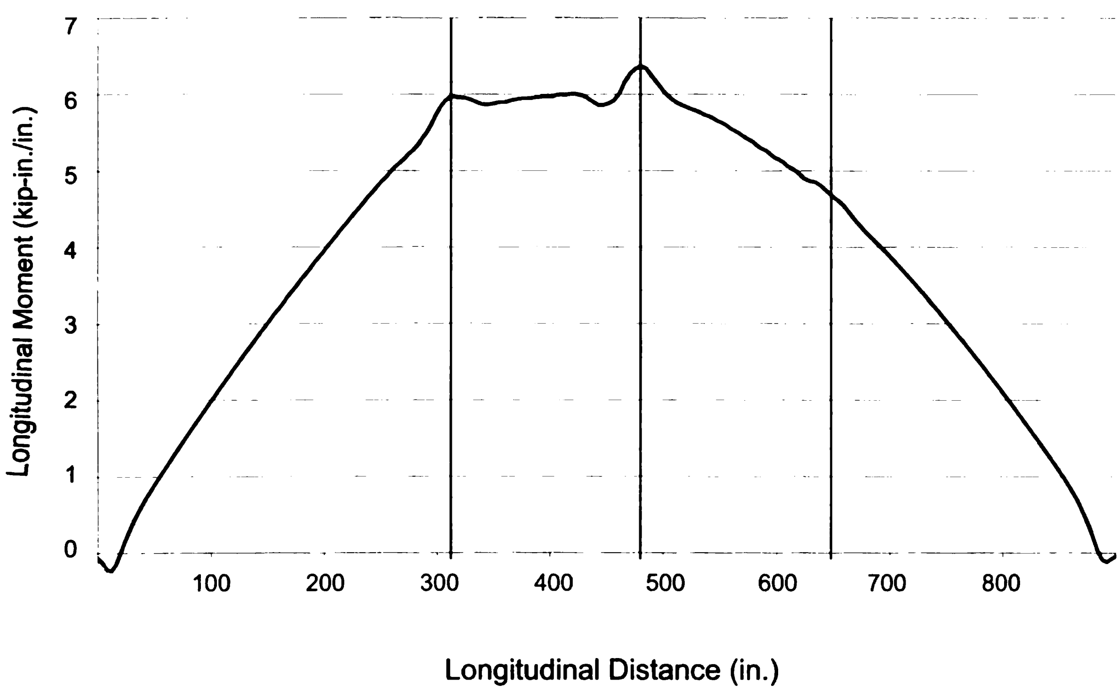

Appendix VII. Bridge Case 6: FE Models Responses

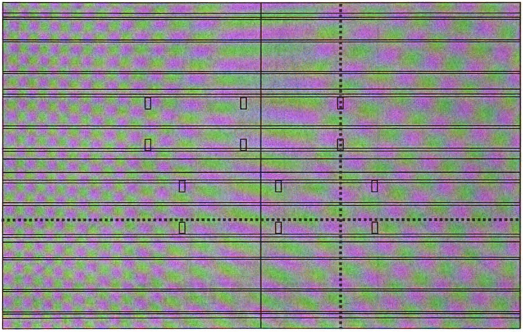

75' Span, 8' Girder Spacing, One Diaphragm: Transverse Moment v. Transverse Distance

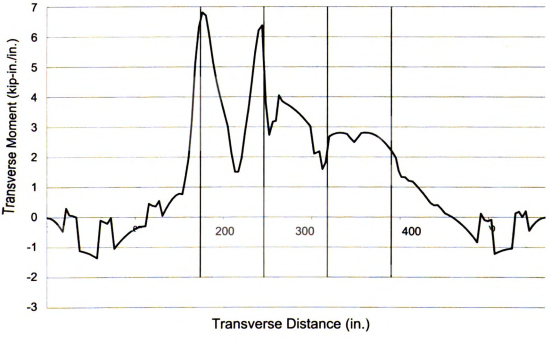

75' Span, 8' Girder Spacing, One Diaphragm: Transverse Moment v. Longitudinal Distance

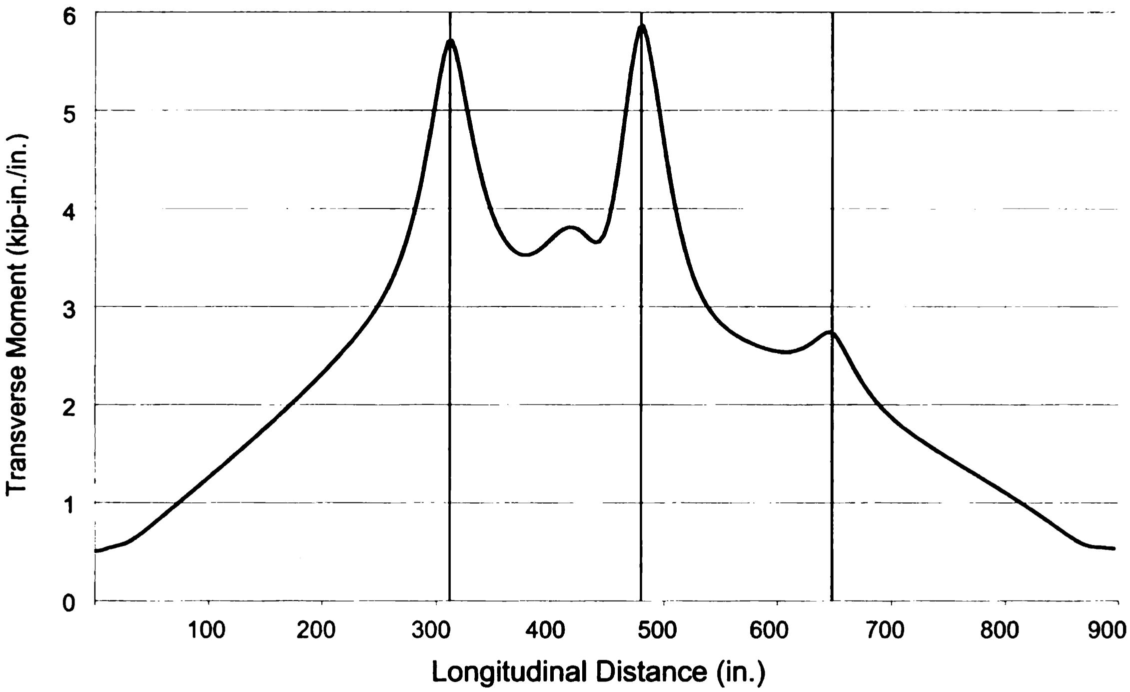

75' Span, 8' Girder Spacing, One Diaphragm: Longitudinal Moment v. Longitudinal Distance

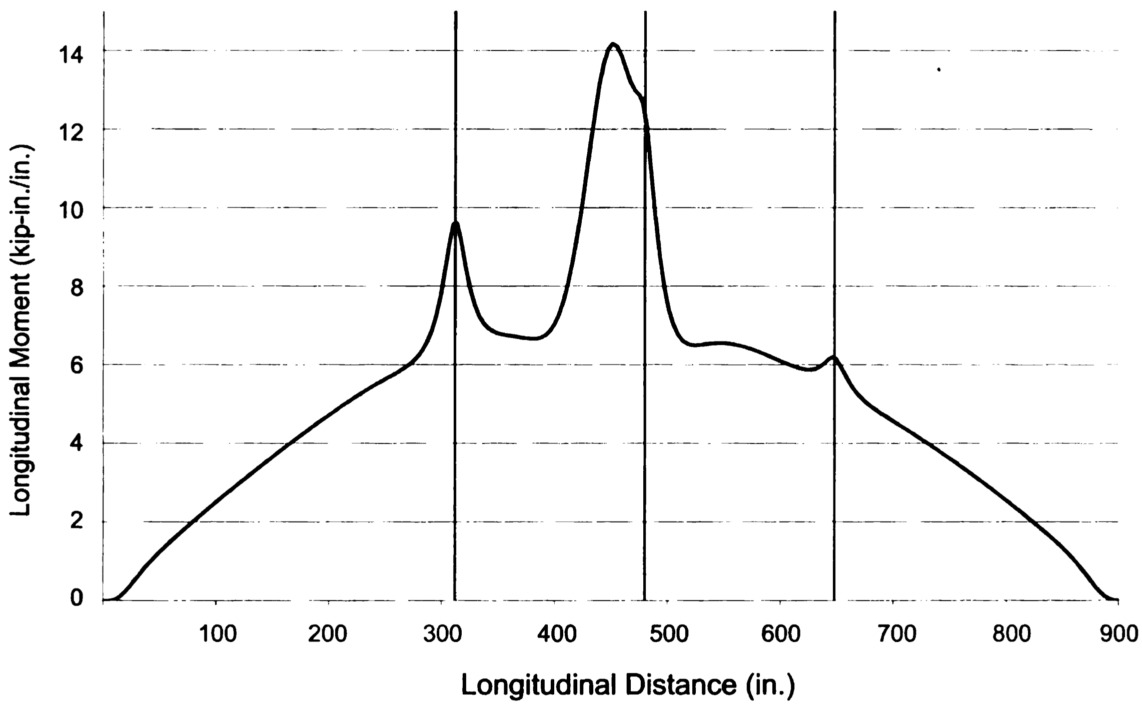

Appendix VIII. Bridge Case 7: FE Models Responses

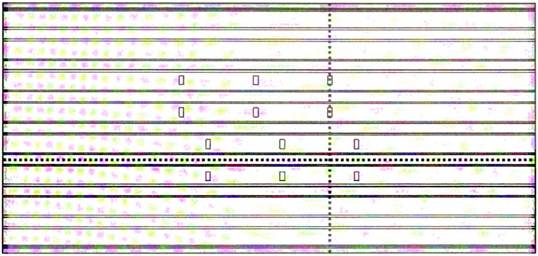

100' Span, 6' Girder Spacing: Transverse Moment v. Transverse Distance

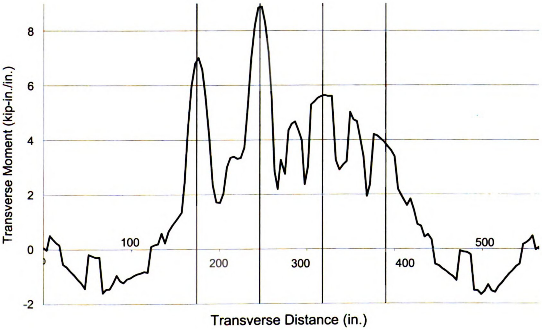

100' Span, 6' Girder Spacing: Transverse Moment v. Longitudinal Distance

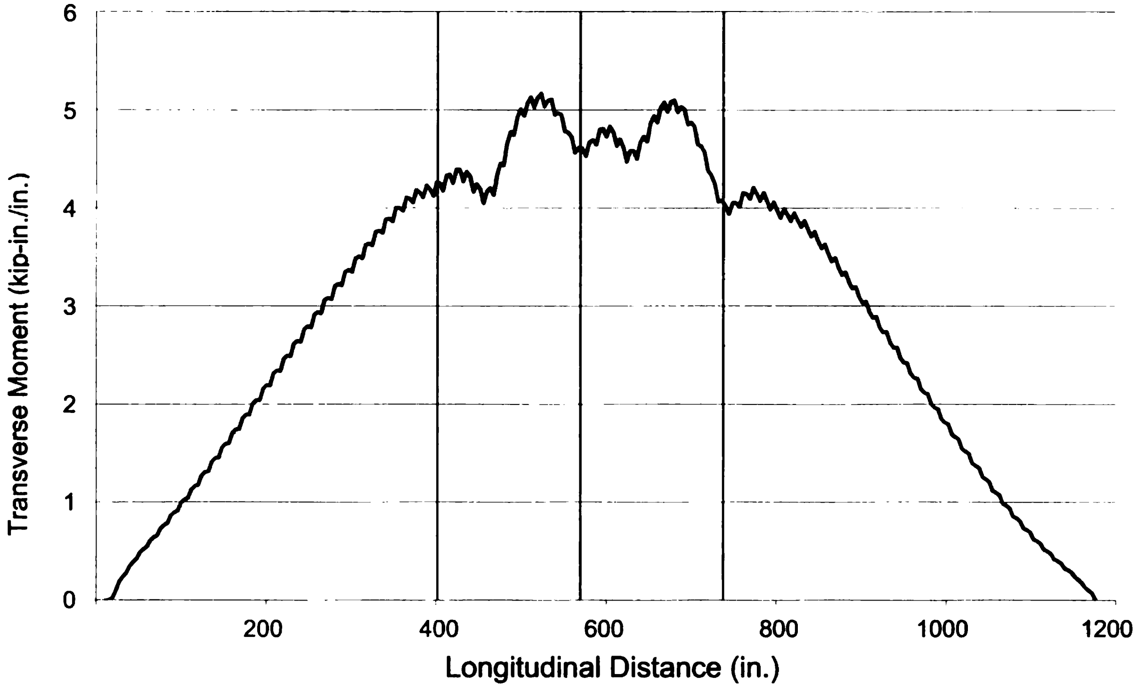

100' Span, 6' Girder Spacing: Longitudinal Moment v. Longitudinal Distance

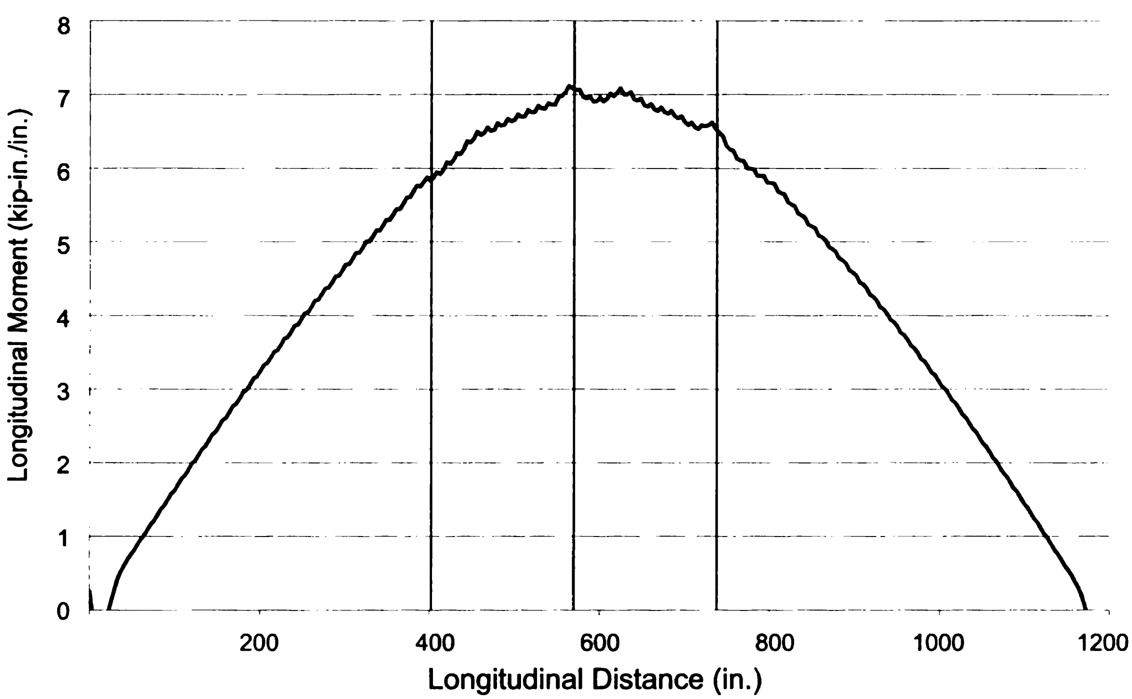

Appendix IX. Bridge Case 8: FE Models Responses

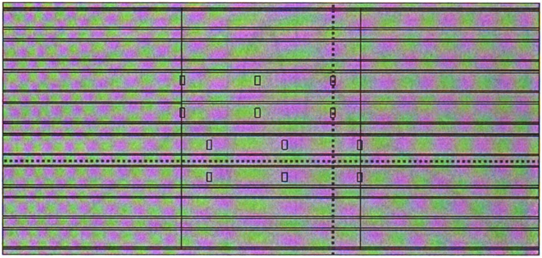

100' Span, 6' Girder Spacing, Two Diaphragms: Transverse Moment v. Transverse Distance

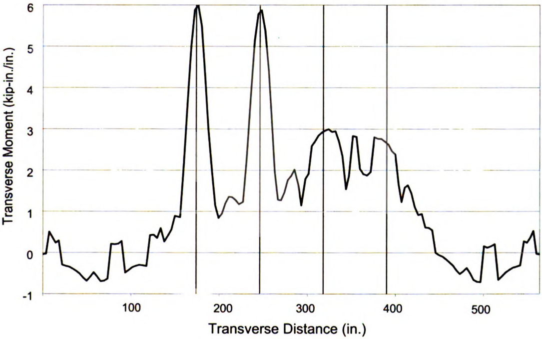

100' Span, 6' Girder Spacing, Two Diaphragms: Transverse Moment v. Longitudinal Distance

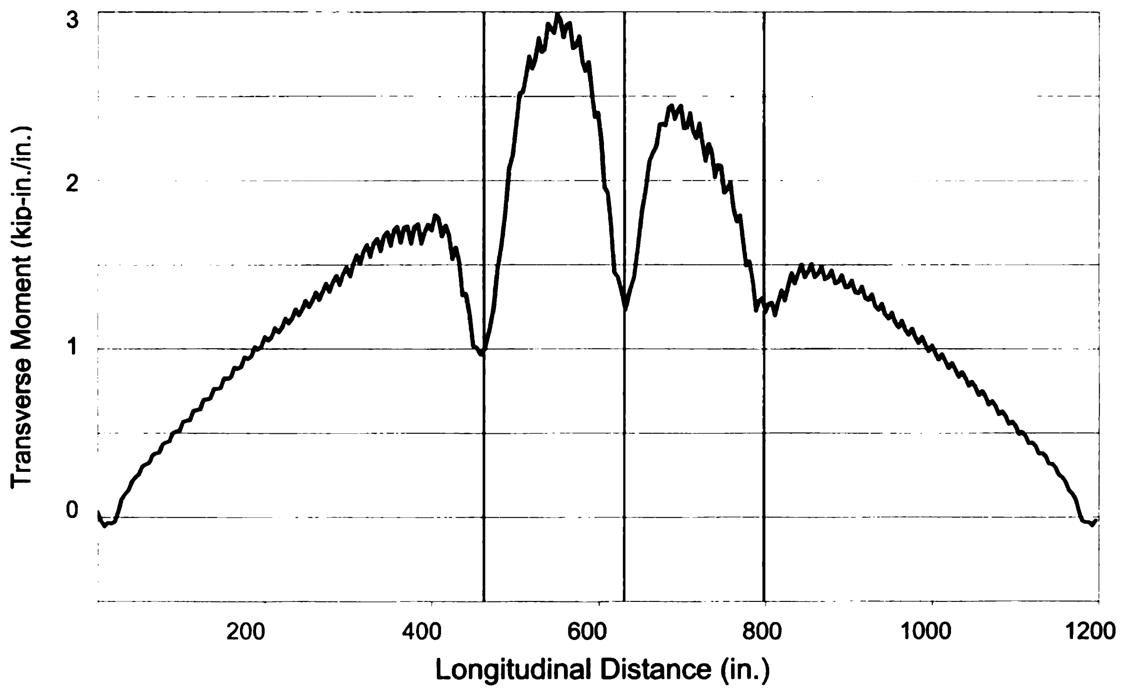

100' Span, 6' Girder Spacing, Two Diaphragms: Longtiudinal Moment v. Longitudinal Distance

Appendix X. Bridge Case 9: FE Models Responses

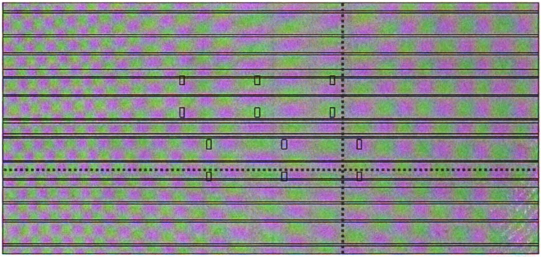

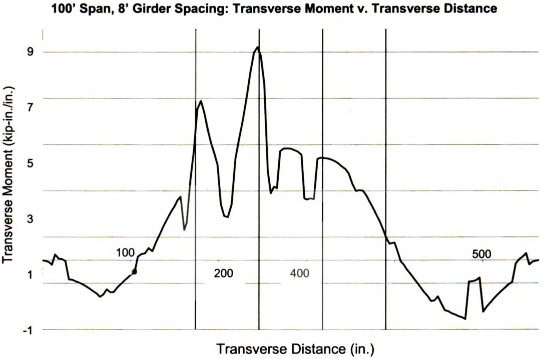

100' Span, 8' Girder Spacing: Transverse Moment v. Longitudinal Distance

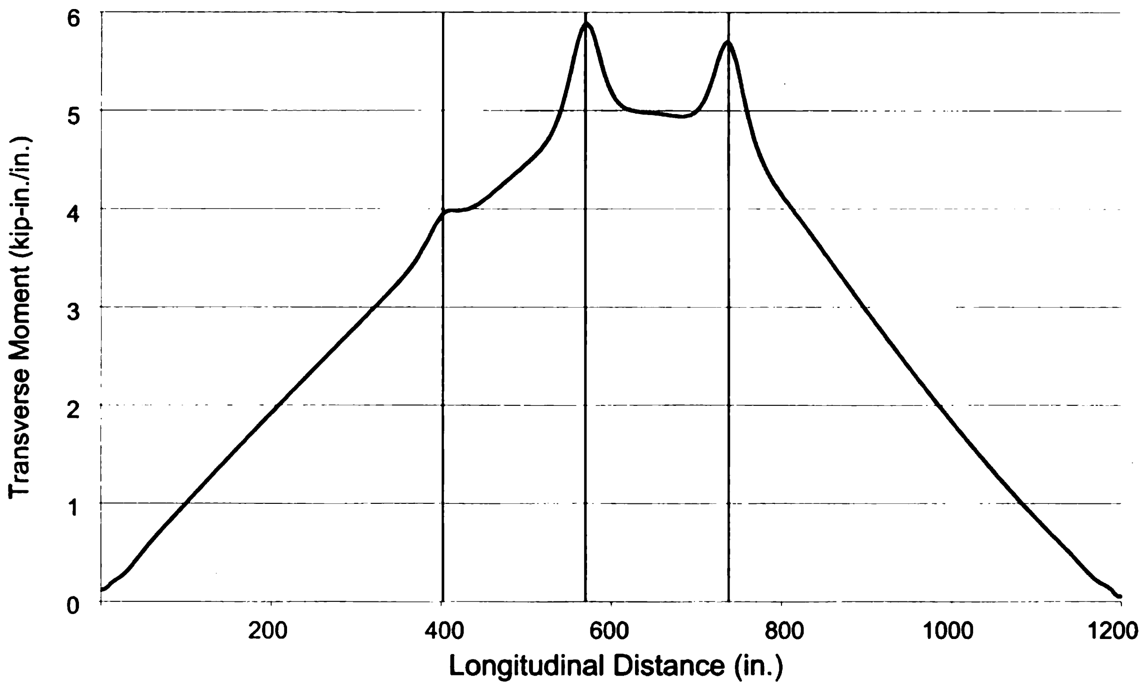

100' Span, 8' Girder Spacing: Longitudinal Moment v. Longitudinal Distance

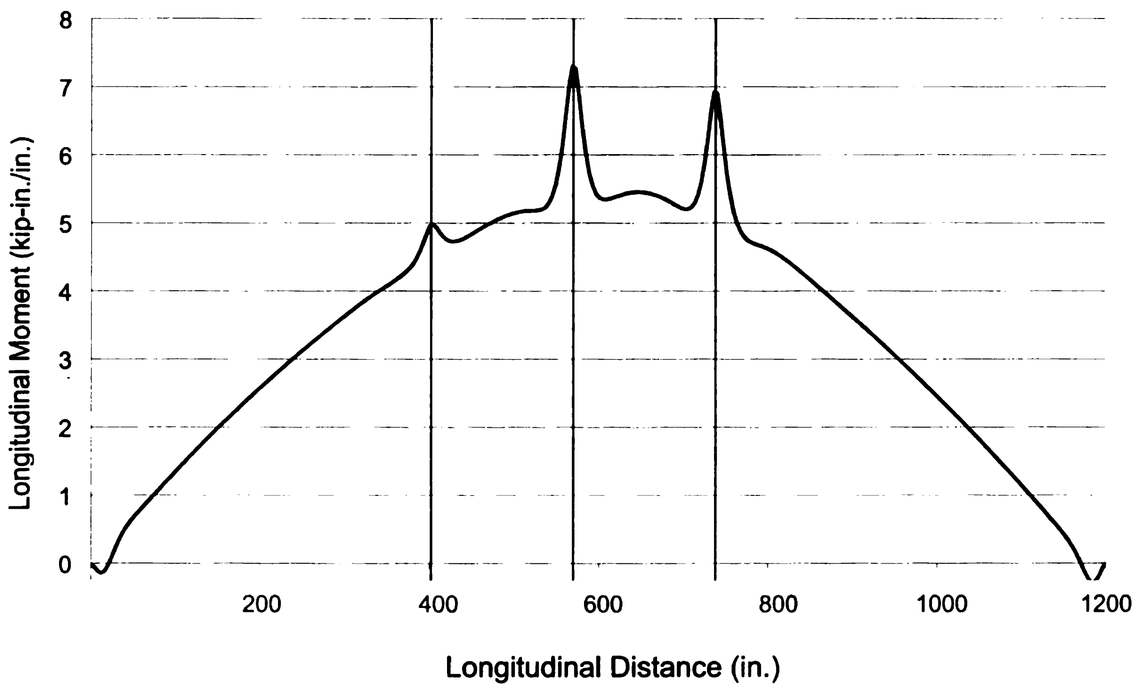

Appendix XI. Bridge Case 10: FE Models Responses

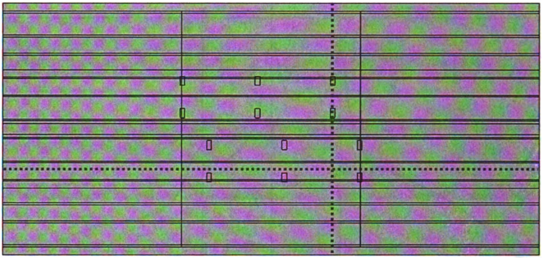

100' Span, 8' Girder Spacing, Two Diaphragms: Transverse Moment v. Transverse Distance

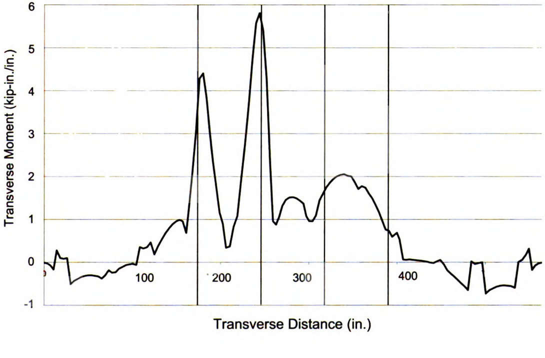

100' Span, 8' Girder Spacing, Two Diaphragms: Transverse Moment v. Longitudinal Distance

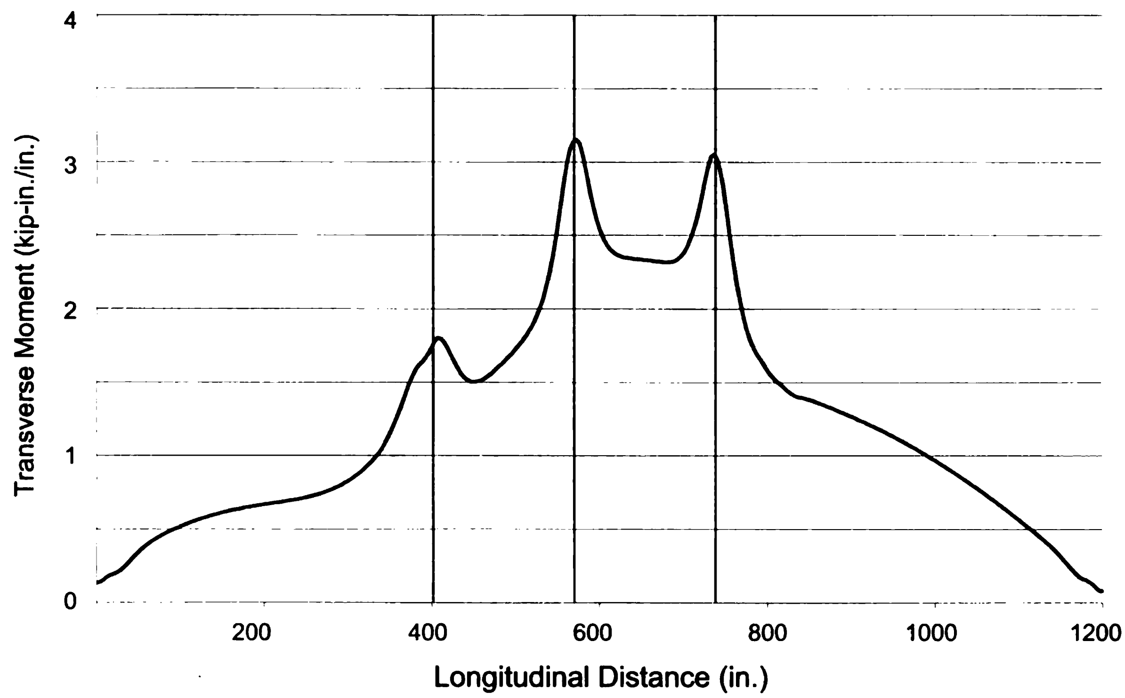

100' Span, 8' Girder Spacing, Two Diaphragms: Longitudinal Moment v. Longitudinal Distance

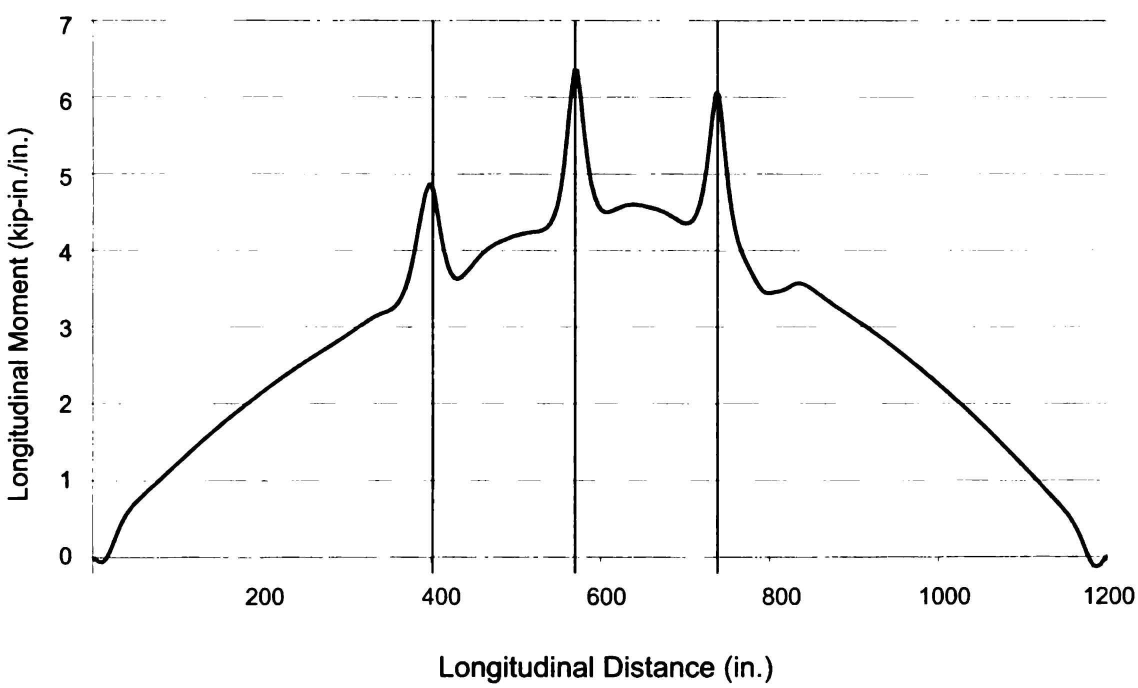

Appendix XII. Bridge Case 11: FE Models Responses

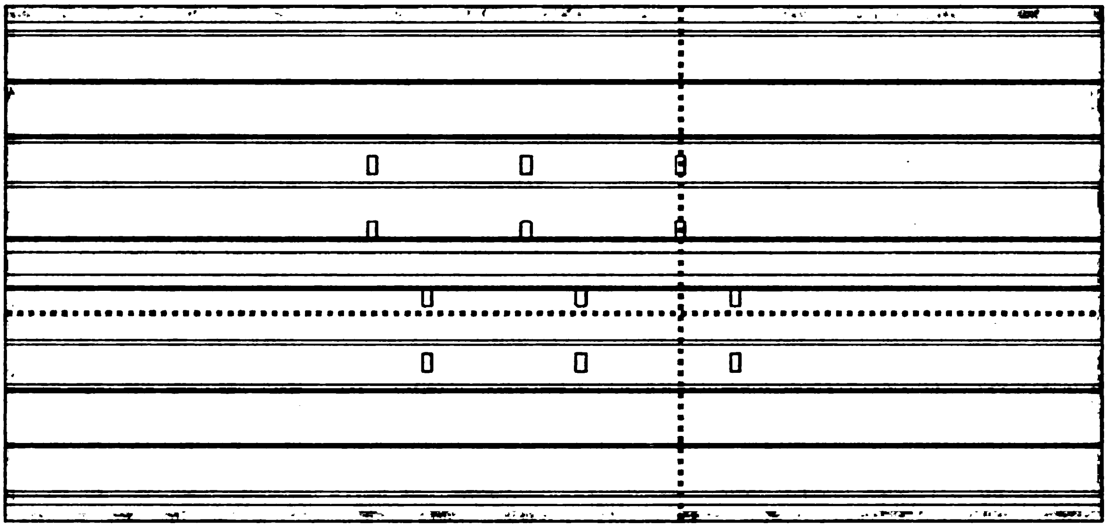

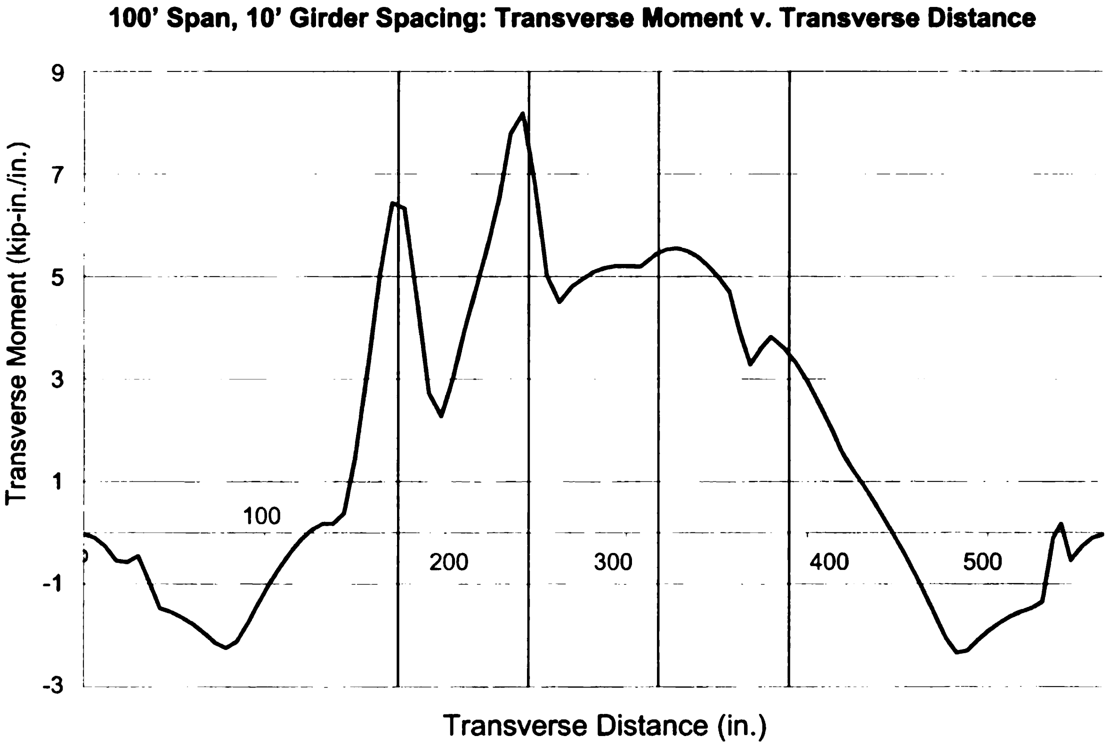

100' Span, 10' Girder Spacing: Transverse Moment v. Longitudinal Distance

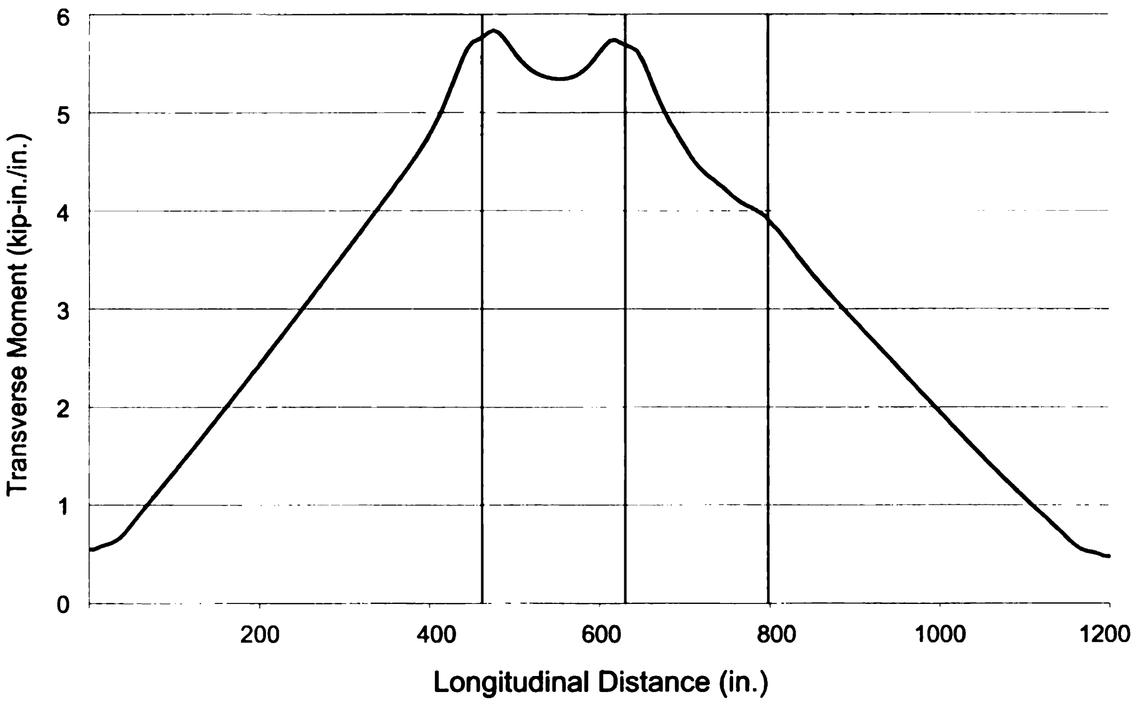

100' Span, 10' Girder Spacing: Longitudinal Moment v. Longitudinal Distance

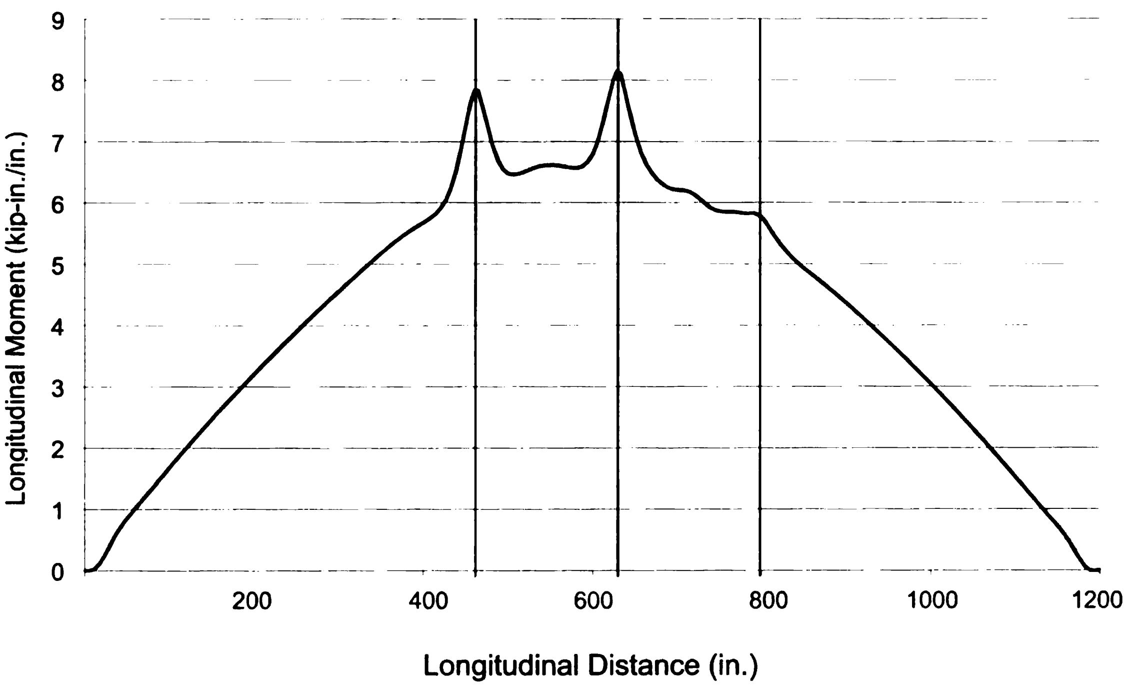

Appendix XIII. Bridge Case 12: FE Models Responses

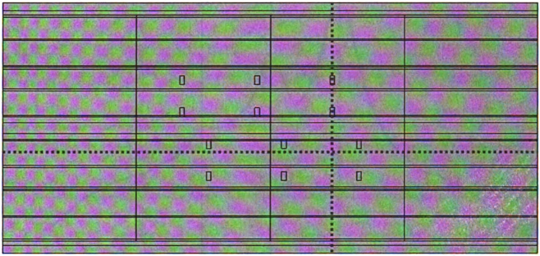

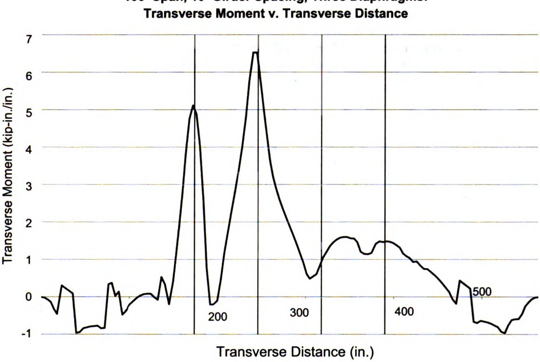

100' Span, 10' Girder Spacing, Three Diaphragms:
Transverse Moment v. Longitudinal Distance

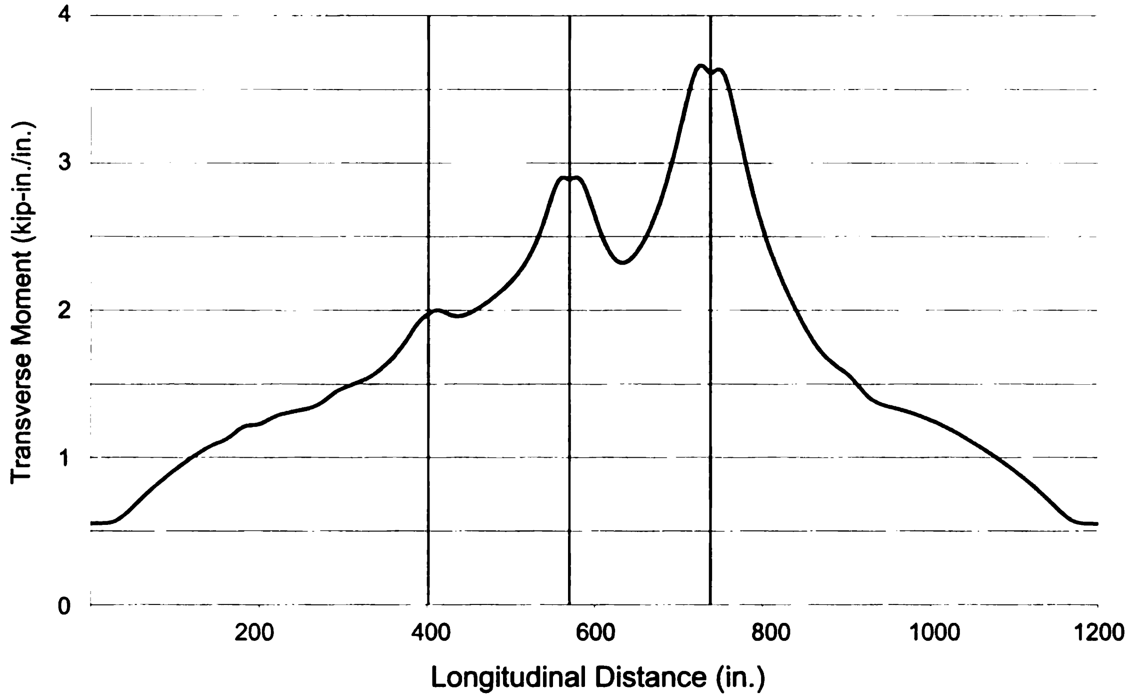

100' Span, 10' Girder Spacing, Three Diaphragms:
Longitudinal Moment v. Longitudinal Distance

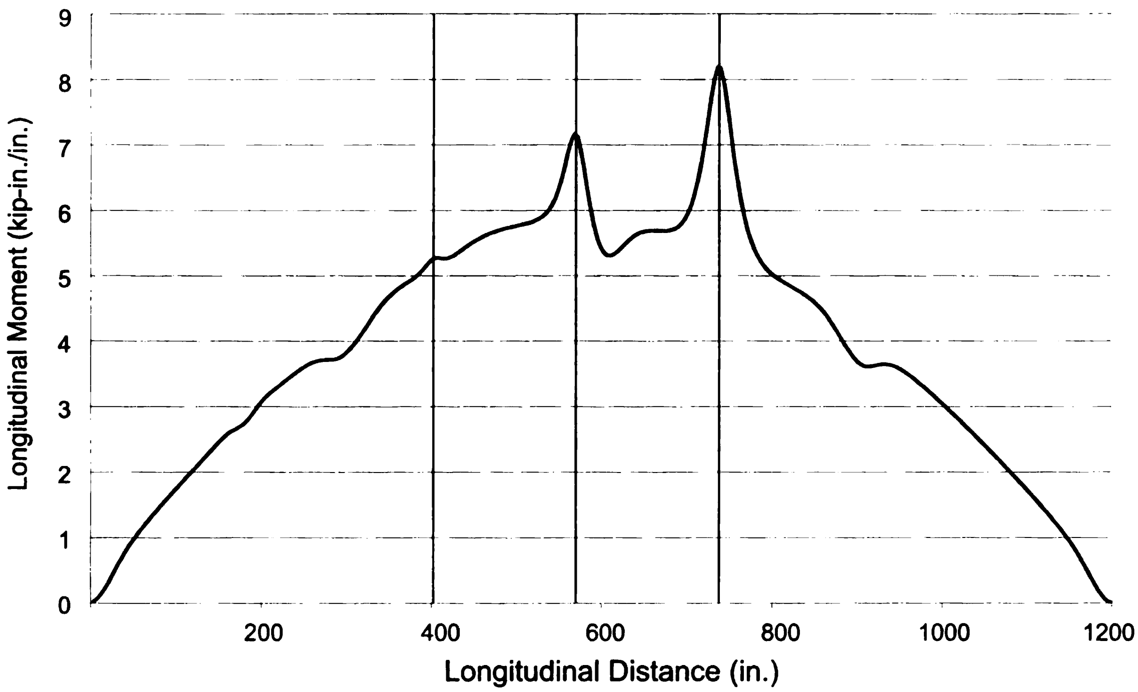

REFERENCES

AASHTO Technology Implementation Group (TIG), "Prefabricated Bridges – Get in, get out, stay out," American Association of State Highway and Transportation Officials, Washington, DC, May 2002.

American Association of Highway Transportation Officials (AASHTO), AASHTO-LRFD Bridge Design Specifications – 2nd Edition, Washington DC, 1998.

Azizinamini, A. (2006) "Bend Steel Plate Girder System for Bridges". United States Patent Application. Pub. No.: US 2006/0265819 A1

Badie, S.S., Kamel, M.R., and Tadros, M.K. (1999). "Precast Pretensioned Trapezoidal Box Beam for Short Span Bridges", *PCI Journal*, 44(1): 48-59.

Barker, R.M. and Puckett, J.A. (1997) Design of Highway Bridges. John Wiley & Sons. New York, NY.

Burgueño, R. and Pavlich, B.S. (2006). "Flexural Performance of Prefabricated Composite Bridge Girder Units," Technical Report CEE-TR-2006-01, Department of Civil and Environmental Engineering, Michigan State University, East Lansing, Michigan.

Chang, S.-P. and Shim, C.-S. (2001). "Continuous Composite Bridges with Precast Decks," *Steel Structures*, 1:123-132.

Computers and Structures (CSI). (2000). SAP 2000 v.7.1 – Integrated Software for Structural Analysis & Design.

Federal Highway Administration, (2004). "Prefabricated Bridge Elements and Systems in Japan and Europe," Federal Highway Administration, International Technology Exchange Program.

Federal Highway Administration. Bridge Rail Guide – New Jersey Barrier. http://www.fhwa.dot.gove/BRIDGE/bridgerail/br054106.cfm. Accessed 5/17/2006.

Freeby, G.A. (2005). "Texas's Totally Prefabricated Bridge Superstructures," *Transportation Research Record: Journal of the Transportation Research Board*, CD 11-S, Transportation Board of the National Academies of Sciences, Washington, D.C., pp. 169-174.

Freeby, G.A., (2006). Personal Communication with B. Pavlich.

Hambly, E.C. (1991) Bridge Deck Behaviour, 2nd Edition. E & FN Spon. London, UK.

Issa, M.A., Idrs, A.-T., Kaspar, I.I., and Khayyyat, S.Y. (1995). "Full-Depth Precast and Precast Prestressed Concrete Bridge Deck Panels," *PCI Journal*, 40(1): 59-80.

Issa, M.A., et al. (1995) "Field Performance of Full Depth Precast Concrete Panels in Bridge Deck Reconstruction," *PCI Journal*, 40(3): 82-108.

Nakmura, S., (2002) "Bending Behavior of Composite Girders with Cold Formed Steel U Section," *Journal of Structural Engineering*. 128(9): 1169-1176.

Nelson, G.C., "Composite Cold-Formed Steel Plate Box Beam," Communication to Michigan Department of Transportation, URS Corporation, Grand Rapids, MI, Spring 2004.

Nelson, G.C., (2005). "Con-Struct Prefabricated Bridge System," 2005 World Steel Bridge Symposium Presentation

Nelson, G.C. (2005). Prefabricated, Prestresed Bridge System and Method of Making the Same Patent Application No. 11/337,206.

Nelson, G.C., (2006). Personal Communication with R. Burgueño

Ohelers, D.J., and Bradford, M.A. (1995). <u>Composite Steel and Concrete Structural Members: Fundamental Behaviour</u>, Elsevier Science, Tarrytown, NY.

Ralls, M.L. and Tang, B.M. (2003). "Laying the Groundwork for Fast Bridge Construction," Public Roads, 67(3).

Shahawy, M.A. (2003). "Prefabricated Bridge Elements and Systems to Limit Traffic Disruption during Construction – A Synthesis of Highway Practice," NCHRP Synthesis 324, National Cooperative Highway Research Program, Transportation Research Board, Washington, D.C.

Simulia. (2007). ABAQUS FEA v.6.7

Taly, N. and Gangarao, H.V.S. (1979). "Prefabricated Press-Formed Steel T-Box Girder Bridge System," *Engineering Journal*, American Institute of Steel Construction, Third Quarter, pp. 75-83.

TRB-RIP, (2006) "Short Span Steel Bridge: Inverted Steel Box," Transportation Research Board of the National Academies, Research in Progress, <u>http://rip.trb.org/browse/dproject.asp?n=5087</u>, accessed online 4/20/06.

Turmo, J., Ramos, G., Aparicio, A.C. (2006) "Shear strength of dry joints of concrete panels with and without steel fibres. Application to precast segmental bridges," *Engineering Structures*, 28: 23-33.

Virlogeux, M. (1999). New Trends in Prestressed Concrete Bridges," *Transportation Research Record* 1696, Paper No. 5B0135, pp. 238-248.

Yakel, A., et al. (2007) "Three Innovative Concepts for Short Span Steel Bridges" NDOR Research Project Number SPR-PL-1.